

**PATENT**

**IN THE UNITED STATES PATENT AND TRADEMARK OFFICE**

*In re* Application of:

Eric N. OLSON

Serial No.: 10/043,658

Filed: January 9, 2002

For: METHODS FOR PREVENTING  
HYPERTROPHY AND HEART FAILURE  
BY INHIBITION OF MEF2  
TRANSCRIPTION FACTOR

Group Art Unit: 1632

Examiner: Woitach, J.

Atty. Dkt. No.: MYOG:024USC1/SLH

Confirmation No.: 7444

**ELECTRONIC FILING SUBMISSION**

Date of Filing: January 12, 2007

**BRIEF ON APPEAL**

## TABLE OF CONTENTS

	Page
I. Real Party in Interest .....	4
II. Related Appeals and Interferences .....	4
III. Status of Claims.....	4
IV. Status of Amendments.....	4
V. Summary of Claimed Subject Matter .....	4
VI. Grounds on Rejection to be Reviewed on Appeal.....	4
VII. Argument.....	5
A. Standard of Review .....	5
B. Rejection Under 35 U.S.C. §112 .....	5
C. Conclusion.....	10
VIII. CLAIMS APPENDIX .....	11
IX. EVIDENCE APPENDIX .....	12
X. RELATED PROCEEDINGS APPENDIX.....	13

**PATENT**

**IN THE UNITED STATES PATENT AND TRADEMARK OFFICE**

*In re* Application of:

Eric N. OLSON

Serial No.: 10/043,658

Filed: January 9, 2002

For: METHODS FOR PREVENTING  
HYPERTROPHY AND HEART FAILURE  
BY INHIBITION OF MEF2  
TRANSCRIPTION FACTOR

Group Art Unit: 1632

Examiner: Woitach, J.

Atty. Dkt. No.: MYOG:024USC1/SLH

Confirmation No.: 7444

**BRIEF ON APPEAL**

**MAIL STOP APPEAL BRIEF - PATENTS**

Commissioner of Patents

P.O. Box 1450

Alexandria, VA 22313-1450

Sir:

This Brief on Appeal is filed in response to the final Office Action mailed May 12, 2006, and the Advisory Action, mailed on September 19, 2006. This brief is due on January 12, 2007, by virtue of the Notice of Appeal filed on September 12, 2006, and the enclosed Petition for Extension of Time (two-month) and payment of fees. Also enclosed are the fees for this brief. No other fees are believed due in connection with this filing. However, should any additional fees be due, appellants authorize the Commissioner to debit Fulbright & Jaworski L.L.P. Deposit Account No. 50-1212/MYOG:024USC1/SLH.

**I. Real Party in Interest**

The real parties in interest of this application are the assignee, the Board of Regents, University of Texas System, Austin TX and the licensee, Myogen Inc. (now Gilead Sciences), Denver CO.

**II. Related Appeals and Interferences**

There are no known related appeals or interferences.

**III. Status of Claims**

Claims 1-31 were filed with the original application, and claims 2, 3, 5-8 and 10-31 have been canceled. Claims 1, 4 and 9 are pending, stand rejected and are appealed.

**IV. Status of Amendments**

No amendments have been offered after the final Office Action.

**V. Summary of Claimed Subject Matter**

Claim 1, drawn to a method of treating hypertrophy in a cardiomyocyte cell comprising the step of inhibiting the function of MEF2, is supported at page 6, lines 25-26, of the Specification.

**VI. Grounds on Rejection to be Reviewed on Appeal**

Whether claims 1, 4 and 9 lack an enabling disclosure under 35 U.S.C. §112, first paragraph.



## **VII. Argument**

### **A. *Standard of Review***

As an initial matter, appellant notes that findings of fact and conclusions of law by the U.S. Patent and Trademark Office must be made in accordance with the Administrative Procedure Act, 5 U.S.C. § 706(A), (E), 1994, and *Dickinson v. Zurko*, 527 U.S. 150, 158 (1999). Moreover, the Federal Circuit has held that findings of fact by the Board of Patent Appeals and Interferences must be supported by “substantial evidence” within the record. *In re Gartside*, 203 F.3d 1305, 1315 (Fed. Cir. 2000). In *In re Gartside*, the Federal Circuit stated that “the ‘substantial evidence’ standard asks whether a reasonable fact finder could have arrived at the agency’s decision.” *Id.* at 1312. Accordingly, it necessarily follows that an Examiner’s position on Appeal must be supported by “substantial evidence” within the record in order to be upheld by the Board of Patent Appeals and Interferences.

### **B. *Rejection Under 35 U.S.C. §112, First Paragraph***

As stated in previous submissions, the rejection seems to have two aspects – indeed, the examiner has agreed (Advisory Action, page 2). First, there is a question regarding the ability to extrapolate from the acknowledged role of MEF2C in hypertrophic signaling to other MEF2 isoforms, *i.e.*, MEF2A, MEF2B and MEF2D. Second, the examiner argues that even given the proven role of MEF2C in hypertrophy, the specification provides insufficient evidence regarding efficacy of the claimed methods. As explained below, appellants believe that the extrapolation from MEF2C to other isoforms is indeed warranted, and submit that simply alleging unpredictability, as the examiner has done here, cannot shift the burden to appellants to provide clinical evidence of efficacy.

In a previous response, appellants attached a paper by Xu *et al.* (2006) (Exhibit 1). In this paper, the authors reported that MEF2A behaves much as does MEF2C in terms of sarcomeric disorganization, focal elongation, altered gene expression, extracellular matrix remodelling, and ion handling. Thus, there is indeed evidence to indicate that MEF2A, like MEF2C, is involved in hypertrophic signaling. Moreover, other evidence exists indicating that MEF2A and MEF2D form a heterodimer, further suggesting a common role for these two proteins. Mora & Pessin (2000) (Exhibit 2). Moreover, there are additional studies indicating that MEF2A, MEF2C and MEF2D have similar functions with respect to interactions with MASH1 and E12. Black *et al.* (1996) (Exhibit 3). Thus, to suggest that there is no evidentiary basis in the literature for extrapolating from MEF2C to other isoforms of MEF2 simply is not true.

Appellants further two declarations from Dr. Tim McKinsey (Exhibits 4-5) in support of enablement. In the second of these declarations, data were provided showing experiments with one month-old MEF2D knockout mice. Fig. A shows both the knockouts and wild-type littermates subjected to sham operation or thoracic aortic banding (TAB) for 20 days. TAB induced a 27% increase in heart weight-to-tibia length ratio, indicative of cardiac hypertrophy. The hypertrophic response to TAB was eliminated in animals lacking a functional *MEF2D* gene. Fig. B shows animals were treated as described in Fig. A. Left ventricles were fixed and stained with hematoxylin (red) and Mason's trichrome (blue) to reveal cardiac muscle and fibrotic lesions, respectively. Thus, this figure shows the MEF2D, in addition to MEF2A and MEF2C, plays a role in cardiac hypertrophy.

Despite this considerable showing, the examiner argues in the Advisory Action that one of skill in the art would still doubt the ability to target MEF2 generally. However, this argument

is based on a selective reading of the art, and a legally inappropriate treatment of factual submissions, such as failing to address the evidence regarding MEF2A and MEF2D, cited above. The examiner argues that “sound scientific arguments supported by scientific references” against MEF2 as a therapeutic target have been provided. However, as evidenced in both McKinsey declarations, the examiner’s view of the cited references is quite distinct from that of the skilled artisan. For example, the examiner has cited Zhang *et al.* (2002; Exhibit 6) and McKinsey *et al.* (2002; Exhibit 7) as indicating that MEF2 is not an enabled target for hypertrophic therapy, whereas Dr. McKinsey, ***lead author of one of the papers***, comes to the opposite conclusion:

[Zhang *et al.*] provides *in vivo* evidence that unphosphorylated Class II HDACs associate with and repress MEF2, and that pro-hypertrophic stimuli lead to phosphorylation-dependent release of class II HDACs from MEF2. Once HDACs are released, MEF2 can and does initiate transcription of fetal genes, leading to development of hypertrophy.... The fact that ... dominant repressive HDACs are anti-hypertrophic is not only validation for a role for HDACs in hypertrophy, it also shows direct proof that inhibiting MEF2 and MEF2 dependent gene upregulation is anti-hypertrophic.

McKinsey Declaration (A), para. 5. Clearly, there are no definitive answers in the cited art, but the proposition upon which appellants’ claims are based – that MEF2 (including various forms thereof) is a hypertrophic signaling agent – is clearly borne out by the evidence of record. The fact that the specification fails to provide evidence for each isoform is not dispositive, nor is the relative complexity in the pathway. What *is* dispositive, here, are the plain statements of the cited articles and the opinion of Dr. McKinsey, which stand in stark contrast to the examiner’s position.

In an attempt to avoid this evidence in favor of enablement, the examiner side-steps the issue by arguing that just because MEF2 contributes to the induction of hypertrophic signaling, that does not mean that inhibition of this target would be therapeutic given the alleged

requirement for other factors and the complexity of the system overall. This statement is nonsensical. Indeed, MEF2 is *necessary* but not *sufficient* for hypertrophy, but under such facts, one of skill in the art *would* believe that inhibition of MEF2 would block hypertrophy. Thus, the examiner's argument devolves into the same one as discussed below – the alleged lack of proof *in vivo* that inhibition would be therapeutic.

The examiner has also argued that to the extent appellants rely on the prior art for enablement of, *e.g.*, gene therapy, appellants are also handicapped by the shortcomings of that art. However, just because there are limitations with respect to, *e.g.*, gene therapy, that does not mean that one of skill in the art cannot make and use the invention. Thus, the field of gene therapy is to the point where general allegations regarding targeting, duration of expression and specificity simply do not stand up. The PTO has issued hundreds of patents on such therapies, and regardless of the fact that “each application is examined on its own merits,” the PTO cannot now maintain that gene therapy is *per se* not enabled. There are simply too many examples where the alleged limitations to gene therapy have been overcome, circumvented or otherwise are not relevant. Thus, an attack on *this* form of gene therapy should have *some* bearing of limitations that are *unique* to this invention. In other words, it is entirely inappropriate to cast *generalized* dispersions on the claimed invention, but then turn around and require *specific* evidence of efficacy. Simply put, the PTO cannot “have its cake and eat it too.”

The only specific attack on MEF2 gene therapy is that inhibiting MEF2 generally would not be believed to inhibit cardiac hypertrophy. With all due respect to the PTO, appellants have submitted an expert declaration (McKinsey Declaration A; Exhibit 4) and a recently published paper on this precise point (Xu *et al.*, 2006; Exhibit 1), both documents *supporting* the position that down-regulating MEF2 would indeed be therapeutic of cardiac hypertrophy. The examiner

again attempts to argue that Xu *et al.* (2006) proves this not to be the case by selectively quoting from the article. However, the concluding statement from that paper, which is far more indicative of the authors' conclusions than the examiner's quotations, **supports** appellants' position: "In conclusion, we provide the first proof-of-principle that MEF2 can dominantly drive dilated cardiomyopathy *in vivo*, potentially in association with a primary alteration in a subset of ion handling genes and extracellular matrix associated genes." This statement **clearly** supports MEF2 as a target, and taken with appellants' other evidence, it is submitted that the record supports, and does not refute, enablement.

Another efficacy-related point raised by the examiner, also raised in prior actions, is the question of **how** one would seek to inhibit MEF2. It is again argued that no materials necessary to practice the claimed invention are provided. Again, as noted in the previous response, this is not true. Pages 23-30 provide a detailed explanation of **how** one can achieve inhibition of MEF2 signaling:

Thus, in a particular embodiment of the present invention, there are provided methods for the treatment of cardiac hypertrophy. These methods exploit the inventors' observation, described in detail below, that MEF2 appears to up-regulate the expression of genes involved in the hypertrophic response. At its most basic, this embodiment will function by reducing the *in vivo* activity of MEF2 in individuals suspected of having undergone a hypertrophic response, currently undergoing a hypertrophic response, or in danger of cardiac hypertrophy. This may be accomplished by one of several different mechanisms. First, one may block the expression of the MEF2 protein. Second, one may directly block the function of the MEF2 protein by providing an agent that binds to or inactivates the MEF2 protein. And third, one may indirectly block the effect of MEF2 by interfering with one or more targets of MEF2.

Specification at page 23. The text goes on to describe a variety of materials that can be used to implement each of these embodiments, and how they can be administered. For example, page 24 of the specification states that "[t]he therapeutic compositions of the present invention may be


administered in a manner similar to the administration of current treatments for heart conditions, such as aspirin, nitrates and beta blockers.” Agents such as antisense polynucleotides, ribozymes, organochemical compositions, antibodies that block an active site or binding site on MEF2, or molecules that mimic an MEF2 target are all described, and the examiner cannot simply dismiss these as not valid. Thus, it is untrue that the specification fails to provide information on *how* to achieve the claimed inhibition of MEF2. And while this information may be general in nature, it is commensurate with appellants’ observations – that MEF2 is a target for anti-hypertrophic therapy.

In sum, upon review of the relevant *Wands* factors, the evidence submitted *in favor* of appellants’ position and the dearth of *evidence* supporting the PTO’s position, it is again submitted that the PTO has failed to shift the burden to appellants to defend their presumptively enabling disclosure. *In re Marzocchi*, 439 F.2d 220, 224, 169 USPQ 367, 370 (CCPA 1971). Reversal of the rejection is respectfully requested.

**C. Conclusion**

In light of the foregoing, appellants respectfully submit that all claims are enabled. Therefore, reversal of the rejection is respectfully requested.

Respectfully submitted,



Steven L. Highlander  
Reg. No. 37,642  
Attorney for Appellants

Date: January 12, 2007

## **VIII. CLAIMS APPENDIX**

1. A method of treating hypertrophy in a cardiomyocyte cell comprising the step of inhibiting the function of MEF2.

4. The method of claim 1, wherein said method further comprises inhibiting the upregulation of a gene upregulated by MEF2.

9. The method of claim 4, wherein the agent that inhibits the function of said genes is an antisense construct.

## **IX. EVIDENCE APPENDIX**

Exhibit 1 – Xu *et al.*

Exhibit 2 – Mora & Pessin

Exhibit 3 – Black *et al.*

Exhibit 4 – Declaration of Timothy McKinsey (A)

Exhibit 5 – Declaration of Timothy McKinsey (B)

Exhibit 6 – Zhang *et al.*

Exhibit 7 – McKinsey *et al.*



**X. RELATED PROCEEDINGS APPENDIX**

[NONE]

Transmittal Form to Commissioner for Patents  
January 12, 2007  
Our reference: MYOG:024USC1  
Client reference:

bcc: BethLynn Maxwell, Esq.  
Ray Wheatley, MS  
Madhavi Chander, Ph.D.  
Eric Olson, Ph.D.

# EXHIBIT 1

## MEF2A and MEF2C Induce Dilated Cardiomyopathy in Transgenic Mice\*

Jian Xu<sup>1,2</sup>, Nanling L. Gong<sup>3,5</sup>, Ilona Bodi<sup>6</sup>, Bruce J. Aronow<sup>2</sup>, Peter H. Backx<sup>3,5</sup>, Jeffery D. Molkentin<sup>2</sup>

<sup>1</sup>Department of Pharmacology and <sup>2</sup>Pediatrics, University of Cincinnati, Cincinnati Children's Hospital Medical Center, Cincinnati, OH 45229 USA

<sup>3</sup>Departments of Physiology and Medicine, <sup>4</sup>Heart & Stroke Richard Lewar Centre,

<sup>5</sup>Division of Cardiology, University of Toronto, Toronto Ontario M5S 3E2 Canada

<sup>6</sup>University of Cincinnati, Department of Surgery, Cincinnati OH 45267 USA

Running title: MEF2 Induces Cardiomyopathy

Address Correspondence to: Jeffery D. Molkentin, Division of Molecular Cardiovascular Biology, Cincinnati Children's Hospital Medical Center, 3333 Burnet Ave, Cincinnati, OH 45229. Fax: 513-636-5958. e-mail: [jeff.molkentin@cchmc.org](mailto:jeff.molkentin@cchmc.org)

Cardiac hypertrophy and dilation are mediated by neuro-endocrine factors and/or mitogens, as well as through internal stretch and stress sensitive signaling pathways, which in turn transduce alterations in cardiac gene expression through specific signaling pathways. The transcription factor family known as myocyte enhancer factor 2 (MEF2) has been implicated as a signal-responsive mediator of the cardiac transcriptional program. For example, known hypertrophic signaling pathways that utilize calcineurin, calmodulin-dependent protein kinase, and mitogen-activated protein kinases can each affect MEF2 activity. Here we demonstrate that MEF2 transcription factors induce dilated cardiomyopathy and the lengthening of myocytes. Specifically, multiple transgenic mouse lines with cardiac-specific overexpression of MEF2A or MEF2C presented with cardiomyopathy at baseline, or were predisposed to more fulminant disease following pressure overload stimulation. The cardiomyopathic response associated with MEF2A and MEF2C was not further altered by activated calcineurin, suggesting that MEF2 functions independent of calcineurin in this response. In cultured cardiomyocytes, MEF2A, MEF2C, and MEF2VP16 overexpression induced sarcomeric disorganization and focal elongation. Mechanistically, MEF2A and MEF2C each programmed similar profiles of altered gene expression in the heart that included extracellular matrix remodeling, ion handling, and metabolic genes. Indeed, adenoviral transfection of cultured

cardiomyocytes with MEF2A, or adult myocytes from the hearts of MEF2A transgenic mice, each showed reduced transient outward K<sup>+</sup> currents (I<sub>to</sub>), consistent with the alterations in gene expression observed in transgenic mice and partially suggesting a proximal mechanism underlying MEF2-dependent cardiomyopathy.

Myocyte enhancer factor 2 (MEF2)<sup>1</sup> was originally identified as a muscle-enriched DNA binding activity from differentiated myotubes, although it is now recognized to be widely distributed in most tissues (1). MEF2 DNA binding activity consists of homo- and heterodimers of four separate gene products in mammals, referred to as *Mef2a-d* (2,3). MEF2 dimers bind to the consensus sequence CTA(A/T)<sub>4</sub>TAG present in the 5' transcriptional regulatory regions of most skeletal and cardiac muscle structural genes characterized to date (2,3). In general, *Mef2a-d* genes are widely expressed in the adult vertebrate organism, although a number of specific regulatory functions have been identified in immune, skeletal muscle, cardiac muscle, and neuronal cells (4-7).

MEF2 factors are related to another MADS-box containing transcription factor known as serum response factor (SRF) (8). Similar to SRF, members of the MEF2 family have been implicated in regulating inducible gene expression in response to mitogen and/or stress stimulation. In the heart, myocytes undergo developmental and pathophysiologic hypertrophy in response to neuro-endocrine-, mitogen- and stress-stimulation. Such stimuli activate intracellular signal transduction cascades resulting in the modification of

transcription factor activity and the reprogramming of cardiac gene expression. A number of lines of evidence suggest that MEF2 factors might regulate inducible gene expression in response to stimuli that underlie the cardiac hypertrophic response. For example, MEF2 DNA binding activity in the heart was shown to be up-regulated 2-3 fold by both pressure and volume overload hypertrophy (9). MEF2 DNA binding activity was also shown to be enhanced in myopathic hearts from *mdx:Myod*<sup>-/-</sup> mice (10). *Mef2c* null mice have altered cardiac gene expression and die during early embryonic development with arrested heart tube morphogenesis, suggesting a critical role in developmental growth (7). Mice expressing a dominant negative mutant of MEF2C in the heart also die during postnatal development with attenuated ventricular growth (10). Lastly, a portion of *Mef2a* null mice die suddenly during the perinatal period with dilated right ventricles, myofibrillar disorganization, and mitochondrial structural abnormalities (11).

Hypertrophic stimulation of the adult heart is associated with activation of a number of intracellular signaling pathways including mitogen-activated protein kinase (MAPK), calcineurin, protein kinase C (PKC), calmodulin-dependent protein kinase (CaMK), insulin-like growth factor (IGF-1) pathway constituents, and altered intracellular Ca<sup>2+</sup> handling (12,13). Consistent with the activation of these discrete intracellular signaling pathways, MEF2 factors can be activated by Ca<sup>2+</sup> (14-18), calcineurin (14,19-21), p38 MAPK (5,22-26), big-MAPK-1 (BMK1) (26,27), and CaMK (28). More provocatively, MEF2 factors are also regulated through association with class II histone deacetylases (HDAC) in the nucleus (17,29-31). In fact, Ca<sup>2+</sup> signaling through CaMK was shown to directly regulate MEF2 transcription factors through a mechanism involving phosphorylation of HDAC4/5, resulting in their extrusion from the nucleus, thus permitting MEF2 to activate transcription (17,32-34). As an extension of these studies, MEF2 has also been indirectly implicated as a regulator of cardiac hypertrophy through the observation that *HDAC9* null mice develop exaggerated hypertrophy and have enhanced MEF2 reporter gene activation in

the heart (35). Finally, MEF2 factors have been implicated in regulating cardiac hypertrophy through the use of a MEF2-dependent  $\beta$ -galactosidase reporter transgene (36). MEF2 reporter mice showed enhanced  $\beta$ -galactosidase staining in the hypertrophic hearts of both calcineurin and CaMK transgenic mice (28,35). Despite each of the lines of evidence discussed above, the hypothesis that MEF2 transcription factors promote the cardiac hypertrophic response has yet to be directly evaluated *in vivo*.

Here we generated multiple independent lines of transgenic mice that overexpress either MEF2A or MEF2C specifically in the heart. These lines demonstrated a dosage sensitive induction of dilated cardiomyopathy with a progressive loss in ventricular performance. Moreover, surgical induction of pressure overload hypertrophy produced more fulminant disease in MEF2 transgenic mice. However, crossing MEF2A or MEF2C transgenic mice with transgenic mice expressing activated calcineurin did not enhance hypertrophy, suggesting that MEF2 might function independent of calcineurin-directed hypertrophy in the adult heart. In depth assessment of altered gene expression in the hearts of both MEF2A and MEF2C transgenic mice using Affymetrix™ arrays suggested a number of mechanistic associations with the cardiomyopathic disease response mediated through MEF2.

## MATERIALS AND METHODS

**Animal Models and Procedures** - MEF2A and MEF2C cardiac-specific transgenic mice were generated by fusing the full-length human MEF2A or mouse MEF2C cDNA to the murine  $\alpha$ -myosin heavy chain promoter (37), followed by injection of the DNA into newly fertilized mouse embryos (FVB/N background). Pathological hypertrophy was induced by constriction of the transverse aortic arch, a procedure referred to as transverse aortic constriction (TAC). The aorta was visualized through a median sternotomy and 7-0 silk ligature was tied around it and a 27-gauge wire between the right brachiocephalic and left common carotid arteries, after which the wire was removed to generate a defined constriction (38). Cardiac-specific transgenic mice expressing the activated calcineurin cDNA ( $\Delta$ CnA) were described

previously (39). For echocardiography, mice were anesthetized with 2% isoflurane and hearts were visualized using a Hewlett Packard Sonos 5500 instrument and a 15 MHz transducer. Cardiac ventricular dimensions were measured on M-mode three times for the number of animals indicated.

*Histological Analysis* - Histological analysis of hypertrophy and fibrosis was performed in hearts fixed overnight in 10% phosphate buffered formalin and processed into paraffin blocks for sectioning. Serial 5  $\mu$ m sections were cut and stained with H&E, Masson's trichrome, or wheat germ agglutinin-tetramethylrhodamine

isothiocyanate (TRITC) conjugate (50  $\mu$ g/ml) to visualize cellular membranes for measuring myocytes cross-sectional areas (at least 100 cells per heart were measured from 4 independent mice). *Dot Blotting and RT-PCR* - Dot blotting and RT-PCR to quantify mRNA levels were performed as previously described (40). Primers employed in the RT-PCR analyses are listed in Supplemental Table 1.

*Western Blotting and Immunocytochemistry* - Western blotting and immunocytochemistry were performed as previously described (40,41). The following antibodies were used: MEF2C rabbit polyclonal Ab (Cell Signaling, 1:500), MEF2A rabbit polyclonal Ab (Santa Cruz, 1:1000), glyceraldehyde 3-phosphate dehydrogenase (GAPDH) mAb (Research Diagnostics, 1:5000),  $\alpha$ -actinin mAb (Sigma, 1:300),  $\alpha$ -tubulin mAb (Santa Cruz, 1:200), myosin mAb (Sigma, 1:250), FAK (Upstate Biotechnologies, 1:400), phospho-Try397-FAK (Upstate Biotechnologies, 1:400).

*Cardiomyocyte Cultures and Recombinant Adenovirus* - All *in vitro* experiments were performed in neonatal ventricular myocytes isolated from 1-2 day old rats as previously described (40). cDNAs encoding MEF2A (human), MEF2B (mouse), MEF2C (mouse), MEF2D (mouse), MEF2C (amino acids 1-143) fused to the VP16 (MEF2VP16) transcriptional activation domain, and dominant negative R3T-MEF2C mutant was used to generate recombinant adenovirus. These cDNAs were subcloned into the pShuttle vector for the Adeno-X system (BD BioSciences, Clontech) to generate replication-deficient adenoviruses. A MEF2

containing adenovirus, Ad $\beta$ gal (control), or AdGFP (control) were used to infect cultured cardiomyocytes at an approximate multiplicity of infection of 50 for a period of 2 hrs, followed by analysis 24, 36, or 48 hrs afterwards (40). Under these conditions greater than 98% of the cells showed expression of the viral gene insert. Assessment of cultured rat neonatal cardiomyocyte cell surface area (hypertrophy) was performed as previously described (from at least 200 cells in three separate experiments each) (42).

*Affymetrix gene expression profiling and bioinformatics* - Total RNA samples were prepared from individual high expressing MEF2A transgenic hearts at 2 weeks of age and compared with 2 wildtype hearts at 2 weeks of age. Alternatively, a separate array was performed on cardiac RNA collected from line 2 MEF2C transgenic mice and wildtype controls at 4 weeks of age. Biotin-labeled target cRNA was prepared from T7-transcribed cDNA made from 10  $\mu$ g of the total RNA using the Affymetrix-recommended protocol (43,44) and hybridized for expression analysis to the Affymetrix U74Av2 GeneChip using antibody-based fluorescence signal amplification. GeneChips were scanned in the Affymetrix 425S scanner using Affymetrix MicroArray Suite version 5.0. Intensity data was scaled to a target of 1500 and the results were analyzed using both MicroArray Suite 5.0 and GeneSpring 5.0.3 (Silicon Genetics, Inc., Redwood City, CA). Data values used for filtering and clustering were "Signal", "Signal Confidence", "Absolute Call" (Absent/Present), and "Change" (Increase, Decrease, Unchanged) as implemented in MicroArray Suite 5.0. Data were normalized as follows: the 50th percentile of all measurements was used as a positive control for each array. Measurements for each gene was divided by this synthetic positive control, assuming that this was at least 10. The bottom tenth percentile signal level was used as a test for correct background subtraction. The measurement for each gene in each sample was divided by the average of the corresponding value in the two wildtype samples, assuming that the value was at least 1.0. Genes regulated consistently between the replicates were identified by data filtering using a Student's T-test  $p < 0.01$  among genes that were called "Present" in

the MEF2 transgenic samples. Gene category information was based on all publicly available gene ontology information from the Gene Ontology consortium (<http://www.geneontology.org/>) as harvested from SwissProt, GeneCards, Compugen, Locus Link, and GenBank as well as exhaustive Medline literature searches.

*Electrophysiological Recordings in Neonatal Cardiomyocytes* - Neonatal rat cardiomyocytes were isolated and cultured as described previously (45). For patch-clamp recording experiments,  $1.5 \times 10^5$  myocytes were plated on laminin-coated coverslips in 35-mm culture dishes. After 24 hours in culture, the medium was replaced by serum-free medium and virus infections were performed (10 multiplicity of infection for AdGFP and AdMEF2A). Typically, more than 95% of the myocytes showed AdGFP expression 36 hours after infection. Whole-cell voltage-clamp recordings were done as described previously (45,46) at room temperature to measure transient outward ( $I_{to}$ ) and inward rectifier (IK1)  $K^+$  currents, at least 36 hours after serum withdrawal and infection with AdMEF2A. Myocytes were perfused for at least 15 minutes before measurements were performed with a solution containing (in mmol/L): NaCl 140, KCl 4,  $CaCl_2$  2,  $MgCl_2$  1,  $CdCl_2$  0.5, HEPES 10, and glucose 10, pH 7.4. The intracellular solution contained (in mmol/L) KCl 140,  $MgCl_2$  1, EGTA 10, HEPES 10, and MgATP 5, pH 7.25. Whole-cell currents were filtered at 2 kHz (Axon 200A amplifier; Axon Instruments, Inc).

*Electrophysiological Recordings in Adult Cardiomyocytes From Whole Hearts* - Single ventricular myocytes were obtained from both ventricles of adult mice (3 month old) of both sexes. The cell isolation technique used in these experiments has been previously described (47). All current recordings were obtained in the whole-cell, voltage-clamp configuration of the patch clamp technique by using 1.60 OD borosilicate glass electrodes (Garner Glass Company). Cell capacitance was measured using voltage ramps of 1V/sec from a holding potential of 0 mV. Series resistance was within the range of 2 to 11 M $\Omega$ . Most of the data presented in these studies were obtained with electrodes having a resistance of 0.5-

3 M $\Omega$ . Whole cell  $Ca^{2+}$ -independent transient outward  $K^+$  currents ( $I_{to}$ ) were evoked by a series of depolarizing voltage steps (680 ms) from -40 mV to +80 mV in 10 mV increments from a holding potential of -40 mV at a frequency of 0.5 Hz. Ventricular cardiomyocytes were perfused with normal Tyrode solution containing (in mmol/l): NaCl 138, KCl 4,  $CaCl_2$  2,  $MgCl_2$  1, glucose 10, HEPES 10,  $NaH_2PO_4$  0.33, adjusted to pH 7.4 with NaOH.  $I_{Ca}$  was largely eliminated by 0.3 mM  $CdCl_2$  included in the recording solution. The pipette solution contained (in mmol/l): Potassium-glutamate 120, KCl 10,  $MgCl_2$  2, HEPES 10, EGTA 5 and Mg-ATP 2, pH 7.2 with KOH. Cell capacitance was estimated by integrating the area under an uncompensated capacity transient elicited by a 25 mV hyperpolarizing test pulse (25 ms) from a holding potential of 0 mV.  $I_{to}$  was defined as the difference between the peak transient current and the steady state current at the end of a 500 ms voltage clamp pulse. All experiments were carried out at room temperature (20-22°C). Whole cell currents were analyzed with Clampfit 6.03 software (Axon Instruments). Pooled data are expressed as means $\pm$ SE. All current amplitudes were normalized to the cell capacitance and expressed as densities (pA/pF).

*Measurement of Adult Cardiomyocyte length and Width* - Wildtype and MEF2A transgenic adult mouse hearts (2 months age) were dissected, washed in ice-cold cannulation buffer (10 mM 2,3-butanedione monoxime, 25  $\mu$ M  $CaCl_2$  in MEM) and perfused with digestion media (1 mg/ml BSA, 90 units/ml collagenase, 10 mM 2,3-butanedione monoxime, 25  $\mu$ M  $CaCl_2$  in MEM) until the myocardium began to visually dissolve. Perfused hearts were flushed with digestion media, dissociated and filtered through a 200  $\mu$ M mesh into MEM containing 10 mM 2,3-butanedione monoxime and 10  $\mu$ M  $CaCl_2$ . Cells were collected by centrifugation and resuspended in 4% paraformaldehyde for fixation. Isolated cardiomyocytes were photographed and length and width were measured with NIH image software from approximately 200 cells from each mouse, from which length/width ratios were calculated.

*Statistical Analysis*--- Data are expressed as means ( $\pm$  SEM). Differences between experimental groups were evaluated for statistical significance

using Student's *t* test, one-way ANOVA or two-way ANOVA. *P* values < 0.050 were considered to be statistically significant.

## RESULTS

**Characterization of MEF2A and MEF2C transgenic mice** - While a number of reports have suggested a role for MEF2 in regulating the hypertrophic growth of the adult myocardium, it has yet to be formally evaluated. To directly investigate the ability of MEF2 to induce the cardiac hypertrophic response we generated a series of cardiac-specific transgenic mice using the  $\alpha$ -myosin heavy chain promoter. cDNAs encoding MEF2A and MEF2C were selected for overexpression since they were proposed to be the predominant MEF2 isoforms expressed in the post-natal mouse heart (10). Three individual MEF2A lines were initially generated and characterized by 1.9- 3.5- and 4.2-fold more MEF2A protein in the heart when normalized to GAPDH (Fig 1A). Overexpression of MEF2A resulted in three different migrating species of MEF2A that collapsed upon calf intestinal alkaline phosphatase treatment, suggesting different phosphorylation isoforms (data not shown). The highest expressing line demonstrated neonatal lethality between 2-4 weeks of age with significant elevations in heart-weight normalized to body-weight, while the low and medium expressing MEF2A transgenic lines showed no lethality and had normal heart weights up to three months of age (Fig 1B). High expressing MEF2A transgenic mice showed severe impairment in ventricular performance at 3 weeks of age as assessed by echocardiography (Fig 1C). Low expressing MEF2A transgenic mice had essentially normal ventricular performance (data not shown), while medium expressing transgenic mice showed a functional deficit at two and three months of age, as well as ventricular chamber dilation (Fig 1C, Table 1). It is interesting to note that medium expressing MEF2A transgenic mice show dramatic reductions in cardiac functional performance and dilation before increases in heart weight are present, suggesting that any manifestation or propensity towards heart weight increase could be secondary to the reduction in ventricular function. High expressing MEF2A

transgenic mice at 3 weeks of age also manifested a severe reduction in fractional shortening and dramatic dilation of the left ventricles (Table 1). Associated with this dosage-dependent profile of cardiomyopathy, high expressing transgenic mice showed increased expression of hypertrophy/stress-associated genes such as atrial natriuretic factor (ANF) and skeletal  $\alpha$ -actin at 3 weeks of age (Fig 1D). Medium-expressing transgenic mice also eventually showed increased expression of these stress marker genes as they aged and developed hypertrophy as a secondary consequence of reduced functional performance (data not shown).

Low and medium expressing lines had normal heart weights up to three months of age, despite a progressive deterioration in ventricular performance. To more carefully evaluate the hypertrophic program associated with MEF2A-mediated cardiomyopathy, eight-week old low- and medium-expressing transgenic mice were subjected to TAC for two weeks to induce cardiac pressure overload. Wildtype mice showed a 33% increase in heart weight normalized to tibia length, while low and medium expressing MEF2A transgenic mice showed a 44% and 91% increase, respectively ( $P < 0.05$ ) (Fig 2A). Moreover, medium expressing MEF2A transgenic mice showed significantly greater pulmonary congestion measured by lung-weight to tibia length ( $P < 0.05$ ) (Fig 2B), greater cellular hypertrophy in the heart measured by direct assessment of myofiber diameters ( $P < 0.05$ ) (Fig 2C), and greater decompensation in ventricular performance as assessed by echocardiography ( $P < 0.05$ ) (Fig 2D). Histological assessment also demonstrated greater cardiac enlargement and ventricular wall dilation in MEF2A medium expressing transgenic mice compared with wildtype controls (Fig 2E). Echocardiography showed a greater dilation in left ventricular chamber dimension in both systole and diastole (data not shown). Echocardiographic data were also used to examine left ventricular wall and septal thickness versus left ventricular chamber radius, referred to as the H/R ratio (Fig 2F). Medium expressing transgenic mice have a smaller ratio at baseline (sham) compared with wildtype and low expressing mice (Fig 2F). Pressure overload for two weeks lead to an increase in the H/R ratio in wildtype and low expressing



transgenic mice, suggesting concentric hypertrophy, yet the medium expressing mice did not, and even showed a relative reduction in the ratio, showing more dilation (Fig 2F). Thus, increased myocardial MEF2A expression predisposed the myocardium to greater functional decompensation and dilation. However, the increase in heart weight associated with MEF2A-dependent cardiomyopathy following TAC stimulation may or may not be a direct effect (see discussion).

Three independent MEF2C expressing transgenic lines were also initially generated, although one died before breeding age with a severely compromised heart, and one died during pregnancy with ventricular dilation (Fig 3A, lines 1 and 3 died). The only viable remaining line (line 2) showed only 1.6-fold overexpression of MEF2C in the heart by western blotting (Fig 3B), suggesting that MEF2C overexpression is not well tolerated, similar to the lethality observed in MEF2A transgenic mice with 4.2-fold overexpression. Indeed, MEF2C transgenic mice presented with a similar cardiomyopathic phenotype as characterized in MEF2A transgenic mice. Specifically, MEF2C transgenic mice first showed a progressive baseline decrease in fractional shortening and ventricular chamber dilation, followed thereafter by an increase in ventricular-weight normalized to body-weight or tibia length (Fig 3C,D, Table 2). Induction of hypertrophy/stress-associated marker genes such as ANF, b-type natriuretic peptide (BNP),  $\beta$ -myosin heavy chain, and skeletal  $\alpha$ -actin was also observed at one-month of age (Fig 3E). Ventricular-weight or tibia lengths were used to assess hypertrophy over total heart weight (as used in MEF2A transgenic mice) because MEF2C transgenic mice had large atrial clots, consistent with a heart failure phenotype and poor ventricular function (Fig 3A). MEF2C transgenic mice were also subjected to TAC stimulation to assess enhancement in hypertrophic enlargement as described in MEF2A transgenic mice. However such attempts failed due to extreme lethality in MEF2C mice at only 1-3 days following pressure overload stimulation, consistent with the hypothesis that MEF2C overexpression induces

fulminant cardiomyopathy that renders the mice intolerant to additional insults (data not shown). In conclusion, MEF2A and MEF2C each appear to induce a similar profile of cardiomyopathy in the mouse heart, with a functional deficit significantly preceding hypertrophic enlargement.

***MEF2A and MEF2C do not phenotypically interact with calcineurin in the heart***

- A number of reports have suggested that calcineurin can directly activate MEF2 transcriptional and/or DNA binding activity (14,19-21). To evaluate the potential importance of calcineurin as an upstream activator of MEF2-induced cardiac hypertrophy, MEF2A and MEF2C transgenic mice were both crossed with transgenic mice expressing activated calcineurin (39). Previously, the degree of cardiac hypertrophy induced by the same activated calcineurin transgene was shown to be dramatically enhanced by intercrossing into the *HDAC9*-/- genetic background (35). However, the degree of cardiac hypertrophy induced by activated calcineurin was not increased in either MEF2A or MEF2C transgenic mice at 7 and 9 weeks of age as assessed by gravimetry and echocardiography (Fig 4A-C), nor were myocyte cellular areas increased more than that seen with just the activated calcineurin transgene (data not shown). VW/BW was measured in MEF2C crossed mice given large atrial clots not seen in MEF2A transgenic mice. The relative degree of functional decompensation associated with the MEF2C transgene was not enhanced by the presence of the activated calcineurin transgene (Fig 4D). Thus, on a phenotypic level, calcineurin does not overtly function upstream of MEF2A or MEF2C in regulating the hypertrophic or myopathic response of the heart.

***Phenotypic assessment of MEF2 overexpression in cultured cardiomyocytes and adult hearts***

- To further investigate the potential mechanisms whereby MEF2A or MEF2C overexpression might induce dilated cardiomyopathy in transgenic mice, a reductionist approach was employed in cultured neonatal rat cardiomyocytes using recombinant adenoviruses for MEF2A, MEF2B, MEF2C, MEF2D, and MEF2VP16. We first investigated if MEF2A, MEF2C, or MEF2VP16 overexpression

alone would induce hypertrophy over 24 or 48 hrs. However, none of the MEF2 recombinant adenoviruses used here induced substantial cardiomyocyte hypertrophy, while control experiments with adenoviruses expressing activated MAKP kinase 6 (MKK6), GATA4, activated calcineurin, or SRF showed pronounced hypertrophy (data not shown). Moreover, neither AdMKK6 nor Ad $\Delta$ CnA showed greater hypertrophy when co-infected with AdMEF2A, AdMEF2C, or AdMEF2VP16, supporting the contention that MEF2 does not function downstream of calcineurin in regulating cardiomyocyte hypertrophy, and further questioning whether it functions downstream of p38 in this capacity (Data not shown). Taken together, these data suggest that neither MEF2A nor MEF2C directly regulate the cardiac hypertrophic response, but that the minor hypertrophy observed in MEF2A and MEF2C transgenic mice could result as a secondary consequence of the reduction in ventricular function associated with other more proximal alterations in gene expression (see discussion).

While MEF2 overexpression did not promote cardiac hypertrophy in cultured neonatal myocytes, a very prominent degeneration in sarcomeric organization and focal elongation was observed due to MEF2A, MEF2B, MEF2C, MEF2D, and MEF2VP16 overexpression (Fig 5, and data not shown). Specifically, MEF2 overexpression induced profound disorganization in the sarcomeric proteins myosin heavy chain and  $\alpha$ -actinin (Fig 5). In contrast, staining of intermediate filaments with antibody against  $\alpha$ -tubulin showed normal intracellular architecture, suggesting a degree of specificity for alterations in sarcomeric proteins (Fig 5). Such disorganization in sarcomeres could be due to a specific function of MEF2 in regulating the expression of a subset of sarcomeric genes, or due to other specific alterations in gene expression that secondarily lead to sarcomeric disorganization, such as associated with dilation (see discussion). Indeed, MEF2A, MEF2C, and MEF2VP16 overexpression produced a remarkable phenotype of elongation or focal projections in 2 or more axis, which was not observed with SRF overexpression (Fig 5). This

phenotype of elongation and sarcomeric disorganization due to MEF2 overexpression in culture is consistent with the observed dilation that occurs in MEF2A and MEF2C transgenic mice.

To further examine the affect of MEF2 overexpression on myocyte architecture and reorganization the phosphorylation status of focal adhesion kinase (FAK) at Tyr397 was examined, given that stretching and changes in adhesion characteristics of myocytes often lead to activation of FAK. Indeed, AdMEF2A infected neonatal myocytes showed an approximate 2-fold increase in FAK phosphorylation, while AdMEF2C myocytes showed a 50% increase, without a change in total FAK protein (Fig 6A). Consistent with this phenotype of altered adhesion and extracellular matrix effects, AdMEF2A and AdMEF2C infected myocytes also showed a dramatic increase in type-X collagen expression (Fig 6B). Finally, myocytes from 2 month-old wildtype and MEF2A (medium) transgenic mice were isolated, fixed, and measured for length and width (Fig 6C). Myocytes from transgenic hearts showed a significant increase in their length/width ratios, suggesting one mechanism whereby dilation occurs in these hearts, although changes in the extracellular matrix and myocyte attachment could also be important factors in mediating the observed cardiomyopathic phenotype.

**Global assessment of altered gene expression in MEF2A and MEF2C hearts** - While MEF2A and MEF2C overexpression induced cardiomyopathy, the potential downstream transcriptional targets or pathways that mediate this phenotype are unknown. Here we generated RNA from the hearts of two wildtype and two MEF2C transgenic mice (line 2) at 4 weeks of age, as well as two wildtype and two MEF2A high expressing transgenic mice at 2 weeks of age for analysis of total gene expression alterations using the Affymetrix<sup>TM</sup> mouse chip set U74v2 containing 36,000 genes. Approximately 1.2 and 1.8% of all genes were altered in expression by 2-fold or more in MEF2C and MEF2A transgenic hearts, respectively. However, we were most interested in profiles of genes that might suggest common pathway alterations due to MEF2 overexpression. Three unique sub-sets of genes were observed as being

altered in MEF2 transgenic hearts, including genes involved in the extracellular matrix and remodeling (Supplemental Table 2), genes involved in ion handling (Supplemental Table 3), and genes involved in metabolism (Supplemental Table 4). Since the microarray analyses with MEF2A and MEF2C transgenic mice were performed at different ages (2 versus 4 weeks), the data are not listed together. These early time points were selected for RNA analysis since they precede fulminant heart disease and might suggest more proximal mechanisms.

The first subset of gene alterations included proteins involved in the extracellular matrix or its regulation. The most interesting of these genes were selected for confirmation by RT-PCR, including  $\beta$ 5-integrin,  $\alpha$ 5-integrin, biglycan, lumican, periostin, matrix G1a protein (MGP), connective tissue growth factor (CTGF), and fibulin, all of which were each significantly up-regulated in the hearts of MEF2C transgenic mice (Fig 7A). Most of these gene alterations were also observed in MEF2A transgenic hearts (data not shown). These alterations in extracellular matrix associated genes and cell attachment genes are especially interesting as they suggest a role in ventricular dilation and remodeling.

A significant subset of metabolic genes were also significantly altered in both MEF2A and MEF2C transgenic heart, consistent with a previous assertion that MEF2 can regulate or participate in controlling the expression of genes involved in mitochondria energy production and general metabolism (11,20,21). However, cardiomyopathy in general is known to be associated with similar alterations in metabolic genes, as observed here, characterized by decreased expression of fatty acid-related metabolic genes and increased expression of glycolytic genes (see discussion).

Finally, a unique profile of altered ion handling genes was also identified in MEF2A and MEF2C transgenic hearts. Specifically, high expressing MEF2A transgenic mice showed increased expression of genes such as *Pkd2l2*, *Kcnd2*, *Kcnk3*, *Kcnj3*, *Kcnk2*, *Kcnj4*, *Mg29*, and many others (Supplemental Table 3). Many of these same genes were also significantly altered in

MEF2C transgenic mice. For example, *Kcnd2*, *Kcnk3*, and *Cacna2d2* were down-regulated 3.6, 1.9, and 2.1 fold in MEF2C hearts, respectively, and *Kcnk1* and *Fxyd6* were up-regulated 2.6 and 2.0 fold, respectively. The MEF2A array data was confirmed by RT-PCR from low, medium and high expressing MEF2A transgenic mice (Fig 7B). In all cases, RT-PCR from high expressing MEF2A transgenic mice confirmed the array data. However, only some of these changes were observed in medium expressing MEF2A transgenic mice, while no alterations were observed in the low expressing MEF2A transgenic mice (Fig 7B). Such alterations in ion handling genes is especially interesting given that *Mef2a* null mice die from sudden death, suggesting predisposition to arrhythmia (11) (see discussion).

To explore the potential biologic relevance of one of the three gene profiles described above, an assessment of correlative ionic currents was performed in cultured cardiomyocytes infected with AdMEF2A + AdGFP (green fluorescent protein), or AdGFP alone as a control. Whole cell voltage clamp recordings were performed at room temperature (see methods). While no significant changes in inward rectifying currents was observed (data not shown), MEF2A overexpressing myocytes displayed a very prominent reduction in transient outward  $K^+$  current (Fig 8A,B). Consistent with the adenoviral overexpression data in neonatal cardiomyocytes, adult myocytes isolated from MEF2A transgenic mice showed a nearly identical profile of reduced transient outward  $K^+$  current ( $P < 0.05$ ) (Fig 8C). This reduction in  $I_o$  is consistent with the pronounced decrease in *Kcnd2* gene expression (Fig 7B), which is the predominant pore-forming alpha-subunit of the transient outward current in rodent cardiomyocytes. Alterations in *Kv4.2* gene expression and  $I_o$  current has been shown to modulate the cardiac action potential profile and calcium entry and promote cardiac hypertrophy/myopathy (see discussion). In conclusion, these data suggest at least one regulatory paradigm whereby MEF2 regulates expression of a subset of genes that has a direct influence on cardiomyocyte physiology and the potential to induce a cardiomyopathic phenotype *in vivo*.

## DISCUSSION

### *Evidence for MEF2 as a Hypertrophic Mediator -*

Here we presented the first experimental evidence that MEF2 transcription factors are capable of inducing cardiomyopathy *in vivo*. While previous lines of evidence have indirectly suggested a potential role for MEF2 factors in regulating cardiac hypertrophy, they did not directly address the ability of MEF2 to program such a response. An inference to MEF2 as a hypertrophic mediator can also be made based on known similarities between SRF and MEF2, both of which are MADS box-containing DNA binding factors that respond to stress, developmental, and mitogen stimulation. Transgenic mice overexpressing SRF in the mouse heart were previously shown to have a phenotype of hypertrophic cardiomyopathy, reminiscent of MEF2A and MEF2C transgenic mice (48). Interesting, overexpression of SRF in cultured neonatal cardiomyocytes induced a phenotype that was reminiscent of hypertrophy, including increased sarcomeric organization and increased cell surface area, yet MEF2 overexpression did not (Fig 5).

MEF2A and MEF2C are also directly phosphorylated by p38 MAPK, resulting in enhanced transcriptional activity (5,22-26). Furthermore, a p38-docking domain was recently identified in MEF2A, MEF2C, and MEF2D that was necessary for efficient p38-mediated phosphorylation (24). These studies suggested a role for MEF2 in regulating cardiac hypertrophy given the data that p38 itself is a modulator of this response (49). However, while p38 prominently regulates the hypertrophic growth of neonatal cardiomyocytes in culture, recent studies in transgenic and gene-targeted mouse models suggest that this kinase is not a positive mediator of the hypertrophic response and may, in fact, even inhibit it in some studies (50-52). Thus, MEF2 is unlikely to function as a hypertrophic mediator downstream of signals (phosphorylation) from p38, consistent with the inability of AdMKK6 to generate enhanced hypertrophic growth when co-infected with AdMEF2A or AdMEF2C (data not shown). However, chronic activation of p38 in the hearts of transgenic mice results in profound myopathy and dilation, suggesting that MEF2

could mediate pathologic responses downstream of p38 in the heart, such as dilation (53).

Ca<sup>2+</sup> acting through the Ca<sup>2+</sup>-sensitive phosphatase calcineurin can also activate MEF2 transcriptional and/or DNA binding activity, possibly through direct dephosphorylation (14,19-21). For example, MEF2 reporter transgenic mice showed enhanced activity in the extensor digitorum longus when crossed with transgenic mice expressing activated calcineurin in their skeletal muscle (19). The expression of the MEF2-lacZ reporter was also reduced with the calcineurin inhibitor cyclosporine A or a transgene expressing the calcineurin regulatory protein known as modulatory calcineurin interacting protein (MCIP), collectively suggesting that calcineurin regulates the MEF2-lacZ reporter transgene in skeletal muscle (54). However, these results depend on the specificity of the MEF2-dependent reporter, which utilized concatamers of an AT-rich element from the desmin regulatory region placed upstream of a minimal heat shock promoter (36). Interestingly, this AT-rich element can also bind the muscle enriched transcription enhancer factor 1 (TEF-1) family of DNA binding proteins (55). TEF-1 was also shown to directly mediate hypertrophy responsive gene expression in cardiac myocytes (56). Thus, the conclusion that calcineurin dominantly functions upstream of MEF2 in striated muscle requires further investigation. We did not observe an increase in cardiac hypertrophy or the degree of functional decompensation between MEF2A and MEF2C transgenic mice crossed with activated calcineurin transgenic mice. In contrast, a synergistic increase in hypertrophy was observed when calcineurin transgenic mice were crossed with mice lacking *HDAC9*, suggesting that the degree of calcineurin-regulated hypertrophy could still be dramatically augmented with a specific pathway interaction (35). In conclusion, while calcineurin is known to function as a potent regulator of the cardiac hypertrophic response, partially through activation of nuclear factor of activated T-cell (NFAT) transcription factors (39), MEF2 is unlikely to be a significant downstream hypertrophic effector of calcineurin in the heart, although it could still participate in maladaptive responses downstream of calcineurin.

More recently, MEF2 factors have been indirectly implicated in mediating cardiac hypertrophy through their interaction with class II HDAC transcriptional repressors (17,29-31). Olson and colleagues demonstrated a fundamental paradigm whereby class II HDACs shuttle between the cytoplasm and nucleus in a signal-dependent manner to regulate the transcriptional activity of MEF2 factors (17,32-35). The extrusion of HDAC4/5 from the nucleus, which permits MEF2 transcriptional activity, is mediated by direct phosphorylation of HDAC4/5 through CaMK, PKC, and protein kinase D (PKD) (17,32-34,57). Given this paradigm, loss of specific class II HDACs should activate MEF2, potentially leading to cardiac hypertrophy. Indeed, *HDAC9* null mice develop exaggerated hypertrophy following pressure overload or when crossed with the calcineurin transgene (35). However, class II HDACs interact with a large array of transcription factors other than MEF2. For example, we have observed an indirect interaction between class II HDACs and NFAT transcription factors, suggesting a role as downstream effector of HDAC (58). Despite the likelihood that HDACs function through other transcription factors to control hypertrophy, it is also possible that MEF2 overexpression is without a primary influence on hypertrophy because it is completely inhibited by endogenous class II HDACs. However, the ability of MEF2 to promote cardiomyopathy and dilation would then have to be independent of HDAC regulation.

Loss-of-function approaches have also suggested a role for MEF2 in regulating cardiac hypertrophy/cardiomyopathy. For example, mice expressing a dominant negative mutant of MEF2C in the heart using the  $\alpha$ -myosin heavy chain promoter die during postnatal development, presumably due to a phenotype of ventricular dilation and attenuated ventricular growth (10). These results suggest that MEF2 transcriptional activity is required for postnatal maturation of the heart, also referred to as developmental hypertrophy, but do not address the role of MEF2 in mediating the pathologic hypertrophic response of the adult myocardium. Another point to consider is that *Mef2a* null mice die suddenly during the perinatal period with dilated right

ventricles, myofibrillar disorganization, and mitochondrial structural abnormalities, consistent with the hypothesis that MEF2 activity is necessary for efficient developmental hypertrophy (11).

The data presented here show a dosage-dependent cardiomyopathic phenotype and a progressive reduction in ventricular performance associated with MEF2A or MEF2C overexpression in the heart. Such reductions in cardiac function can promote a secondary neuro-endocrine stimulated hypertrophy as the heart attempts to compensate. Such an indirect influence could also enhance TAC-induced cardiac hypertrophy, as observed here. Thus, some increase in heart weight could result as a secondary consequence of decreased ventricular performance that leads to a secondary neuro-endocrine driven response, while the remaining increase in heart weight could result from dilation itself and the addition of sarcomeres in series. For example, myocytes from MEF2A transgenic mice were noticeably altered in their length/width ratios, consistent with a dilated phenotype or an addition of sarcomeres in series (and a loss of cross-sectional area). Addition of sarcomeres in series can lead to overall increases in heart weight, thus being suggestive of hypertrophy at the whole organ level, although at the cellular level MEF2A does not appear to regulate the more classically defined index of hypertrophy associated with increased cross-sectional area. Indeed, MEF2 overexpression in cultured neonatal cardiomyocytes did not promote definitive hypertrophy. However, MEF2 overexpression in neonatal myocytes did promote noticeable sarcomeric disorganization and focal elongation, consistent with its ability to induce dilated cardiomyopathy with compromised ventricular performance *in vivo* (see below).

The phenotype of MEF2 overexpressing transgenic mice and adenoviral infected neonatal cardiomyocytes is reminiscent of transgenic mice expressing an activated MEK5 mutant in the heart or in adenoviral infected myocytes (59). Interesting, MEF2 is directly phosphorylated by BMK1, which is directly activated by MEK5 (26,27). Expression of activated MEK5 induced elongation of cardiac myocytes in culture, while activated MEK5 transgenic mice showed addition of sarcomeres in series with a loss in myocyte

cross-sectional area (59). Activated MEK5 transgenic mice also showed profound ventricular dilation, reduced fractional shortening, and activation of hypertrophic gene expression. This overall phenotype is remarkably similar in nearly every respect to our observations in MEF2A/C transgenic mice and adMEF2A/C infected neonatal myocytes, which is particularly relevant given the known ability of MEK5-BMK1 to directly activate MEF2 by phosphorylation (26,27).

A final issue that should be discussed relates to the relevance of MEF2 overexpression as a means to understanding its functional role. The degree of MEF2A or MEF2C protein overexpression that produced viable lines was rather mild and arguably within a "physiologic" range, suggesting that the observed cardiomyopathic phenotype was not due to grossly unspecific effects associated with massive overexpression.

**Non-Hypertrophic Functions of MEF2** - MEF2 has been implicated as a mediator of apoptosis in a cell-type dependent manner. For example, MEF2 has been implicated as a necessary regulator of cell death in T lymphocytes, or T cell hybridomas in response to calcium signals (15,60). In contrast, enhanced MEF2 activity is associated with the survival of cultured primary neurons or neuronal-like cell lines (61-64). For example, inhibition of MEF2 in neuronal cultures with a dominant negative mutant of MEF2 or with specific kinases that inactivate MEF2, enhanced cell death (62-64). Here we also investigated the ability of MEF2 to alter cell death of neonatal cardiomyocytes in culture to determine if it functioned in a pro-survival or pro-apoptotic manner. Cardiomyocytes were infected with recombinant adenoviruses encoding MEF2A, MEF2B, MEF2C, MEF2D or a dominant negative MEF2C mutant (R3T). While overexpression of wildtype MEF2A-D had no effect on baseline DNA laddering, expression of a dominant negative MEF2C mutant increased DNA laddering, suggesting that MEF2 activity was protective against apoptosis in cardiomyocytes similar to neurons (data not shown).

MEF2 was originally named myocyte-specific enhancer binding factor-2, based on its

induction in differentiated skeletal muscle cells and based on its ability to regulate expression of numerous muscle-specific genes. Indeed, MEF2 binding sites have been identified within the promoters of most skeletal and cardiac muscle expressed structural genes examined to date (2,3). Moreover, loss of *Mef2c* in gene-targeted mice resulted in a loss or downregulation in multiple cardiac structural genes in the developing heart (7). Thus, MEF2 has been proposed to function as a mediator of contractile gene expression in striated muscle. This assertion is indirectly supported by our analysis of MEF2 overexpression in cultured cardiomyocytes, where sarcomeric disorganization was prominent (Fig 5). Such alterations in sarcomeric organization could be attributed to mismatches in gene expression for structural and sarcomeric proteins, which would further promote cardiomyopathy *in vivo*. While this hypothesis is attractive, it is unlikely since few consistent alterations were observed in the expression levels of structural and sarcomeric genes in MEF2A or MEF2C mice, or even in adenoviral infected neonatal cardiomyocytes overexpressing very high levels of MEF2C also subjected to array analysis (data not shown). Thus, MEF2A and MEF2C do not appear to induce cardiomyopathy or sarcomeric disorganization through a mechanism involving direct imbalances in expression of sarcomeric genes. However, these results do not mean that loss of MEF2 activity has no impact on expression of cardiac structural genes, as previously described.

In contrast to the lack of alterations in structural genes associated with increased MEF2 activity in cardiomyocytes, MEF2 overexpression promoted dramatic alterations in a subset of genes encoding ion handling proteins, or genes that indirectly modulate ion handling. One of these genes, *Kcnd2*, encodes a pore-forming Kv4.2 alpha-subunit of the cardiac  $I_{to}$  and thereby controls  $I_{to}$  density in the rodent myocardium (65). The physiological significance of this observed MEF2-dependent alteration in *Kcnd2* expression was verified by patch clamping in cultured cardiomyocytes following acute AdMEF2A infection, and in adult myocytes isolated from MEF2A transgenic mice. Reductions in  $I_{to}$  current density are the major cause for action potential duration prolongation (65) in heart disease and

have been linked to elevated  $\text{Ca}^{2+}$  entry through L-type  $\text{Ca}^{2+}$  channels, enhanced contractility and promotion of cardiac hypertrophy via calcineurin-dependent pathways, as well as delayed repolarization affecting the synchrony of inward  $\text{Ca}^{2+}$  fluxing (66). Since MEF2 is itself directly regulated by  $\text{Ca}^{2+}$  concentration, the observed effects of MEF2 on  $I_{\text{to}}$  suggests a complex and dynamic feedback network for the regulation of cardiac function (electrical and contractile properties), hypertrophy and altered gene expression. It is also interesting to note that CaMK has been shown to also regulate  $I_{\text{to}}$  in atrial cardiac myocytes (67), especially interesting given the known relationship whereby CaMK can regulate MEF2 activity through HDAC4/5 nuclear extrusion (33,34).

That MEF2 factors might specifically regulate a subset of ion handling genes is supported by the observation that MEF2 proteins are most prominently expressed in excitable tissues, such as heart, skeletal muscle, and brain. Indeed, *Mef2a* deletion promoted a phenotype of sudden death and cardiomyopathy in mice (11). However, hearts from *Mef2a* null mice were reported to have no alterations in expression of the arrhythmia promoting genes *KVLQT1*, *minK*, *MERG*, and *SCN5A* (11). None of these same genes were altered in our MEF2A or MEF2C overexpressing hearts either, excluding this specific subset of ion handling genes (Supplemental Table 3). Thus, a more selected subset of genes likely contributes to the cardiomyopathic phenotype observed in MEF2A and MEF2C transgenic hearts. Indeed,

alterations in a subset of ion handling genes, such as encoded by *Kcnd2*, has already been reported to induce cardiac hypertrophy and myopathy (68,69), as well as being able to modulate hypertrophy induced by  $\alpha$ -adrenergic stimulation (46) or pressure overload (70). Thus, we propose that the alterations in ion handling genes might function as a primary disease-inducing lesion partially underlying the MEF2-mediated cardiomyopathy. While this prediction would be difficult to directly prove, it is nonetheless consistent with relatively rapid profile of current alterations that occurred in AdMEF2A infected cultured cardiomyocytes (within 36 hrs). Moreover, consensus MEF2 DNA binding sites are present in the promoters of the *Kcnj3*, *Kcnk2*, and *Kcnk3* genes (data not shown). The observed changes in a subset of metabolic genes may have some direct regulatory relationships, or it could also represent early secondary changes associated with the impending cardiomyopathic phenotype in MEF2A and MEF2C transgenic hearts. In contrast, the observed alterations in extracellular matrix and cell attachment associated genes may represent a more primary disease mechanism underlying the propensity towards ventricular dilation associated with MEF2 overexpression *in vivo*, or the sarcomeric disorganization and focal elongation observed in culture. In conclusion, we provide the first proof-of-principle that MEF2 can dominantly drive dilated cardiomyopathy *in vivo*, potentially in association with a primary alteration in a subset of ion handling genes and extracellular matrix associated genes.



**Footnotes:**

<sup>1</sup>Abbreviations: Ad, adenovirus; ANF, atrial natriuretic factor; BMK-1, big MAPK 1; BNP, b-type natriuretic peptide; CaMK, calmodulin-dependent protein kinase; CTGF, connective tissue growth factor; FAK, focal adhesion kinase; FS, fractional shortening; GAPDH, glyceraldehyde 3-phosphate dehydrogenase; GFP, green fluorescent protein; HW/BW, heart-weight divided by body-weight; HW/TL, heart-weight divided by tibia length; HDAC, histone deacetylase; IGF-1, insulin-like growth factor 1;  $I_{to}$ , transient outward current; MAPK, mitogen-activated protein kinase; MCIP, modulatory calcineurin interacting protein; MEF2, myocyte enhancer factor 2; MGP, matrix Gla protein; PKC, protein kinase C; PKD, protein kinase D; SRF, serum response factor; TAC, transverse aortic constriction; TEF-1, transcription enhancer factor 1; VW/BW, ventricular-weight divided by body-weight.

**Acknowledgement**

This work was supported by the National Institutes of Health (to J.D.M.) J.X. was supported by a Pre-Doctoral Fellowship from the Ohio Valley Affiliate branch of the American Heart Association (0215048B). J.D.M. is an Established Investigator of the American Heart Association. This work was also supported by a Canadian Institutes for Health Research (CIHR grant and a Career Investigator with the Heart and Stroke Foundation (HSF) of Ontario (to P.H.B). N.L.G. holds postdoctoral fellowships from the Heart & Stroke Foundation of Canada, the TACTICS-CIHR program at the University of Toronto and the Faculty of Medicine at the University of Toronto.

**REFERENCES**

1. Gossett, L. A., Kelvin, D. J., Sternberg, E. A., and Olson, E. N. (1989) *Mol. Cell. Biol.* **9**, 5022-5033
2. Black, B. L., and Olson, E. N. (1998) *Annu. Rev. Cell Dev. Biol.* **14**, 167-196
3. Molkenstin, J. D., and Olson, E. N. (1996) *Proc. Natl. Acad. Sci. USA* **93**, 9366-9373
4. Rao, S., Karray, S., Gackstetter, E. R., and Koshland, M. E. (1998) *J. Biol. Chem.* **273**, 26123-26129
5. Han, J., Jiang, Y., Li, Z., Kravchenko, V. V., and Ulevitch, R. J. (1997) *Nature* **386**, 296-299
6. Skerjanc, I. S., and Wilton, S. (2000) *FEBS Lett.* **472**, 53-56
7. Lin, Q., Schwarz, J., Bucana, C., and Olson, E. N. (1997) *Science* **276**, 1404-1407
8. Shore, P., and Sharrocks, A. D. (1995) *Eur. J. Biochem.* **229**, 1-13
9. Molkenstin, J. D., and Markham, B. E. (1993) *J. Biol. Chem.* **268**, 19512-19520
10. Kolodziejczyk, S. M., Wang, L., Balazsi, K., DeRepentigny, Y., Kothary, R., and Megeney, L. A. (1999) *Curr. Biol.* **9**, 1203-1206
11. Naya, F. J., Black, B. L., Wu, H., Bassel-Duby, R., Richardson, J. A., Hill, J. A., and Olson, E. N. (2002) *Nat. Med.* **8**, 1303-1309
12. Molkenstin, J. D., and Dorn, II. G. W. 2nd. (2001) *Annu. Rev. Physiol.* **63**, 391-426
13. Balke, C. W., and Shorofsky, S. R. (1998) *Cardiovasc. Res.* **37**, 290-299
14. Mao, Z., and Wiedmann, M. (1999) *J. Biol. Chem.* **274**, 31102-31107
15. Youn, H. D., Sun, L., Prywes, R., and Liu, J. O. (1999) *Science* **286**, 790-793
16. Youn, H. D., Grozinger, C. M., and Liu, J. O. (2000) *J. Biol. Chem.* **275**, 22563-22567
17. Lu, J., McKinsey, T. A., Nicol, R. L., and Olson, E. N. (2000) *Proc. Natl. Acad. Sci. USA* **97**, 4070-4075
18. Pan, F., Ye, Z., Cheng, L., and Liu, J. O. (2004) *J. Biol. Chem.* **279**, 14477-14480
19. Wu, H., Naya, F. J., McKinsey, T. A., Mercer, B., Shelton, J. M., Chin, E. R., Simard, A. R., Michel, R. N., Bassel-Duby, R., Olson, E. N., and Williams, R. S. (2000) *EMBO J.* **19**, 1963-1973
20. Lin, J., Wu, H., Tarr, P. T., Zhang, C. Y., Wu, Z., Boss, O., Michael, L. F., Puigserver, P., Isotani, E., Olson, E. N., Lowell, B. B., Bassel-Duby, R., and Spiegelman, B. M. (2002) *Nature* **418**, 797-801



21. Handschin, C., Rhee, J., Lin, J., Tarr, P. T., and Spiegelman, B. M. (2003) *Proc. Natl. Acad. Sci. USA*. **100**, 7111-7116
22. Cox, D. M., Du, M., Marback, M., Yang, E. C., Chan, J., Siu, K. W. McDermott, and J. C. (2003) *J. Biol. Chem.* **278**, 15297-15303.
23. Zhao, M., New, L., Kravchenko, V. V., Kato, Y., Gram, H., di Padova, F., Olson, E. N., Ulevitch, R. J., and Han, J. (1999) *Mol. Cell. Biol.* **19**, 21-30
24. Yang, S-H., Galanis, A., and Sharrocks, A. D. (1999) *Mol. Cell. Biol.* **19**, 4028-4038.
25. Ornatsky, O. I., Cox, D. M., Tangirala, P., Adnreeucci, J. J., Quinn, Z. A., Wrana, J. L., Prywes, R., Yu, Y. T., and McDermott, J. C. (1999) *Nuc. Acids Res.* **27**, 2646-2654
26. Marrinissen, M. J., Chiariello, M., Pallante, M., and Gutkind, J. S. (1999) *Mol. Cell. Biol.* **19**, 4289-4301
27. Kato, Y., Kravchenko, V. V., Tapping, R. I., Han, J., Ulevitch, R. J., and Lee, J-D. (1997) *EMBO J.* **16**, 7054-7066
28. Passier, R., Zeng, H., Frey, N., Naya, F. J., Nicol, R. L., McKinsey, T. A., Overbeek, P., Richardson, J. A., Grant, S. R., and Olson, E. N. (2000) *J. Clin. Invest.* **105**, 1395-1406
29. Miska, E. A., Karlsson, C., Langley, E., Nielsen, S. J., Pines, J., and Kouzarides, T. (1999) *EMBO J.* **18**, 5099-5107
30. Sparrow, D. B., Miska, E. A., Langley, E., Reynaud-Deonauth, S., Kotecha, S., Towers, N., Spohr, G., Kouzarides, T., and Mohun, T. J. (1999) *EMBO J.* **18**, 5085-5098
31. Wang, A. H., Bertos, N. R., Vezmar, M., Pelletier, N., Crosato, M., Heng, H. H., Th'ng, J., Han, J., and Yang, X. J. (1999) *Mol. Cell. Biol.* **19**, 7816-7827
32. McKinsey, T.A., Zhang, C. L., and Olson, E. N. (2001) *Mol. Cell. Biol.* **21**, 6312-6321.
33. Lu, J., McKinsey, T. A., Zhang, C. L., and Olson, E. N. (2000) *Mol. Cell.* **6**, 233-244
34. McKinsey, T. A., Zhang, C. L., Lu, J., and Olson, E. N. (2000) *Nature* **408**, 106-111
35. Zhang, C. L., McKinsey, T. A., Chang, S., Antos, C. L., Hill, J. A., and Olson, E. N. (2002) *Cell* **110**, 479-488
36. Naya, F. J., Wu, C., Richardson, J. A., Overbeek, P., and Olson, E. N. (1999) *Development* **126**, 2045-2052
37. Palermo, J., Gulick, J., Colbert, M., Fewell, J., and Robbins, J. (1996) *Circ. Res.* **78**, 504-509.
38. Wilkins, B. J., Dai, Y. S., Bueno, O. F., Parsons, S. A., Xu, J., Plank, D. M., Jones, F., Kimball, T. R., and Molkentin, J. D. (2004) *Circ. Res.* **94**, 110-118
39. Molkentin, J. D., Lu, J. R., Antos, C. L., Markham, B., Richardson, J., Robbins, J., Grant, S. R., and Olson, E. N. (1999) *Cell* **93**, 215-228
40. De Windt, L. J., Lim, H. W., Haq, S., Force, T., and Molkentin, J. D. (2000) *J. Biol. Chem.* **275**, 13571-13579
41. Parsons, S. A., Millay, D. P., Wilkins, B. J., Bueno, O. F., Tsika, G. L., Neilson, J. R., Liberatore, C. M., Yutzey, K. E., Crabtree, G. R., Tsika, R. W., and Molkentin, J. D. (2004) *J. Biol. Chem.* **279**, 26192-26200
42. Taigen, T., De Windt, L. J., Lim, H. W., and Molkentin, J. D. (2000) *Proc. Natl. Acad. Sci. USA*. **97**, 1196-1201
43. Cho, R. J., Huang, M., Campbell, M. J., Dong, H., Steinmetz, L., Sapinoso, L., Hampton, G., Elledge, S. J., Davis, R. W., and Lockhart, D. J. (2001) *Nat. Genetics* **27**, 48-54
44. Notterman, D. A., Alon, U., Sierk, A. J., and Levine, A. J. (2001) *Cancer Res.* **61**, 3124-3130
45. Wickenden, A. D., Kaprielian, R., Parker, T. G., Jones, O. T., and Backx, P. H. (1997) *J. Physiol.* **504**, 271-286
46. Zobel, C., Kassiri, Z., Nguyen, T. T., Meng, Y., and Backx, P. H. (2002) *Circulation* **106**, 2385-2391
47. Petrashevskaya, N. N., Bodi, I., Rubio, M., Molkentin, J. D., and Schwartz, A. (2002) *Cardiovasc Res.* **54**, 117-132

48. Zhang, X., Azhar, G., Chai, J., Sheridan, P., Nagano, K., Brown, T., Yang, J., Khrapko, K., Borrás, A. M., Lawitts, J., Misra, R. P., and Wei, J. Y. (2001) *Am. J. Physiol. Heart Circ. Physiol.* **280**, H1782-H1792
49. Liang, Q., and Molkenin, J. D. (2003) *J. Mol. Cell. Cardiol.* **35**, 1385-1394
50. Braz, J. C., Bueno, O. F., Liang, Q., Wilkins, B. J., Dai, Y. S., Parsons, S., Braunwart, J., Glascock, B. J., Klevitsky, R., Kimball, T. F., Hewett, T. E., and Molkenin, J. D. (2003) *J. Clin. Invest.* **111**, 1475-1486
51. Zhang, S., Weinheimer, C., Courtois, M., Kovacs, A., Zhang, C. E., Cheng, A. M., Wang, Y., and Muslin, A. J. (2003) *J. Clin. Invest.* **111**, 833-841
52. Nishida, K., Yamaguchi, O., Hirotsu, S., Hikoso, S., Higuchi, Y., Watanabe, T., Takeda, T., Osuka, S., Morita, T., Kondoh, G., Uno, Y., Kashiwase, K., Taniike, M., Nakai, A., Matsumura, Y., Miyazaki, J., Sudo, T., Hongo, K., Kusakari, Y., Kurihara, S., Chien, K. R., Takeda, J., Hori, M., and Otsu, K. (2004) *Mol. Cell. Biol.* **24**, 10611-10620
53. Liao, P., Georgakopoulos, D., Kovacs, A., Zheng, M., Lerner, D., Pu, H., Saffitz, J., Chien, K., Xiao, R. P., Kass, D. A., and Wang, Y. (2001) *Proc. Natl. Acad. Sci. USA.* **98**, 12283-12288
54. Wu, H., Rothermel, B., Kanatous, S., Rosenberg, P., Naya, F. J., Shelton, J. M., Hutcheson, K. A., DiMaio, J. M., Olson, E. N., Bassel-Duby, R., and Williams, R. S. (2001) *EMBO J.* **20**, 6414-6423
55. Karasheva, N., Tsika, G., Ji, J., Zhang, A., Mao, X., and Tsika, R. (2003) *Mol. Cell. Biol.* **23**, 5143-5164
56. Karns, L. R., Kariya, K., and Simpson, P. C. (1995) *J. Biol. Chem.* **270**, 410-417
57. Vega, R. B., Harrison, B. C., Meadows, E., Roberts, C. R., Papst, P. J., Olson, E. N., and McKinsey, T. A. (2004) *Mol. Cell. Biol.* **24**, 8374-8385
58. Dai, Y.-S., Xu, J., and Molkenin, J. D. (2005) *Mol. Cell. Biol.* **25**, 9936-9948
59. Nicol RL, Frey N, Pearson G, Cobb M, Richardson J, Olson EN. (2001) *EMBO J.* **20**, 2757-2767
60. Liu, W., Youn, H. D., Liu, J. O. (2001) *Eur. J. Immunol.* **31**, 1757-1764
61. Mao, Z., Bonni, A., Xia, F., Nadal-Vicens, M., and Greenberg, M. E. (1999) *Science.* **286**, 785-790
62. Okamoto, S., Krainc, D., Sherman, K., and Lipton, S. A. (2000) *Proc. Natl. Acad. Sci. USA.* **97**, 7561-7566
63. Gong, X., Tang, X., Wiedmann, M., Wang, X., Peng, J., Zheng, D., Blair, L. A., Marshall, J., and Mao, Z. (2003) *Neuron* **38**, 33-46
64. Linseman, D. A., Cornejo, B. J., Le, S. S., Meintzer, M. K., Laessig, T. A., Bouchard, R. J., and Heidenreich, K. A. (2003) *J. Neurochem.* **85**, 1488-1499
65. Sah, R., Ramirez, R. J., Oudit, G. Y., Gidrewicz, D., Trivieri, M. G., Zobel, C., and Backx, P. H. (2003) *J. Physiol.* **546**, 5-18
66. Harris, D. M., Mills, G. D., Chen, X., Kubo, H., Berretta, R. M., Votaw, V. S., Santana, L. F., and Houser, S. R. (2005) *Circ. Res.* **96**, 543-550
67. Tessier, S., Karczewski, P., Krause, E. G., Pansard, Y., Acar, C., Lang-Lazdunski, M., Mercadier, J. J., and Hatem, S. N. (1999) *Circ. Res.* **85**, 810-819.
68. Wickenden, A. D., Lee, P., Sah, R., Huang, Q., Fishman, G. I., and Backx, P. H. (1999) *Circ. Res.* **85**, 1067-1076
69. Kassiri, Z., Zobel, C., Nguyen, T. T., Molkenin, J. D., and Backx, P. H. (2002) *Circ. Res.* **90**, 578-585
70. Lebeche, D., Kaprielian, R., del Monte, F., Tomaselli, G., Gwathmey, J. K., Schwartz, A., and Hajjar, R. J. (2004) *Circulation.* **110**, 3435-3443.

## FIGURE LEGENDS

Figure 1. Generation of MEF2A transgenic mice. (A) Western blot for MEF2A protein in the hearts of wildtype (WT), low, medium, and high expressing MEF2A transgenic mice. GAPDH protein was measured as a loading control. (B) Heart-weight normalized to body-weight (HW/BW) in wildtype, low, and medium MEF2A transgenic mice at 3 months of age, and wildtype and high expressing mice at 3 weeks of age (N=5-8 mice per group). \*P<0.05 versus wildtype. (C) Echocardiographic assessment of fractional shortening (FS) in wildtype, medium and high expressing MEF2A transgenic mice at the indicated times. (N=4-6 mice per group) \*P<0.05 versus wildtype of the same age. (D) Relative mRNA expression of ANF and skeletal  $\alpha$ -actin in wildtype, low, medium and high expressing MEF2A mice at 3 weeks of age (N=3-4 hearts per group). \*P<0.05 versus wildtype. Abbreviations not defined in text: Sk  $\alpha$ -actin, skeletal  $\alpha$ -actin.

Figure 2. Characterization of MEF2A transgenic mice following pressure overload stimulation. (A) Heart-weight normalized to tibia length in wildtype, low, and medium expressing MEF2A transgenic mice at 2 months of age following a sham or transverse aortic constriction (TAC) surgical procedure for 2 weeks. (N=5-8 mice per group) \*P<0.05 versus sham of the same genotype; #P<0.05 versus wildtype TAC. (B) Lung-weight normalized to tibia length as an indication of heart failure in wildtype, low, and medium expressing MEF2A transgenic mice at 2 months of age following a sham or TAC surgical procedure for 2 weeks. (N=5-8 mice per group) \*P<0.05 versus sham of the same genotype; #P<0.05 versus wildtype TAC. (C) Cardiomyocyte surface area in hearts from wildtype, low, and medium expressing MEF2A transgenic mice following a sham or TAC surgical procedure for 2 weeks. (N=5 hearts per group) \*P<0.05 versus sham of the same genotype; #P<0.05 versus wildtype TAC. (D) Cardiac fractional shortening (FS) in wildtype, low, and medium expressing MEF2A transgenic mice at 2 months of age following a sham or TAC surgical procedure for 2 weeks. (N=5-8 mice per group) #P<0.05 versus wildtype TAC. (E) H&E-stained histological cross-section of hearts from wildtype and medium expressing MEF2A transgenic mice at 2 months of age following a sham or TAC surgical procedure for 2 weeks. (F) Echocardiography measured H/R ratio in sham mice and after TAC stimulation in the indicated groups. The H/R ratio indicates dilation versus concentric hypertrophy and is the ratio of the average of the left ventricular wall and septal thickness divided by 1/2 left ventricular end diastolic dimension (LVED).

Figure 3. Generation and characterization of MEF2C transgenic mice. (A) H&E-stained histological cross-section of hearts from wildtype (WT) and 3 different cardiac-specific MEF2C transgenic mouse lines at 4-6 weeks of age. (B) Western blot for MEF2C and GAPDH protein from hearts of wildtype and MEF2C transgenic mice (line 2). (C) Ventricular-weight to body-weight (VW/BW) in wildtype and line 2 MEF2C transgenic mice at the indicated times (N=5-6 mice per group) \*P<0.05 versus wildtype of the same age. (D) Fractional shortening (FS) in wildtype and line 2 MEF2C transgenic mice at the indicated times (N $\geq$ 5 mice per group) \*P<0.05 versus wildtype of the same age. (E) Relative mRNA expression of the indicated genes in wildtype and line 2 MEF2C transgenic mice at 1 month of age (N=4 hearts per group). \*P<0.05 versus wildtype. Abbreviations not defined in text:  $\alpha$ -MHC,  $\alpha$ -myosin heavy chain;  $\beta$ -MHC,  $\beta$ -myosin heavy chain; Sk  $\alpha$ -actin, skeletal  $\alpha$ -actin.

Figure 4. Crossing MEF2A and MEF2C transgenic mice with activated calcineurin transgenic mice (A) Heart-weight normalized to body-weight (HW/BW) in wildtype mice, medium expressing MEF2A transgenic mice, activated calcineurin transgenic mice ( $\Delta$ CnA), and double transgenic mice at 9 weeks of age (N=4-5 mice per group) \*P<0.05 versus wildtype. (B) Ventricular-weight normalized to body-weight (VW/BW) in wildtype mice, line 2 MEF2C transgenic mice, activated calcineurin transgenic mice

( $\Delta$ CnA), and double transgenic mice at 7 weeks of age (N=4-5 mice per group). \* $P$ <0.05 versus wildtype. (C) Echocardiography measured left ventricular (LV) wall thickness in wildtype mice, line 2 MEF2C transgenic mice, activated calcineurin transgenic mice ( $\Delta$ CnA), and double transgenic mice at 7 weeks of age (N=4-5 mice per group). \* $P$ <0.05 versus wildtype. (D) Echocardiography measured fractional shortening (FS) in wildtype mice, line 2 MEF2C transgenic mice, activated calcineurin transgenic mice ( $\Delta$ CnA), and double transgenic mice at 7 weeks of age (N=4-5 mice per group).

Figure 5. Confocal immunocytochemistry of neonatal cardiomyocyte cellular architecture and sarcomeric organization following Ad $\beta$ gal, AdMEF2A, AdMEF2C, AdMEF2VP16, and AdSRF infection. MEF2A, MEF2C, and MEF2VP16 lead to disorganization in myosin heavy chain and  $\alpha$ -actinin, yet the intermediate filament network as assessed with  $\alpha$ -tubulin antibody was not altered. As a control, AdSRF overexpression did not induce the same phenotypic disorganization in sarcomeres or cellular elongation. Identical results were observed in three independent experiments.

Figure 6. Assessment of indexes of ventricular remodeling (A) Western blot for phosphorylated FAK and total FAK from neonatal rat cardiomyocyte cultures infected with the indicated adenoviruses for 24 hrs. (B) RT-PCR from type-X $\alpha$ 1 collagen (rat) from neonatal rat cardiomyocyte cultures infected with the indicated adenoviruses for 24 hrs. (C) Measurement of myocyte length and width ratios from adult MEF2A transgenic mice at 2 months of age. Three wildtype and five transgenic hearts were disassociated and approximately 200 myocytes were measured from each (\* $P$ <0.05 versus wildtype).

Figure 7. RT-PCR confirmation of altered gene expression in MEF2A/C transgenic hearts. (A) Semi-quantitative RT-PCR for mRNA levels in separate hearts of wildtype and line 2 MEF2C transgenic mice for the indicated subset of extracellular matrix associated genes. L7 mRNA levels serve as a control for equal amplification and loading. Similar results were observed in two additional independent experiments, although from the same 2 mice in each group. (B) Semi-quantitative RT-PCR for mRNA levels in separate hearts of wildtype, low, medium, and high expressing MEF2A transgenic mice for the indicated subset of ion handling genes. Similar results were observed in two additional independent experiments, although from the same two mice in each group.

Figure 8. Whole-cell voltage-clamp recordings of  $K^+$  currents in cultured neonatal cardiomyocytes 36 hours following adenoviral infection with AdMEF2A plus AdGFP, AdGFP alone, or in adult myocytes from MEF2A transgenic mice. (A) Representative current recordings in response to step depolarizations between -40 mV and +60 mV (by 10 mV) from a holding potential of -80 mV followed by a brief 40 msec prepulse to -40 mV. (B) Current-voltage relationships for  $I_{K0}$  currents. Symbols represent mean  $\pm$  SEM for 6 cells with AdGFP and 4 cells with AdMEF2A + AdGFP. (C) Current-voltage relationships for  $I_{K0}$  currents from adult wildtype (WT) or MEF2A transgenic myocytes from disassociated hearts. Ten wildtype and five transgenic hearts were disassociated, generating 37 and 35 myocytes for recording, respectively.

Table 1. Echocardiography in wildtype (WT) and MEF2A medium and high transgenic (TG) mice.

	WT 1month	TG 1month	WT 2month	TG 2month	WT 3month	TG 3month	WT 3weeks	TG 3weeks
		Med		Med		Med		High
LVED	3.39 ± 0.10	3.38 ± 0.05	3.66 ± 0.16	4.19 ± 0.08*	3.88 ± 0.12	4.43 ± 0.11*	2.53 ± 0.24	3.71 ± 0.16*
LVES	2.21 ± 0.11	2.17 ± 0.09	2.48 ± 0.23	3.42 ± 0.19*	2.43 ± 0.06	3.55 ± 0.11*	1.40 ± 0.11	2.96 ± 0.09*
Septum	0.96 ± 0.06	1.08 ± 0.06	1.07 ± 0.09	1.03 ± 0.06	1.33 ± 0.09	1.10 ± 0.06	0.79 ± 0.02	0.78 ± 0.09
LV	0.87 ± 0.05	1.00 ± 0.07	1.20 ± 0.12	0.83 ± 0.13	1.27 ± 0.02	1.03 ± 0.06*	0.69 ± 0.06	0.64 ± 0.03
FS (%)	34.65 ± 2.23	35.95 ± 2.28	32.58 ± 3.99	18.61 ± 2.86*	37.11 ± 0.97	19.89 ± 0.92*	44.14 ± 2.35	20.16 ± 0.91*

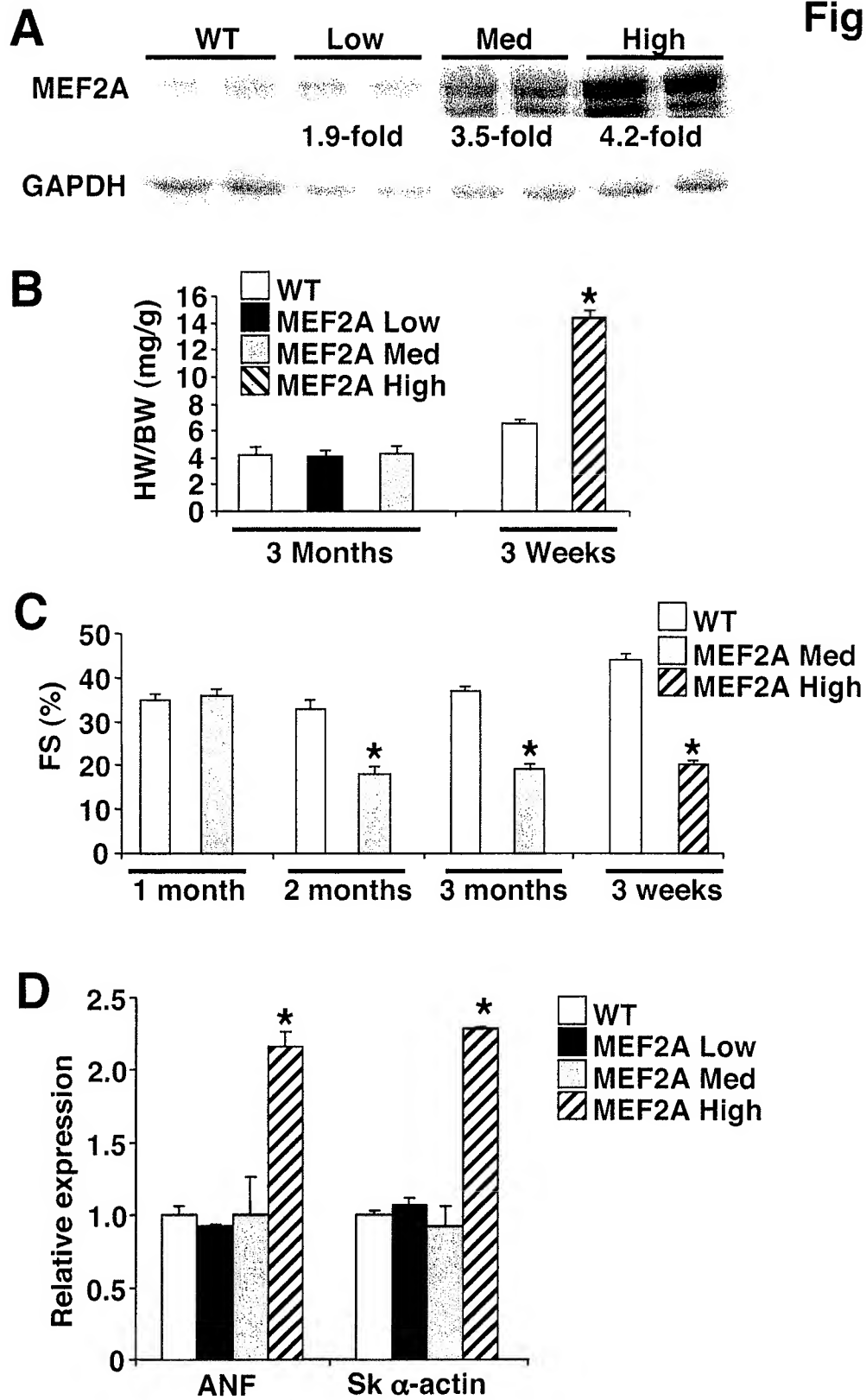
All measurements are means ± SEM, and each animal was measured three separate times. Septal and left ventricular (LV) wall thicknesses were assessed in systole and shown as millimeters (mm). Additional abbreviations used: LVED, left ventricular end-diastolic dimension; LVES, left ventricular end-systolic dimension; FS, fractional shortening. \*P<0.05, TG versus age-matched control. Four to six mice were analyzed in each group.

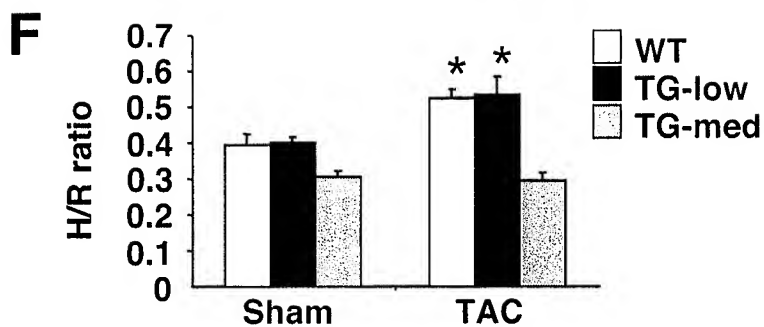
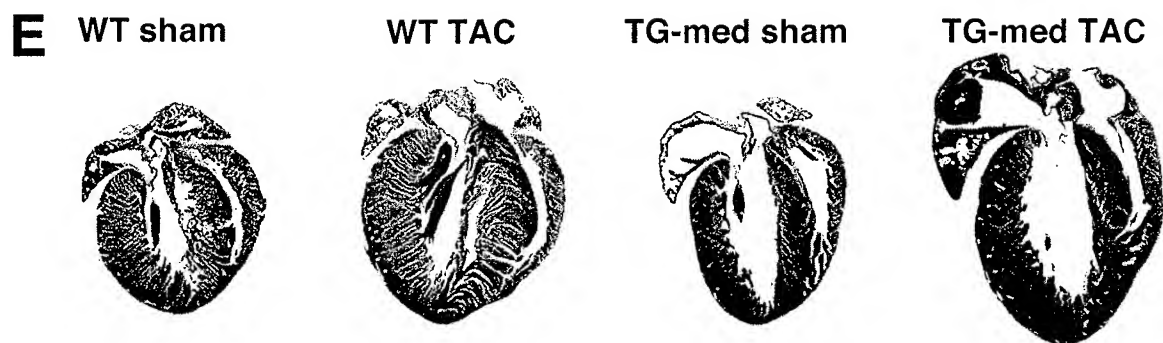
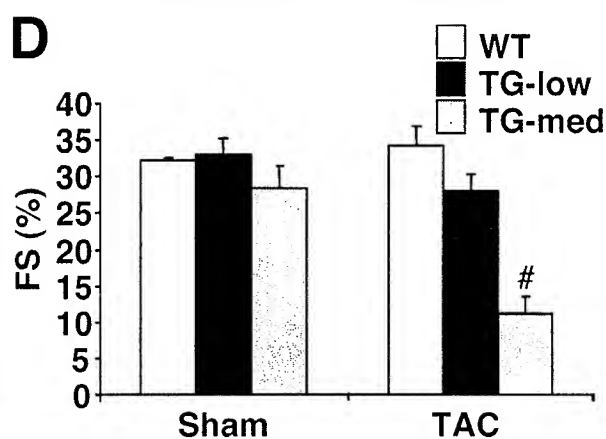
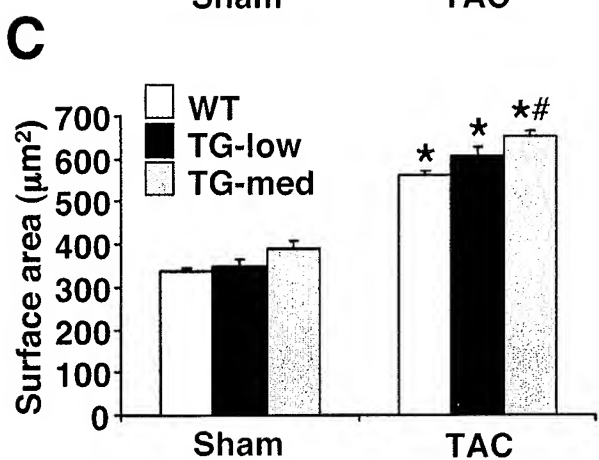
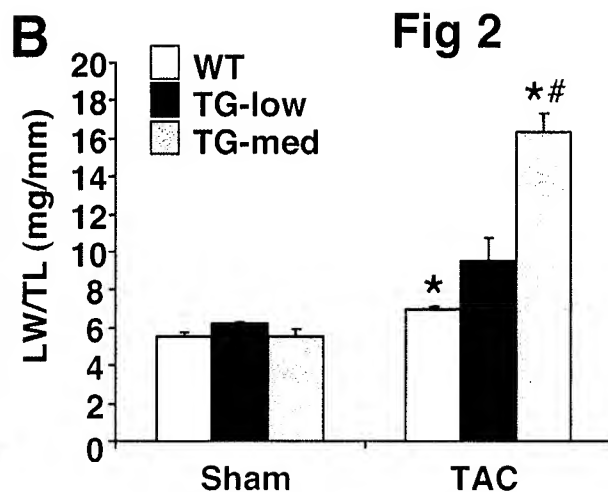
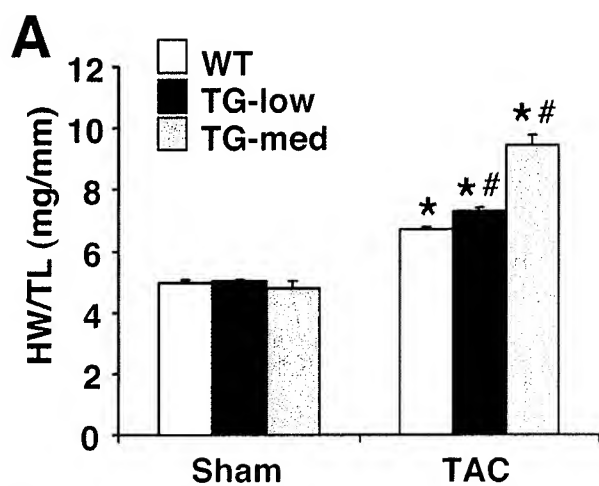
Table 2. Echocardiography in wildtype (WT) and MEF2C transgenic (TG) mice

	WT1month	TG 1month	WT 2month	TG 2month	WT 3month	TG 3month
LVED	2.88 ± 0.23	3.55 ± 0.62	3.54 ± 0.25	4.73 ± 0.56*	3.48 ± 0.17	5.25 ± 0.39*
LVES	1.72 ± 0.08	2.54 ± 0.79	2.28 ± 0.31	3.83 ± 0.75*	2.05 ± 0.15	4.45 ± 0.47*
Septum	0.92 ± 0.03	0.82 ± 0.11	1.07 ± 0.10	0.78 ± 0.20*	1.18 ± 0.11	0.87 ± 0.11*
LV	0.83 ± 0.15	0.76 ± 0.12	1.02 ± 0.08	0.76 ± 0.08*	1.09 ± 0.09	0.78 ± 0.07*
FS (%)	39.90 ± 7.48	29.65 ± 9.94	35.92 ± 5.53	19.61 ± 7.60*	40.93 ± 5.53	15.31 ± 4.47*

All measurements are means ± SEM, and each animal was measured three separate times. Septal and left ventricular (LV) wall thicknesses were assessed in systole and shown as millimeters (mm). Additional abbreviations used: LVED, left ventricular end-diastolic dimension; LVES, left ventricular end-systolic dimension; FS, fractional shortening. \*P<0.05, TG versus age-matched control. Five or more mice were analyzed in each group.

**Fig 1**





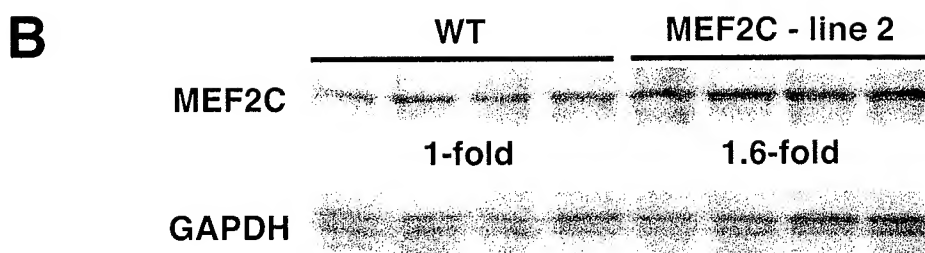
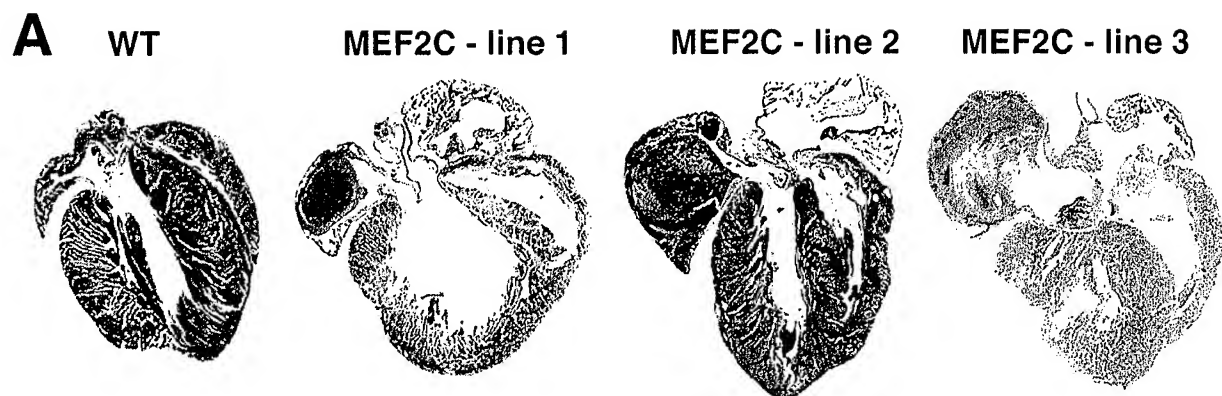


**Fig 3**

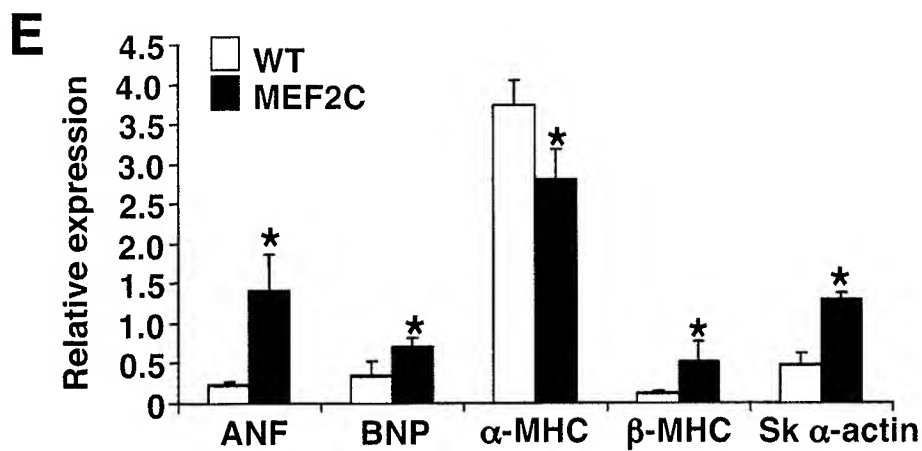
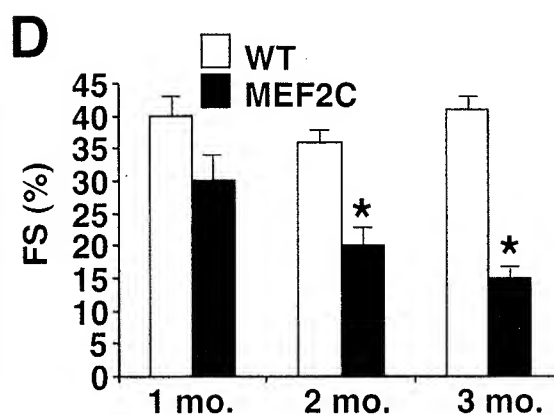
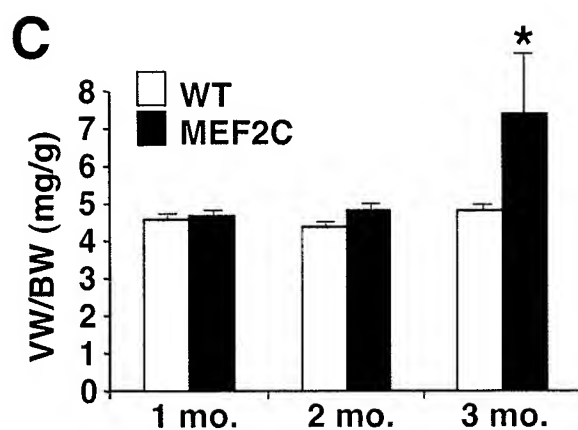
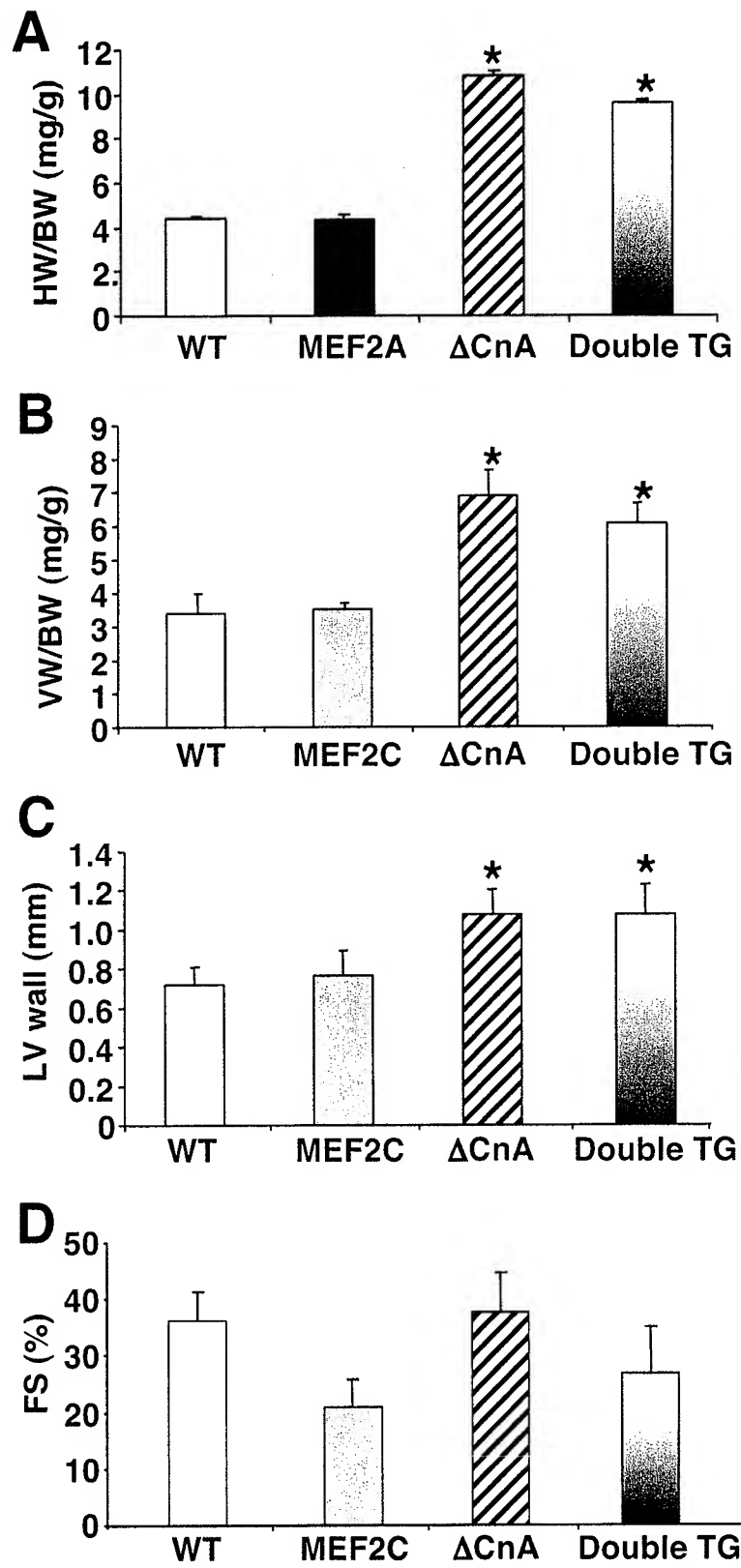




Fig 4



**Fig 5**

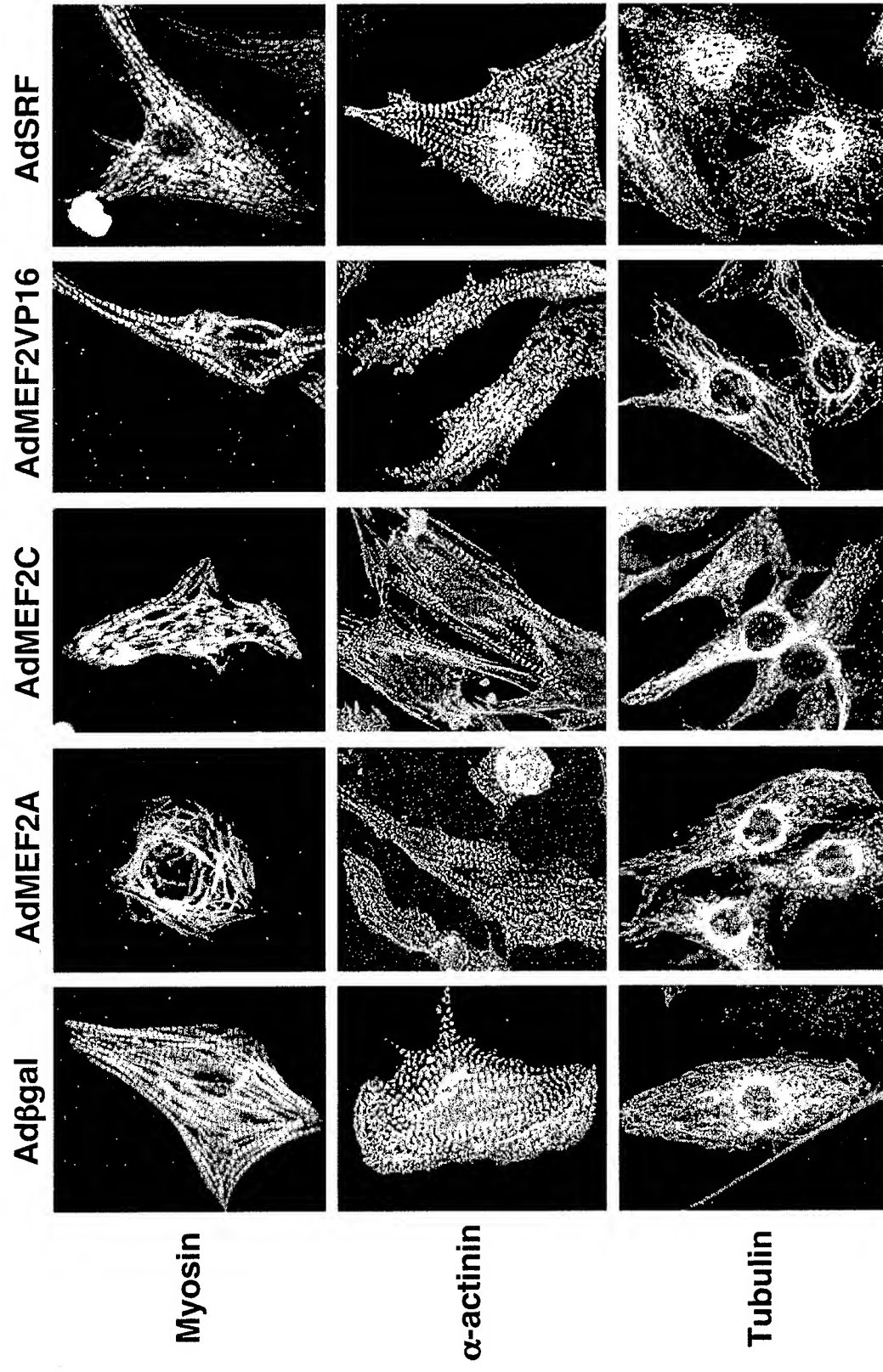


Fig 6

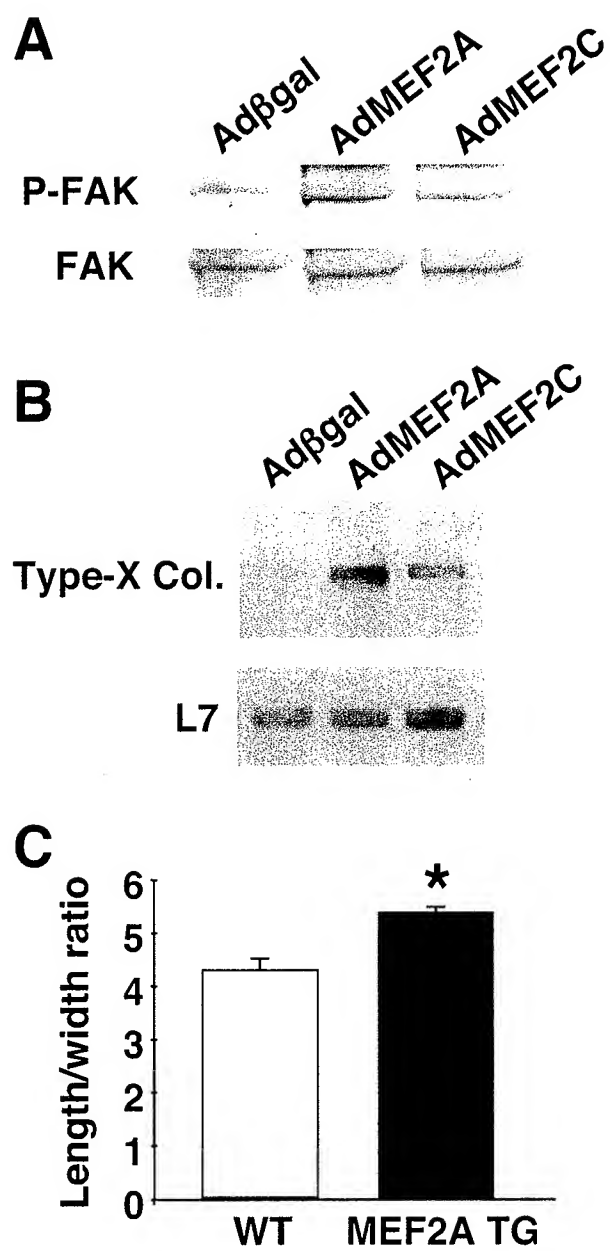


Fig 7

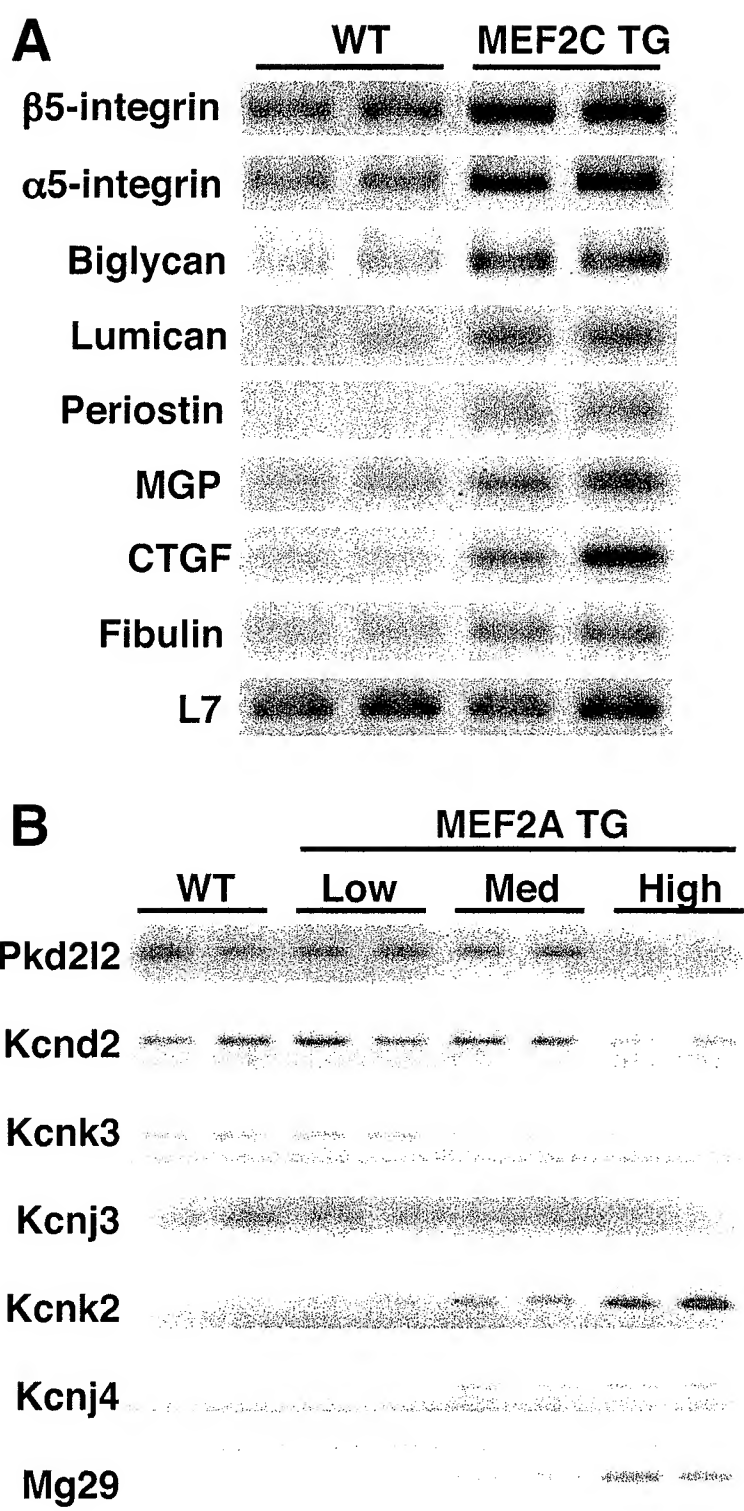
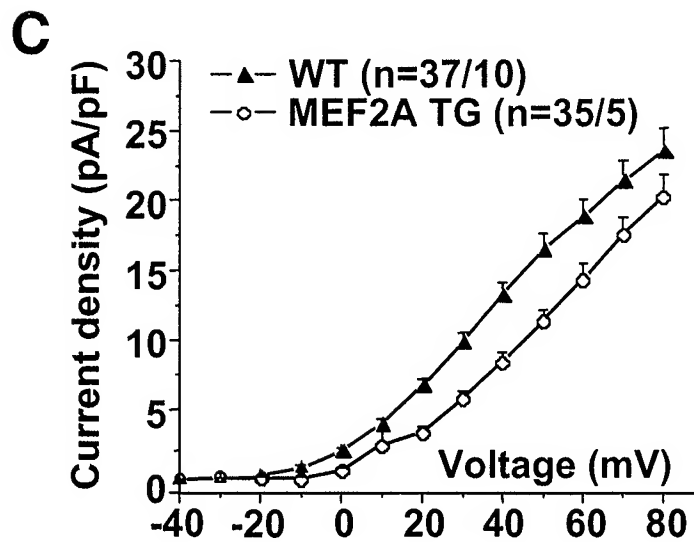
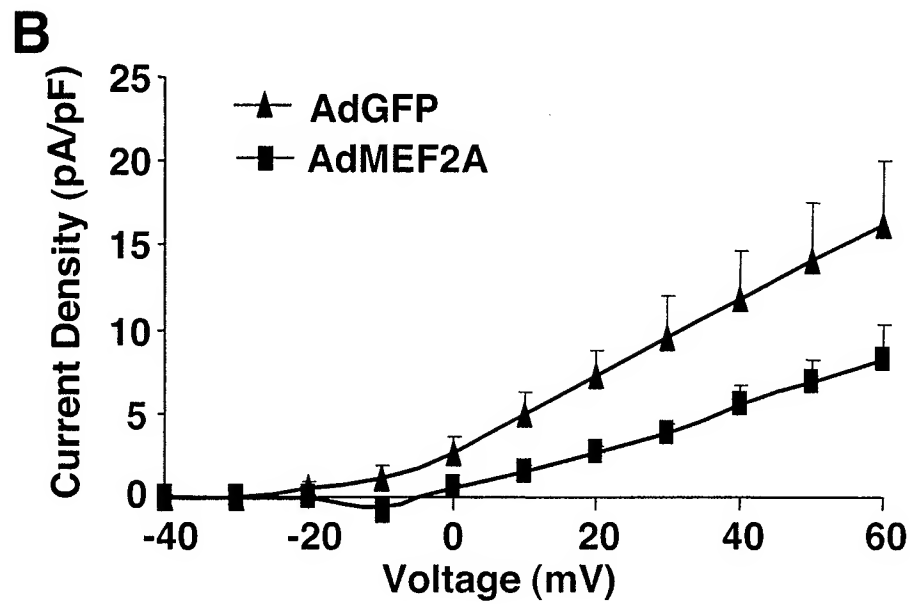
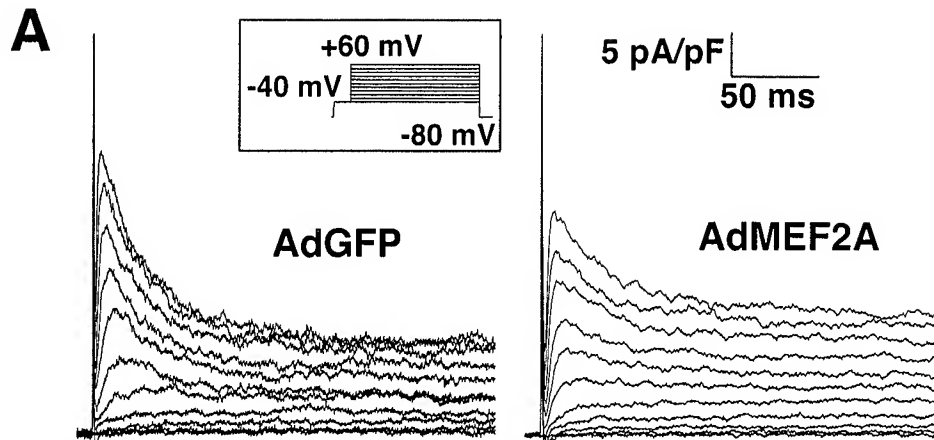


Fig 8



**Supplemental Tables.**

Supplemental Table 1. List of oligonucleotide primers used for RT-PCR of the indicated genes

Genes	Primers	
ANF	5'	5'-GCCCTGAGTGAGCAGACTG
	3'	5'-CGGAAGCTGTTGCAGCCTA
BNP	5'	5'-CTGCTGGAGCTGATAAGAGA
	3'	5'-AGTCAGAAACTGGAGTCTCC
SK $\alpha$ -actin	5'	5'-AGAAGGAGATCACAGCTCTG
	3'	5'-TACACGTCAAAAACAGGCGC
CTGF	5'	5'-CAGCTTGTGGCAAGTAAGTTTG
	3'	5'-GCTTTATCACCTGCACAGCATT
Lumican	5'	5'-TCTCGTTGCTGGTGGTATTAC
	3'	5'-AACTTGGCTGATTTCCATGCAA
MGP	5'	5'-AGCAGAGGTGGCGAGCTAAA
	3'	5'-TAATGCTACTGCAGGAGATAT
Periostin	5'	5'-AGCAAGTCCAAACACAGAGTTC
	3'	5'-ACTGTGCAAAGACTTAGCTGTA
Fibulin2	5'	5'-TGCTGTGACTCTGTAACCTAAC
	3'	5'-AGGAACACAGTGGATGAAGGA
Biglycan	5'	5'-CCAACCCTGTTATGCTTCCTGA
	3'	5'-CTCCTTGATCCTCGTCTTGAT
Interin $\alpha$ 5	5'	5'-AGAGAACCAGGAAGTCTGC
	3'	5'-CTGACTTGTCTAAGTCAGGG
Integrin $\beta$ 5	5'	5'-TACAGAAAGCCCATCTCCACA
	3'	5'-GAACACCAGAGTCTCCTTGC
Kcnj3	5'	5'-TCAGTAGTCAACATTTCAATTAGAA
	3'	5'-ACATGCAGAAATCATACTGTTCC
PKD2L2	5'	5'-AAGTTATGTCGTCTCTGTTTGTG
	3'	5'-TGTAAGTGTGCTGTAGCAGTCGC
Kcnk3	5'	5'-CGCGAATTCCGAGAAATGTGAA
	3'	5'-TGACCTGGACAAAACACCTTG
Kcnd2	5'	5'-ATCTCTTTAGTGTCTTTCCACTG
	3'	5'-CACATATGGGTGTTTGCAGGG
Kcnk2	5'	5'-AACGCCGATTAGCACAATCTAA
	3'	5'-AATGCCACATGATCACGTAAGC
Kcnj4	5'	5'-AGAGCAAGATCACGGTGCTG
	3'	5'-TTCCCTGCGATAGGAAATATTGT
Mg29	5'	5'-ACTGGCCCATCAACTACTTTAG
	3'	5'-ATAGCTAGAGAAACCAGACACC
L7	5'	5'-GAAGCTCATCTATGAGAAGGC
	3'	5'-AAGACGAAGGAGCTGCAGAAC
TypeX-Col.	5'	5'-ATAAGGCTCTAGCGCATCATGAAT
	3'	5'-ATACTGCGTTGCTGACATAAGAGT

Supplemental Table 2. mRNA Expression of genes involved in cardiac remodeling and composition of the extracellular matrix in wildtype and MEF2C transgenic hearts.

Name	Relative Gene Expression (ratio)				Genebank
	WT 1	WT 2	TG 1	TG 2	
ADAM19	0.64878	1.35121	3.36720	4.30963	NM_009616
ADAM9	1.02212	0.97788	1.53336	3.21983	NM_007404
biglycan	0.75128	1.24871	2.75767	3.45107	NM_007542
chondroitin sulfate proteoglycan 2	0.77221	1.22778	2.81219	2.49650	NM_019389
connective tissue growth factor	0.94485	1.05514	4.03104	9.25093	NM_010217
elastin	0.82053	1.17946	1.29893	3.61096	NM_007925
fibrillin 1	0.71335	1.28664	1.89387	1.73548	NM_007993
fibroblast growth factor receptor 1	1.17529	0.82471	1.74766	1.98691	NM_010206
fibronectin 1	0.69406	1.30593	1.49676	1.91466	M18194
fibulin 1	0.84113	1.15886	2.33248	3.16772	NM_010180
fibulin 2	0.84439	1.15560	2.49937	2.70906	NM_007992
integrin beta 5	0.86724	1.13275	2.54567	3.48622	NM_010580
laminin, alpha 2	0.90379	1.09620	2.05016	1.80792	NM_008481
lumican	0.85523	1.14476	2.18920	2.05969	NM_008524
matrilin 2	0.86553	1.13446	1.52142	1.38906	NM_016762
matrix gamma-carboxyglutamate (gla) protein	0.95813	1.04186	2.67455	4.32764	NM_008597
microfibrillar associated protein 5	0.87966	1.12033	4.27765	4.59619	NM_015776
microfibrillar-associated protein 2	0.75528	1.24471	1.70992	2.11885	NM_008546
nephronectin	0.69022	1.30977	11.17086	11.10387	NM_033525
osteoblast specific factor 2	0.61511	1.38488	5.29482	7.47862	NM_015784
tenascin C	0.98518	1.01481	4.71654	3.48314	NM_011607
thrombospondin 1	1.16358	0.83641	2.12132	4.53676	NM_011580
tissue inhibitor of metalloproteinase 1	0.80433	1.19566	3.52705	2.80179	NM_011593
procollagen C-proteinase enhancer protein	0.90181	1.09818	1.71083	1.29164	NM_008788
procollagen, type I, alpha 1	0.67721	1.32278	2.37270	2.78462	U08020
procollagen, type I, alpha 2	0.77903	1.22096	2.71956	3.45925	NM_007743
procollagen, type III, alpha 1	1.06096	0.93903	2.10598	2.28781	AK019448
procollagen, type IV, alpha 1	0.75567	1.24432	1.55611	1.63813	J04694
procollagen, type IV, alpha 5	0.97815	1.02184	0.87942	1.47431	Z35168
procollagen, type V, alpha 1	0.84487	1.15512	1.61151	1.46212	NM_015734
procollagen, type V, alpha 2	0.68108	1.31891	2.93712	4.13223	NM_007737
procollagen, type VI, alpha 1	0.95917	1.04082	2.75430	3.90867	NM_009933
procollagen, type VI, alpha 2	0.79436	1.20563	2.62053	2.18290	NM_146007
procollagen, type VI, alpha 3	0.70289	1.29711	1.85295	1.95569	AF064749
procollagen, type VIII, alpha 1	1.03838	0.96162	5.19285	5.55102	NM_007739
procollagen, type XIV, alpha 1	0.88828	1.11171	1.82762	2.13939	AJ131395

Cardiac RNA was collected from two line 2 MEF2C transgenic (TG) and two wildtype mice (WT) at 4 weeks of age and subjected to expression profiling using the Affymetrix U74Av2 array. The common gene names are shown along with the absolute normalized expression data for each sample in the right hand columns along with the Genebank accession number.

Supplemental Table 3. mRNA expression of genes directly or indirectly involved in ion handling or conductance in wildtype and high expressing MEF2A transgenic hearts

Name	<u>Relative Gene Expression (ratio)</u>				<u>Genebank</u>
	<u>WT 1</u>	<u>WT 2</u>	<u>TG 1</u>	<u>TG 2</u>	
voltage-gated sodium channel type X	1.05041	0.94959	0.18213	0.14415	NM_009134
synaptophysin	0.92323	1.07677	0.18407	0.18636	NM_009305
voltage-dependent calcium channel $\alpha_2/d$ subunit 2, Cacna2d2	0.98165	1.01835	0.19515	0.18245	NM_020263
small conductance calcium-activated potassium channel, Kcnn1	1.03327	0.96673	0.17735	0.12462	NM_032397
potassium inwardly-rectifying channel, Kcnj3	1.00869	0.99131	0.32709	0.31788	NM_008426
polycystic kidney disease 2-like 2, Pkd2l2	0.99865	1.00135	0.25970	0.22380	NM_016927
protein distantly related to the g subunit family	0.88964	1.11036	0.25753	0.22457	NM_019432
aquaporin 7	1.03528	0.96472	0.19112	0.17177	NM_007473
aldehyde oxidase 1	1.10392	0.89608	0.32229	0.34346	NM_009676
potassium voltage-gated channel, Kcnd2	1.00294	0.99706	0.15660	0.18380	NM_019697
potassium channel, Kcnk3	1.05136	0.94864	0.23500	0.26085	NM_010608
tramdorin 1	1.01022	0.98978	0.09472	0.12128	NM_153170
synaptotagmin 7	0.94981	1.05019	0.19009	0.23554	NM_173068
aquaporin 4	1.04337	0.95663	0.07746	0.09089	NM_009700
peptidylprolyl isomerase-like 1	1.07418	0.92582	0.22864	0.19289	NM_026845
Na <sup>+</sup> /K <sup>+</sup> transporting ATPase $\alpha_2$	1.12702	0.87298	0.20604	0.19357	NM_178405
GABA-A receptor $\alpha_1$	0.73210	1.26790	304.3776	342.5116	NM_010250
mitsugumin 29, Mg29	1.09065	0.90935	21.97762	20.02845	NM_008596
potassium channel tetramerisation domain containing 3	1.06472	0.93528	4.03101	5.30173	NM_172650
GABA-A receptor $\alpha_1$	0.97313	1.02687	6.52808	7.54893	NM_010250
Na <sup>+</sup> /K <sup>+</sup> transporting ATPase $\beta_4$	0.96921	1.03079	61.95085	63.19544	NM_133690
potassium inwardly-rectifying channel, Kcnj4	1.17995	0.82005	12.14792	14.16595	U11075
potassium channel, Kcnk2	0.97933	1.02067	3.91103	5.16053	NM_010607
receptor activity modifying protein 1	1.01647	0.98353	4.41346	4.35721	NM_016894
FXRD domain-containing ion transport regulator 6, Fxyd6	1.02505	0.97495	2.30911	2.74179	NM_022004
prolyl 4-hydroxylase b	1.04576	0.95424	2.73203	2.71201	NM_011032

Cardiac RNA was collected from two high expressing MEF2A transgenic (TG) and two wildtype mice (WT) at 2 weeks of age and subjected to expression profiling using the Affymetrix U74Av2 array. The common gene names are shown along with the absolute normalized expression data for each sample in the right hand columns along with the Genebank accession number.



Supplemental Table 4. mRNA Expression levels of metabolism related genes in wildtype and MEF2C transgenic hearts

Name	<u>Relative Gene Expression (ratio)</u>				<u>Genebank</u>
	<u>WT 1</u>	<u>WT 2</u>	<u>TG 1</u>	<u>TG 2</u>	
acyl-Coenzyme A thioesterase 2, mitochondrial	0.72290	1.27710	1.78206	2.51946	NM_019736
acyl-Coenzyme A thioesterase 3, mitochondrial	1.11353	0.88647	1.59554	2.59703	NM_022816
carboxylesterase 3	1.25243	0.74757	0.43764	0.06322	NM_053200
carnitine acetyltransferase	1.15009	0.84991	0.65055	0.30442	NM_007760
dihydrolipoamide branched chain transacylase E2	1.20317	0.79683	0.67708	0.32363	NM_010022
dodecenoyl-Coenzyme A delta isomerase	0.99333	1.00667	0.58274	0.33361	NM_010023
fatty acid Coenzyme A ligase, long chain 2	1.19573	0.80427	0.64748	0.50044	NM_007981
carnitine palmitoyltransferase 2	1.07486	0.92514	0.75868	0.43892	NM_009949
lipin 1	1.01569	0.98431	0.79947	0.44745	NM_015763
lipoprotein lipase	1.06856	0.93144	0.71185	0.50400	NM_008509
methylmalonyl-Coenzyme A mutase	0.98646	1.01354	0.74876	0.51665	NM_008650
monoglyceride lipase	0.86654	1.13346	0.70039	0.47586	NM_011844
fructose bisphosphatase 2	1.22179	0.77821	0.22995	0.02915	NM_007994
phosphorylase kinase gamma	1.22352	0.77648	0.47649	0.32077	NM_011079
pyruvate dehydrogenase kinase, isoenzyme 4	1.22013	0.77987	0.53228	0.39312	NM_013743
succinate dehydrogenase complex, subunit A, flavoprotein	1.08810	0.91190	0.61318	0.48923	NM_023281
glycogenin 1	0.99504	1.00496	1.81641	1.85155	NM_013755
phosphofructokinase 1	0.79858	1.20142	1.98908	3.12496	NM_019703

Cardiac RNA was collected from two line 2 MEF2C transgenic (TG) and two wildtype mice (WT) at 4 weeks of age and subjected to expression profiling using the Affymetrix U74Av2 array. The common gene names are shown along with the absolute normalized expression data for each sample in the right hand columns along with the Genebank accession number.

## EXHIBIT 2

## The MEF2A Isoform Is Required for Striated Muscle-specific Expression of the Insulin-responsive GLUT4 Glucose Transporter\*

Received for publication, December 20, 1999, and in revised form, March 10, 2000  
Published, JBC Papers in Press, March 15, 2000, DOI 10.1074/jbc.M910259199

Silvia Mora† and Jeffrey E. Pessin§

From the Department of Physiology and Biophysics, University of Iowa, Iowa City, Iowa 52242

Previously, we have demonstrated that an MEF2 consensus sequence located between –473/–464 in the human GLUT4 gene was essential for both tissue-specific and hormonal/metabolic regulation of GLUT4 expression (Thai, M. V., Guruswamy, S., Cao, K. T., Pessin, J. E., and Olson, A. L. (1998) *J. Biol. Chem.* 273, 14285–14292). To identify the specific MEF2 isoform(s) responsible for GLUT4 expression, we studied the pattern of expression of the MEF2 isoforms in insulin-sensitive tissues. Both heart and skeletal muscle were found to express the MEF2A, MEF2C, and MEF2D isoforms but not MEF2B. However, only the MEF2A protein was selectively down-regulated in insulin-deficient diabetes. Co-immunoprecipitation with isoform-specific antibodies revealed that, in the basal state, essentially all of the MEF2A protein was presented as a MEF2A-MEF2D heterodimer without any detectable MEF2A-MEF2A homodimers or MEF2A-MEF2C and MEF2C-MEF2D heterodimers. Electrophoretic mobility shift assays revealed that nuclear extracts from diabetic animals had reduced binding to the MEF2 binding site compared with extracts from control or insulin-treated animals. Furthermore, immunodepletion of the MEF2A-MEF2D complex from control extracts abolished binding to the MEF2 element. However, addition of MEF2A to diabetic nuclear extracts fully restored binding activity to the MEF2 element. These data strongly suggest that the MEF2A-MEF2D heterodimer is selectively decreased in insulin-deficient diabetes and is responsible for hormonally regulated expression of the GLUT4 gene.

The major insulin-responsive facilitative glucose transporter GLUT4<sup>1</sup> is predominantly expressed in striated muscle and adipocytes, tissues that display insulin-stimulated glucose uptake (1–3). In the basal state, this transporter slowly recycles between a poorly described intracellular storage compartment(s) and the plasma membrane such that the steady-state distribution favors intracellular localization (3, 4). However, following insulin stimulation, there is a dramatic increase in

the rate of GLUT4 exocytosis with a smaller decrease in the rate of plasma membrane endocytosis (4). This redistribution of pre-existing GLUT4 protein provides the major mechanism accounting for the acute insulin-stimulated glucose uptake that occurs in the post-prandial state (1, 3, 5, 6). In addition to this acute regulation of GLUT4-containing vesicle trafficking, the expression of GLUT4 is transcriptionally regulated in a variety of persistent altered metabolic states. For example, states of insulin deficiency induced by either streptozotocin (STZ) treatment or nutritional restriction results in decreased GLUT4 mRNA and protein in adipose tissue and cardiac and skeletal muscle (7–9). The decrease in GLUT4 protein levels directly correlates with a decrease in GLUT4 mRNA and the rate of GLUT4 gene transcription (10). Promoter analysis in tissue cultured 3T3L1 adipocytes has recently identified an insulin-responsive element (–706/–676) located in the 5′-flanking region of the murine GLUT4 gene (11, 12). In addition, analysis of tissue-specific GLUT4 gene expression in the cultured C2C12 muscle cell line demonstrated the necessary requirement for a myocyte enhancer factor 2 (MEF2) cis-DNA regulatory element (13). The importance of the MEF2 site was further supported by expression analysis in transgenic mice that demonstrated the essential function of the human GLUT4 MEF2 site (–473/–464) in both tissue-specific and hormonal/metabolic regulation (14). Importantly, *in vitro* MEF2 sequence-specific binding activity was found to decrease following STZ-induced diabetes (15).

Currently, there are four known members of the mammalian MEF2 family termed MEF2A, MEF2B, MEF2C, and MEF2D (16, 17). These DNA-binding proteins are important transcription factors in both the maintenance and induction of the muscle differentiated phenotype (18–21). These factors bind DNA as homo- and heterodimers but can also form protein-protein interactions with the thyroid hormone receptor (22), and members of the basic helix-loop helix family of transcription factors, such as MyoD or myogenin (18, 20, 22–25).

Although the MEF2 element appears to be essential for GLUT4 expression, the specific MEF2 isoform(s) regulating the tissue-specific and hormonal/metabolic regulation of the GLUT4 gene has not been determined. In this report, we demonstrate that cardiac and skeletal muscle expression of GLUT4 is dependent upon a MEF2A-MEF2D heterodimer. STZ-induced insulin deficiency results in a specific decrease in expression of the MEF2A mRNA and protein. Furthermore, the addition of *in vitro* synthesized MEF2A protein to diabetic nuclear extracts restored the binding activity to a comparable level found in control or insulin-treated animals.

### EXPERIMENTAL PROCEDURES

**Rats**—Male Sprague-Dawley rats (180–200 g) were obtained from Harlan. These animals were either left untreated or made diabetic by an intraperitoneal injection of STZ (90–100 mg/kg body weight) following an overnight fast. Three days following the injection, blood tail samples were checked for glucose concentration using a One-Touch<sup>®</sup>

\* This work was supported in part by Research Grants DK33823 and DK25295 from the National Institutes of Health. The costs of publication of this article were defrayed in part by the payment of page charges. This article must therefore be hereby marked "advertisement" in accordance with 18 U.S.C. Section 1734 solely to indicate this fact.

† Recipient of a postdoctoral fellowship (Formacion de Personal Investigador) from the Ministerio de Educacion y Cultura, Spain.

§ To whom correspondence should be addressed: Dept. of Physiology and Biophysics, University of Iowa, 51 Newton Rd., Iowa City, IA 52242. Tel.: 319-335-7823; Fax: 319-335-7330; E-mail: jeffrey-pessin@uiowa.edu.

<sup>1</sup> The abbreviations used are: GLUT4, muscle/adipose-specific glucose transporter; MEF, myocyte enhancer factor; STZ, streptozotocin; PMSF, phenylmethylsulfonyl fluoride; TPCK, *N*-tosyl-L-phenylalanine chloromethyl ketone; TLCK, *N*<sup>α</sup>-*p*-tosyl-L-lysine chloromethyl ketone.

glucometer (Lifescan, Milpitas, CA). Animals with a glycemia  $\geq 300$  mg/dl were considered diabetic and sacrificed 3–5 days following the STZ injection by CO<sub>2</sub> asphyxiation for removal of tissues. A set of diabetic animals were also treated with human insulin for 7 days with a daily dose of 3 units of regular insulin (Humulin-R) and 2 units of long-acting insulin (Humulin-N) as described previously (26, 27). All tissues were snap-frozen in liquid nitrogen and kept at  $-80^{\circ}\text{C}$  until used. All procedures were reviewed and approved by the University of Iowa Committee for the Care and Use of Animals.

**RNA Isolation and Northern Blot Analysis**—RNA was extracted with guanidinium thiocyanate method using the RNeasy reagent from TelTest (Friendswood, TX) and following the manufacturer's instructions. For Northern blots, 30  $\mu\text{g}$  of total RNA was fractionated in a 1% formaldehyde agarose gel. The samples were then transferred to a Hybond-N nylon membrane (Amersham Pharmacia Biotech) overnight and prehybridized at  $65^{\circ}\text{C}$  for 3–4 h in a solution containing 20% formamide,  $4\times$  SSPE,  $5\times$  Denhardt's, 5% SDS, 10% dextran sulfate, 40 mM HCl, 0.4 mg/ml salmon sperm DNA, and 0.2 mg/ml yeast tRNA. The same solution was used for overnight hybridization at  $65^{\circ}\text{C}$  with  $10^6$  cpm/ml  $^{32}\text{P}$ -random primed labeled probe corresponding to full-length human  $\alpha$ -actin, rat GLUT4, human MEF2A, and mouse MEF2B, MEF2C, and MEF2D cDNAs. The cDNA probes were labeled using [ $\alpha$ - $^{32}\text{P}$ ]dCTP and the Rediprime labeling kit (Amersham Pharmacia Biotech) following manufacturer's directions. After hybridization membranes were washed thoroughly and exposed to film overnight at  $-70^{\circ}\text{C}$ .

**Preparation of Nuclear Extracts and Total Membranes**—Nuclear extracts from heart and skeletal muscle were obtained as described by Thai *et al.* (15) with minor modification. Briefly, frozen tissues were pulverized in liquid nitrogen and then resuspended in homogenization buffer A (250 mM sucrose; 10 mM Hepes, pH 7.6; 25 mM KCl; 1 mM EDTA; 10% glycerol; 0.15 mM spermine; 0.5 mM spermidine; 0.1 mM PMSF; 2  $\mu\text{g}/\text{ml}$  each aprotinin, leupeptin, and pepstatin A; and 6  $\mu\text{g}/\text{ml}$  each TLCK and TPCK). The tissues were homogenized with 10 strokes of a Teflon pestle and filtrated through gauze and centrifuged at  $3,900 \times g$  for 10 min at  $4^{\circ}\text{C}$ . The supernatant was then centrifuged at  $200,000 \times g$  for 1 h at  $4^{\circ}\text{C}$  to obtain a pellet of crude total membranes. The pellet from the low speed centrifugation was resuspended in 10 ml of homogenization buffer A and homogenized in a loose-type Dounce homogenizer. The homogenate was then layered over 0.5 volume of buffer B (1 M sucrose; 10 mM Hepes, pH 7.6; 25 mM KCl; 1 mM EDTA; 10% glycerol; 0.15 mM spermine; 0.5 mM spermidine; 0.1 mM PMSF; 2  $\mu\text{g}/\text{ml}$  each aprotinin, leupeptin, and pepstatin A; and 6  $\mu\text{g}/\text{ml}$  each TLCK and TPCK, followed by centrifugation at  $3,900 \times g$  for 10 min at  $4^{\circ}\text{C}$ . The pellet was then resuspended in buffer A/glycerol (9:1, w/w) and layered over one-third buffer B/glycerol (9:1). The gradient was centrifuged at  $48,000 \times g$  for 30 min at  $4^{\circ}\text{C}$ . The semi-purified nuclear pellet was resuspended in 1 volume of nuclear extraction buffer (10 mM Hepes, pH 7.6, 400 mM KCl, 3 mM MgCl<sub>2</sub>, 0.1 mM EDTA, 10% glycerol, 1 mM dithiothreitol). Nuclear proteins were extracted at  $4^{\circ}\text{C}$  for 30 min and insoluble nuclei precipitated by centrifugation at 13,000 rpm in a microcentrifuge for 15 min. Supernatant was dialyzed against a buffer containing 25 mM Hepes, pH 7.5; 100 mM KCl; 0.1 mM EDTA; 10% glycerol; 1 mM dithiothreitol; 0.1 mM PMSF; 2  $\mu\text{g}/\text{ml}$  pepstatin, aprotinin, and leupeptin; and 6  $\mu\text{g}/\text{ml}$  each of TLCK and TPCK for 2–3 h at  $4^{\circ}\text{C}$ . The extracts were quantified for protein content using BCA method (Pierce) and frozen in small aliquots at  $-70^{\circ}\text{C}$ .

**Western Blot Analysis**—Nuclear extracts (30–50  $\mu\text{g}$ ) were resolved in a 10% SDS-polyacrylamide gel electrophoresis. The fractionated proteins were transferred to nitrocellulose membranes in a buffer containing 25 mM Tris, 190 mM glycine, pH 8.5, at 0.6 A for 6 h at  $4^{\circ}\text{C}$ . Filters were then blotted for 60 min with 5% nonfat dry milk in Tris-buffered saline/Tween buffer (20 mM Hepes, pH 7.5, 150 mM NaCl, 0.2% Tween 20). The nitrocellulose membranes were then probed with a 1:2000 dilution of MEF2A/C or a MEF2D polyclonal antibodies (kindly provided by Dr. Ron Prywes, Columbia University, New York, NY) or a polyclonal GLUT4-specific antibody generated in our laboratory. In addition, we have prepared a polyclonal MEF2A-specific antibody (IA-17) generated against amino acid residues 88–131 of MEF2A and a polyclonal MEF2C-specific antibody (IA-14) generated against amino acid residues 311–351 of MEF2C. The filters were then washed three times with Tris-buffered saline/Tween buffer at room temperature for 10 min and probed for 1 h at room temperature with a goat anti-rabbit horseradish peroxidase-conjugated antibody (Pierce). Membranes were then washed as before and proteins visualized by enhanced chemiluminescence (Pierce).

**In Vitro Translation of MEF2**—*In vitro* transcription and translation was performed using a TNT reticulocyte lysate system from Promega

(Madison, WI) following manufacturer's instructions. For each reaction 1  $\mu\text{g}$  of template DNA corresponding to full-length cDNA of MEF2A, MEF2B, MEF2C, or MEF2D was used.

**Immunoprecipitation**—Nuclear extracts (50–100  $\mu\text{g}$ ) were incubated with 5  $\mu\text{g}$  of MEF2D monoclonal antibody (Transduction Laboratories, San Diego, CA) coupled to goat anti-mouse IgG-agarose beads (Sigma) in 25 mM Hepes, pH 7.6; 100 mM KCl; 0.1 mM EDTA; 10% glycerol; 1% Nonidet P-40; 1 mM sodium vanadate; 1 mM PMSF; 2  $\mu\text{g}/\text{ml}$  of pepstatin, aprotinin, and leupeptin; and 6  $\mu\text{g}/\text{ml}$  each of TLCK and TPCK. Samples were microcentrifuged for 1 min and the pellets washed five times in the above buffer. The samples were then resuspended in Laemli sample buffer, heated for 5 min at  $100^{\circ}\text{C}$ , and subjected to SDS-polyacrylamide gel electrophoresis and Western blot analysis. For immunoprecipitation with the MEF2A antibody, 2 ml of the polyclonal IA-17 antibody were cross-linked to protein A beads with dimethyl pimelimidate reagent using the Immunopure protein A IgG kit (Pierce). Immunoprecipitation was then performed at  $4^{\circ}\text{C}$  as described for the MEF2D antibody above.

**Electrophoretic Mobility Shift Assays**—For electrophoretic mobility shift assays, we used a Gelshift kit obtained from Geneka Biotechnology (Montreal, Canada). For each reaction, 4–10  $\mu\text{g}$  of nuclear extracts were incubated in DNA binding buffer at  $4^{\circ}\text{C}$  for 20 min and subsequently with the labeled oligonucleotide probe corresponding to the MEF2 consensus binding site (Santa Cruz Biotechnology, Santa Cruz, CA) for an additional 20 min at  $4^{\circ}\text{C}$ . The samples were then run in a 5% acrylamide:bisacrylamide gel (38:2) in TGE buffer (250 mM Tris, 1.9 M glycine, and 10.5 mM EDTA). Labeling of the oligonucleotide probes was performed as described by Ausubel *et al.* (28). For immunodepletion experiments, 50–80  $\mu\text{g}$  of nuclear extract were immunoprecipitated as described above using the immunoprecipitation buffer without detergent.

## RESULTS

**Insulin-deficient Diabetes Results in a Selective Decrease in MEF2A Protein Expression in Cardiac and Skeletal Muscle**—Previously, we have demonstrated that the MEF2 consensus cis-DNA element is essential for both tissue-specific and hormonal/metabolic regulation of the GLUT4 gene (15). In addition, nuclear extracts from STZ-induced diabetes bind poorly to this element compared with control tissue extracts. In order to identify the specific MEF2 isoform(s) responsible for the loss of MEF2 binding and GLUT4 transcriptional activity, we initially performed Northern blot analysis of total RNA isolated from control, STZ-induced diabetic, and STZ-diabetic animals treated with insulin for 1 week (Fig. 1). As typically observed, STZ-induced diabetes resulted in decreased GLUT4 mRNA levels in both the heart and hindlimb skeletal muscle. The reduction in GLUT4 mRNA was fully reversible following insulin treatment and was specific as there was no significant change in  $\alpha$ -actin expression. Similarly, the two MEF2D transcripts were also unaffected in STZ-induced diabetes, whether or not the animals were treated with insulin. In contrast, insulin deficiency resulted in decreased levels of the MEF2A and MEF2C mRNA that were also recovered following insulin therapy. As expected, we were unable to detect the presence of any MEF2B transcripts in adult striated muscles consistent with this isoform only expressed at significant amounts during embryonic development (29, 30) (data not shown).

Since previous studies have observed that the relative levels of the MEF2 transcripts do not always correlate with protein expression (31, 32), it was necessary to perform specific Western blots of nuclear extracts. However, due to the high degree of sequence identity between the MEF2 proteins, antibodies selective for the MEF2A and MEF2C isoforms have not been available. Therefore, to distinguish between the MEF2A and MEF2C proteins, we generated specific polyclonal antibodies as described under "Experimental Procedures." To demonstrate the specificity of several MEF2 antibodies, we *in vitro* translated the three MEF2 isoforms (MEF2A, MEF2C, and MEF2D), followed by immunoblotting (Fig. 2). In the absence of any template, none of the antibodies detected any immunore-

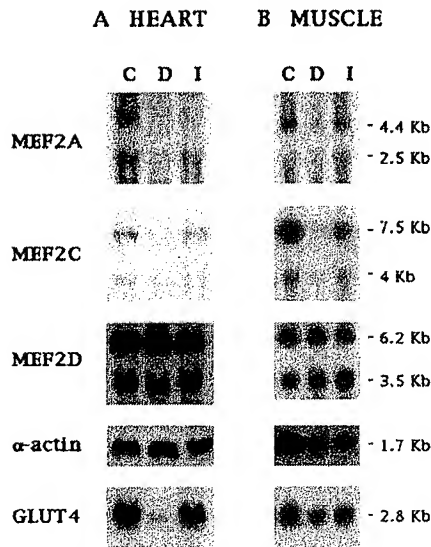


FIG. 1. MEF2A, MEF2C, and GLUT4 mRNA levels are decreased in striated muscle of insulin-deficient diabetic rats. Total heart (A) and hindlimb skeletal muscle (B) RNA (30  $\mu$ g) was isolated from control (C), STZ-diabetic (D), and insulin-treated STZ-diabetic rats (I). The RNA was resolved in an agarose denaturing gel, transferred to a nylon membrane, and probed with full-length  $^{32}$ P-labeled cDNAs corresponding to MEF2A, MEF2C, MEF2D, GLUT4, or  $\alpha$ -actin genes as described under "Experimental Procedures." This is a representative experiment independently performed two times.

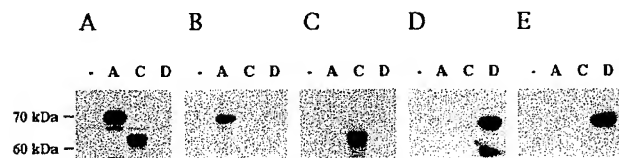


FIG. 2. Western blot analysis of *in vitro* transcribed and translated MEF2 isoforms. The empty vector (—), MEF2A (A), MEF2C (C), and MEF2D (D) cDNAs were *in vitro* translated and resolved by 10% SDS-polyacrylamide gel electrophoresis. The samples were then transferred to a nitrocellulose membrane and immunoblotted with the MEF2A polyclonal antibody provided by Dr. Ron Prywes (A), the MEF2A IA-17 polyclonal antibody (B), the MEF2C IA-14 polyclonal antibody (C), the MEF2D polyclonal antibody obtained from Dr. Ron Prywes (D), and the MEF2D monoclonal antibody obtained from Signal Transduction Laboratories (E) as described under "Experimental Procedures." This is a representative experiment independently performed two times.

active protein. As reported previously (33), an antibody prepared against MEF2A kindly provided by Dr. Ron Prywes cross-reacted with both the MEF2A and MEF2C isoforms but did not detect MEF2D (Fig. 2A). In contrast, the IA-17 antibody was specific for MEF2A, whereas the IA-14 was specific for MEF2C (Fig. 2, B and C). Furthermore, the two MEF2D antibodies (one polyclonal kindly provided by Dr. Ron Prywes, and one monoclonal from Signal Transduction Laboratories) were both specific for MEF2D and did not cross-react with either MEF2A or MEF2C (Fig. 2, D and E). In addition, although the IA-17 MEF2A antibody was capable of immunoprecipitating the native protein, the IA-14 MEF2C was only able to react in Western blots and was incapable of immunoprecipitating the native MEF2C protein (see Fig. 5 and data not shown).

In any case, having established the specificity of these antibodies, we next assessed the expression of the MEF2 isoforms in cardiac and skeletal muscle nuclear extracts from control, diabetic, and insulin-treated diabetic animals (Fig. 3). Immunoblotting with the MEF2A/C antibody demonstrated that one and/or both of these isoforms was decreased in streptozotocin-induced diabetes. The decrease in MEF2A/C immunoreactivity

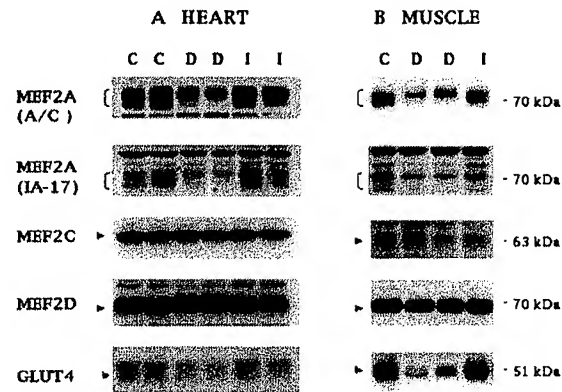


FIG. 3. MEF2A protein is specifically decreased in striated muscle of insulin-deficient diabetic rats. Nuclear extracts were isolated from the heart (A) and hindlimb skeletal muscles (B) of control (C), STZ-diabetic (D), and insulin-treated STZ-diabetic (I) rats. The protein samples (30  $\mu$ g) were resolved by 10% SDS-polyacrylamide gel electrophoresis and transferred to a nitrocellulose membrane. The membranes were then immunoblotted with the MEF2A polyclonal antibody provided by Dr. Ron Prywes, the MEF2A IA-17 polyclonal antibody, the MEF2C IA-14 polyclonal antibody, and the MEF2D monoclonal antibody obtained from Signal Transduction Laboratories as described under "Experimental Procedures." This is a representative experiment independently performed three times.

was specifically due to a loss of MEF2A protein without any effect on the MEF2C protein as detected by the IA-17 and IA-14 antibodies. Furthermore, the diabetic state had no effect on MEF2D protein levels. The changes in MEF2A protein levels directly correlated with the changes in GLUT4 protein. Together, these data suggest that the expression of the MEF2A nuclear protein isoform is selectively down-regulated in insulin-deficient diabetes.

**MEF2A Is Specifically Complexed with MEF2D**—The MEF2 family of transcription factors bind to DNA as either homodimeric or heterodimeric complexes (16). To examine the association state of MEF2A, we initially immunoprecipitated nuclear extracts with the specific MEF2D antibody and determined the amount of co-immunoprecipitated MEF2 isoforms (Fig. 4). In the absence of the MEF2D antibody, all the MEF2A, MEF2C, and MEF2D proteins remained in the supernatant without any protein detected in the immunoprecipitated pellets. In contrast, incubation with the MEF2D antibody resulted in the quantitative depletion of the MEF2D protein from the supernatant and appearance in the immunoprecipitated pellet. Western blots of the MEF2D immunoprecipitates demonstrated that all the MEF2A isoform was co-immunoprecipitated with MEF2D, whereas there was essentially no co-immunoprecipitated MEF2C protein, which was completely retained in the supernatant.

To further confirm the specific interaction of MEF2A with MEF2D, nuclear extracts were immunoprecipitated with the MEF2A-specific antibody (Fig. 5). Under these conditions, the MEF2A protein was completely immunodepleted from the cell extracts. This resulted in the co-immunoprecipitation of approximately 33% of the MEF2D protein, as observed both by its depletion from the supernatant and appearance in the immunoprecipitated pellet. Furthermore, essentially none of the MEF2C protein was immunodepleted from the supernatant following MEF2A immunoprecipitation. Although we were unable to immunoblot the MEF2A immunoprecipitates with the MEF2C antibody due to heavy chain cross-reactivity, these data are consistent with the absence of a MEF2A-MEF2C complex. It should also be noted that, since the MEF2C antibody (IA-14) was unable to immunoprecipitate the native MEF2C protein, we could not examine the co-immunoprecipi-

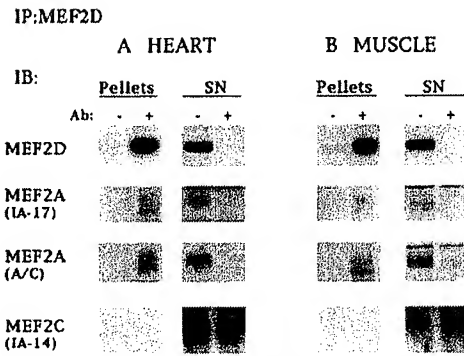


FIG. 4. Immunoprecipitation of MEF2D results in the co-precipitation of MEF2A in striated muscle nuclear extracts. Heart (A) and hindlimb skeletal muscle (B) were obtained from control rats. The nuclear extracts (50  $\mu$ g) were immunoprecipitated with the MEF2D monoclonal antibody, and the resultant pellets and supernatants (SN) were subjected to 10% SDS-polyacrylamide gel electrophoresis and transferred to a nitrocellulose membrane. The membranes were then immunoblotted with the MEF2D polyclonal antibody the MEF2A IA-17 polyclonal antibody, the MEF2A polyclonal antibody (MEF2A/C) and the MEF2C IA-14 polyclonal antibody as described under "Experimental Procedures." This is a representative experiment independently performed three times for each tissue.

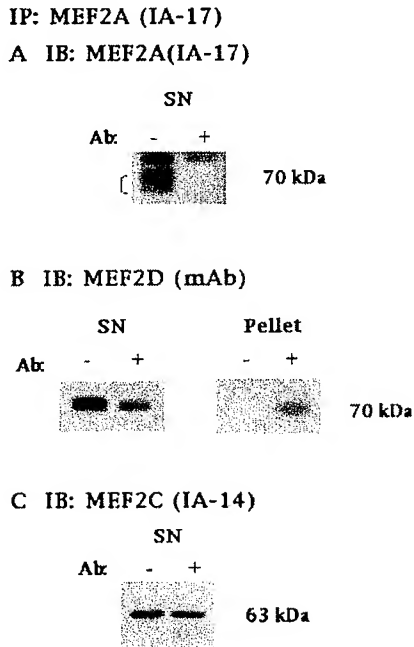


FIG. 5. Immunoprecipitation of MEF2A results in the partial co-precipitation of MEF2D in heart nuclear extracts. Heart nuclear extracts (50  $\mu$ g) were immunoprecipitated with the MEF2A IA-17 polyclonal antibody linked to protein A beads as described under "Experimental Procedures." Equal volumes of samples were resolved by 10% SDS-polyacrylamide gel electrophoresis and transferred to a nitrocellulose membranes. A, the resulting supernatant (SN) was immunoblotted with the MEF2A IA-17 antibody. B, the resulting supernatant (SN) and pellet were immunoblotted with the MEF2D monoclonal antibody. C, the resulting supernatant (SN) was immunoblotted with the MEF2C IA-14 polyclonal antibody as described under "Experimental Procedures." This is a representative experiment independently performed two times.

tation of MEF2C with MEF2A or MEF2D. Nevertheless, these data indicate that the majority of the MEF2A protein existing as a heterodimeric complex with MEF2D, whereas MEF2D is found in both a heterodimeric complex with MEF2A and as a MEF2D-MEF2D homodimeric complex. Importantly, MEF2C is apparently not complexed with either MEF2A or MEF2D

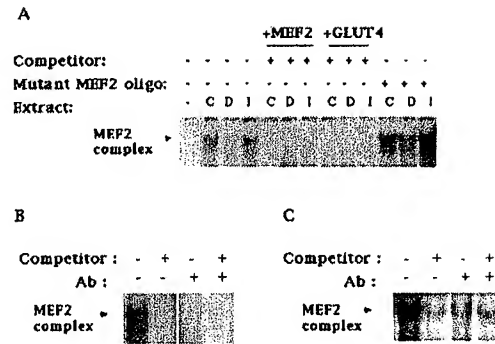


FIG. 6. Insulin-deficient diabetes results in a decrease DNA binding activity to the MEF2 consensus site. A, heart nuclear extracts (10  $\mu$ g) from control (C), STZ-diabetic (D), or insulin-treated STZ-diabetic (I) rats were incubated with a  $^{32}$ P-labeled 25-base pair MEF2 consensus double-stranded oligonucleotide as described under "Experimental Procedures." Specific binding was determined by electrophoretic mobility shift assay in the absence or presence of a 100-fold molar excess of unlabeled muscle creatine kinase (+MEF2) oligonucleotide, a 18-base pair oligonucleotide corresponding to the MEF2 site in the GLUT4 gene (+GLUT4), or a mutated MEF2 oligonucleotide. B, the heart nuclear extracts were first immunodepleted with the MEF2A IA-17 polyclonal antibody and equal volumes of supernatants were subjected to electrophoretic mobility shift assays in the absence and presence of 100-fold excess cold competitor oligonucleotide. C, the heart nuclear extracts were first immunodepleted with the MEF2D monoclonal antibody and equal volumes of supernatants were subjected to electrophoretic mobility shift assays in the absence and presence of 100-fold excess cold competitor oligonucleotide. This is a representative experiment independently performed two times for each antibody.

and therefore must necessarily be present as a homodimeric MEF2C-MEF2C complex, or perhaps complexed to another transcription factor.

**The MEF2A-MEF2D Heterodimeric Complex Interacts with the GLUT4 MEF2-responsive Element**—To assess the functional binding properties of the MEF2 dimeric complexes from heart nuclear extracts, we next examined MEF2 DNA binding by electrophoretic mobility shift assays (Fig. 6). Using a consensus MEF2 double-stranded oligonucleotide, we observed that heart nuclear extracts resulted in a specific decrease in the mobility of the labeled probe. In agreement with previous findings (15), the MEF2-DNA complexed band was substantially reduced in extracts isolated from diabetic animals compared with controls rats but which fully recovered following insulin treatment (Fig. 6A). This binding activity was specifically blocked in the presence of either the myosin creatine kinase or GLUT4 unlabeled MEF2 element but not by a mutant MEF2 oligonucleotide with two substitutions (C  $\rightarrow$  G and A  $\rightarrow$  C), in the consensus core sequence (mutant oligonucleotide sequence: 5'-GATCGCTGTAAACATAACCCGTGCG-3'), that impair MEF2 binding (15). Furthermore, the MEF2 sequence-dependent binding activity was completely lost when the nuclear extracts were immunodepleted with either the MEF2D- or MEF2A-specific antibody (Fig. 6, B and C). These data indicate that the heterodimer MEF2A-MEF2D interacts with the MEF2-responsive element.

**Addition of MEF2A to Nuclear Extracts from Diabetic Animals Restores Binding Activity to the MEF2 Site**—Since nuclear extracts from diabetic animals have reduced levels of MEF2A but have normal amounts of MEF2D, re-addition of MEF2A protein should restore binding activity to this site. To this end, we prepared different dilutions of *in vitro* translated MEF2A protein and compared these to the endogenous MEF2A protein present in control extracts (Fig. 7A). The amount of *in vitro* translated MEF2A protein present in 0.15–0.3  $\mu$ l of transcription reaction was found to be similar to the endogenous

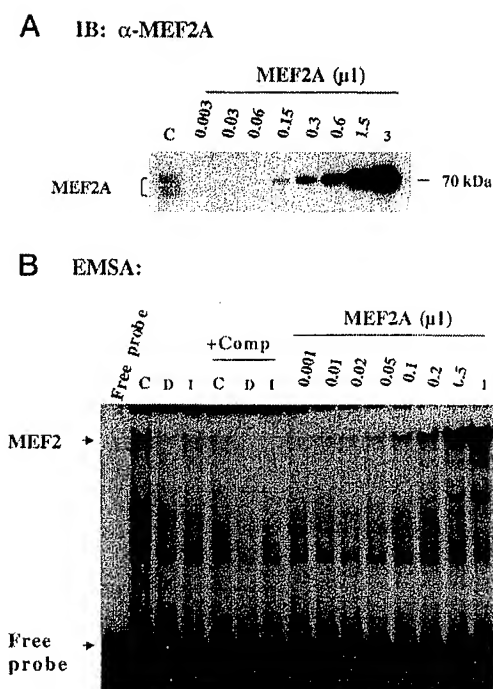


FIG. 7. Addition of *in vitro* translated MEF2A protein restores DNA binding activity in nuclear extracts from diabetic rats. **A**, control heart nuclear extracts from (30  $\mu$ g) and increasing amounts of *in vitro* translated MEF2A protein (0.003, 0.03, 0.06, 0.15, 0.3, 0.6, 1.5, and 3  $\mu$ l of the reaction) were subjected to Western blotting as described under "Experimental Procedures." **B**, nuclear extracts (10  $\mu$ g) obtained from control (C), STZ-diabetic (D), and insulin-treated STZ-diabetic rats (I) were subjected to electrophoretic mobility shift assay using the  $^{32}$ P-labeled 25-base pair MEF2 consensus double-stranded oligonucleotide in the absence or presence of 100-fold excess unlabeled competitor oligonucleotide. The diabetic extracts (10  $\mu$ g) were also pre-mixed with increasing amounts of *in vitro* translated MEF2A (0.001, 0.01, 0.02, 0.05, 0.1, 0.2, 0.5, and 1  $\mu$ l of the reaction), in the same proportion of the samples used for Western blot in panel A. This is a representative experiment independently performed two times.

level of MEF2A in 30  $\mu$ g of control nuclear extracts. The same dilutions were proportionally added to nuclear extracts from diabetic animals and tested for binding activity to the MEF2 site (Fig. 7B). The addition of similar amounts of MEF2A to the diabetic nuclear extracts restored binding up to a level comparable to that observed in the control extract. In fact, further addition of excess MEF2A resulted in increased binding, probably due to both MEF2A-MEF2D complex formation and the presence of MEF2A-MEF2A homodimers. Taken together, these data demonstrate that the MEF2A-MEF2D complex is responsible for binding to the GLUT4 MEF2 site and that the down-regulation of MEF2A protein levels in insulin-deficient diabetes accounts for the lack of GLUT4 gene expression in striated muscle.

#### DISCUSSION

It has been well established that insulin stimulates the recruitment or translocation of pre-formed GLUT4 glucose transporter proteins from intracellular storage sites to the cell surface membrane (1–3, 5). This process is necessary for normal tissue (striated muscle and adipose) insulin sensitivity and the maintenance of whole body glucose homeostasis. However, in addition to the acute stimulation of GLUT4 protein intracellular trafficking, the tissue-specific expression levels of GLUT4 are also regulated by a variety of hormonal/nutritional/metabolic states. For example, GLUT4 expression is markedly up-regulated during muscle and adipose differentiation and fol-

lowing muscle exercise/contraction (34–36). In contrast, states of relative insulin deficiency (type I diabetes and fasting) result in decreased GLUT4 expression (7, 26). Furthermore, although there was no effect on muscle GLUT4 levels in patients with non-insulin-dependent diabetes, there was a selective loss of GLUT4 protein in adipose tissue (37).

Based upon these data, we and others have begun to identify the cis-regulatory elements that are necessary for the tissue-specific and regulated expression of the GLUT4 gene. Recently, we have identified a consensus MEF2 binding sequence located at (–473/–464) in the human GLUT4 gene (13, 15). Deletions or point mutations within this element completely prevented tissue-specific and hormonally/metabolically regulated expression in both differentiating culture muscle C2C12 cells and more importantly in transgenic mice (15). Furthermore, DNA binding activity to this sequence was markedly reduced in nuclear extracts from insulin-deficient diabetic rats but was fully restored following insulin therapy. Thus, these data provide compelling evidence that the MEF2 binding site is, at least, one essential functional element in the expression of the GLUT4 gene.

There are four known members of the mammalian MEF2 family of transcription factor, and since MEF2B expression is restricted to early embryo development (29, 30), the other MEF2 isoforms were likely candidates responsible for the loss of DNA binding activity in nuclear extracts from diabetic animals. To this end, Western blotting using isoform-specific antibodies demonstrated that only the level of MEF2A protein was down-regulated in both skeletal muscle and heart of insulin-deficient diabetic rats. Interestingly, the mRNA of MEF2C was also decreased; however, this did not result in any significant change in protein expression. Previous studies have also observed a discordance in the levels of MEF2 mRNA versus protein, suggesting the presence of post-transcriptional control mechanism(s) (31, 32). In any case, the decrease in MEF2A expression correlated with the decrease in GLUT4 gene expression and reduction in nuclear extract binding activity to the MEF2 consensus sequence. These findings were confirmed by the addition of *in vitro* translated MEF2A protein to diabetic nuclear extracts, which at the appropriate endogenous amount restored the DNA binding activity to the same level as found in control nuclear extracts.

At present, the mechanism(s) regulating MEF2 gene expression and protein levels remains largely unknown. All the MEF2 genes contain large 5'-noncoding regions with multiple spliced exons and large introns. In *Drosophila*, two D-MEF enhancers have been described, one that binds the cardiac homeodomain protein Tinman (38) and another controlled by the basic helix-loop helix transcription factor Twist (39). However, no cis-regulatory sequences have yet been described for any vertebrate MEF2 gene. Alternatively, MEF2A and also MEF2C can be transcriptionally activated by phosphorylation through the p38 mitogen-activated protein kinase (40–43) and protein kinase C isoforms (41). In addition, MEF2C has been reported to undergo nuclear export into the cytoplasm following transforming growth factor- $\beta$  stimulation (44).

Although we cannot exclude these possibilities for the loss of MEF2A expression in muscles of insulin-deficient diabetic rats, an additional mechanism may be envisaged based upon the dimerization of the MEF2 isoforms. In this study, we have also observed that the MEF2A antibody will co-immunoprecipitate approximately one-third of the MEF2D protein, whereas the MEF2D antibody will co-immunoprecipitate essentially all of the MEF2A protein. These data suggest that all the MEF2A protein exists as an MEF2A-MEF2D heterodimer. Since MEF2C is not co-immunoprecipitated with MEF2D, these data



further indicate that the excess MEF2D is present in an MEF2D-MEF2D homodimer. The presence of an MEF2A-MEF2D heterodimer is consistent with studies in the HeLa cell system but is somewhat in disagreement with cultured C2C12 cells (45). In any case, decreased MEF2A expression would therefore increase the relative proportion of MEF2D-MEF2D homodimers. Although it has been suggested that MEF2D homodimers can function as a transcriptional inhibitor (45), we do not feel that this is likely for the GLUT4 promoter. The fact that decreased levels of MEF2A, either in diabetic nuclear extracts or by MEF2A antibody immunodepletion, markedly reduces DNA binding strongly suggests the MEF2D homodimer has a relatively low affinity for the GLUT4 MEF2 element.

In summary, our data demonstrate that MEF2A protein levels are selectively reduced in striated muscle of insulin-deficient diabetic rats. This loss of MEF2A expression accounts for the reduction in DNA binding activity and directly correlates with the decrease in GLUT4 gene expression. Future studies are now needed to determine whether the down-regulation of MEF2A expression occurs at the transcriptional or post-transcriptional level. In addition, further analysis will be necessary to determine the specific functional roles of the MEF2A-MEF2D heterodimer and MEF2D-MEF2D homodimer in the control of GLUT4 transcriptional activity.

**Acknowledgment**—We thank Dr. Ron Prywes for kindly providing the MEF2A/C and MEF2D antibodies.

#### REFERENCES

- Pessin, J. E., Thurmond, D. C., Elmendorf, J. S., Coker, K. J., and Okada, S. (1999) *J. Biol. Chem.* **274**, 2593–2596
- Martin, S., Slot, J., and James, D. (1999) *Cell Biochem. Biophys.* **30**, 89–113
- Kandror, K. V., and Pilch, P. F. (1996) *Am. J. Physiol.* **271**, E1–E14
- Holman, G. D., Lo Leggio, L., and Cushman, S. W. (1994) *J. Biol. Chem.* **269**, 17516–17524
- Zorzano, A., Muñoz, P., Camps, M., Mora, C., Testar, X., and Palacin, M. (1996) *Diabetes* **45**, S70–S81
- St Denis, S., and Cushman, S. (1998) *J. Basic Clin. Physiol. Pharmacol.* **9**, 153–165
- Camps, M., Castello, A., Munoz, P., Monfar, M., Testar, X., Palacin, M., and Zorzano, A. (1992) *Biochem. J.* **282**, 765–772
- Neufer, P. D., Carey, J. O., and Dohm, G. L. (1993) *J. Biol. Chem.* **268**, 13824–13829
- Bourey, R. E., Koranyi, L., James, D., Mueckler, M., and Permutt, A. (1990) *J. Clin. Invest.* **86**, 542–547
- Olson, A. L., Edgington, N. P., Moye-Rowley, W. S., and Pessin, J. E. (1995) *Endocrinology* **136**, 1962–1968
- Cooke, D. W., and Lane, M. D. (1998) *J. Biol. Chem.* **273**, 6210–6217
- Cooke, D. W., and Lane, M. D. (1999) *J. Biol. Chem.* **274**, 12917–12924
- Liu, M. L., Olson, A. L., Edgington, N. P., Moye-Rowley, W. S., and Pessin, J. E. (1994) *J. Biol. Chem.* **269**, 28514–28521
- Tsunoda, N., Cooke, D. W., Ikemoto, S., Maruyama, K., Takahashi, M., Lane, M. D., and Ezaki, O. (1997) *Biochem. Biophys. Res. Commun.* **239**, 503–509
- Thai, M. V., Guruswamy, S., Cao, K. T., Pessin, J. E., and Olson, A. L. (1998) *J. Biol. Chem.* **273**, 14285–14292
- Black, B. L., and Olson, E. N. (1998) *Annu. Rev. Cell. Dev.* **14**, 167–196
- Brand, N. (1997) *Int. J. Biochem. Cell Biol.* **12**, 1467–1470
- Naidu, P. S., Ludolph, D. C., To, R. Q., Hinterberger, T. J., and Konieczny, S. F. (1995) *Mol. Cell. Biol.* **15**, 2707–2718
- Ornatsky, O. I., Andreucci, J. J., and McDermott, J. C. (1997) *J. Biol. Chem.* **272**, 33271–33278
- Molkentin, J. D., Black, B. L., Martin, J. F., and Olson, E. N. (1995) *Cell* **83**, 1125–1136
- Molkentin, J., and Olson, E. (1996) *Proc. Natl. Acad. Sci. U. S. A.* **93**, 9366–9373
- Lee, Y., Nadal-Ginard, B., Mahdavi, V., and Izumo, S. (1997) *Mol. Cell. Biol.* **17**, 2745–2755
- Black, B. L., Ligon, K. L., Zhang, Y., and Olson, E. N. (1996) *J. Biol. Chem.* **271**, 26659–26663
- Black, B. L., Molkentin, J. D., and Olson, E. N. (1998) *Mol. Cell. Biol.* **18**, 69–77
- Brand-Saberi B., and Christ, B. (1999) *Cell Tissue Res.* **296**, 199–212
- Richardson, J. M., Balon, T. W., Treadway, J. L., and Pessin, J. E. (1991) *J. Biol. Chem.* **266**, 12690–12694
- Olson, A. L., and Pessin, J. E. (1994) *Endocrinology* **134**, 271–276
- Ausubel, F., Brent, R., Kingston, R. E., Moore, D. D., Seidman, J. G., Smith, J. A., and Struhl, K. (1994) *Current Protocols in Molecular Biology*, pp. 3.10.1–3.10.5, John Wiley & Sons, New York
- Morisaki, T., Sermsuvitayawong, K., Byun, S. H., Matsuda, Y., Hidaka, K., Morisaki, H., and Mukai, T. (1997) *J. Biochem. (Tokyo)* **122**, 939–946
- Molkentin, J. D., Firulli, A. B., Black, B. L., Martin, J. F., Hustad, C. M., Copeland, N., Jenkins, N., Lyons, G., and Olson, E. N. (1996) *Mol. Cell. Biol.* **16**, 3814–3824
- Yu, Y. T., Breithart, R. E., Smoot, L. B., Lee, Y., Mahdavi, V., and Nadal-Ginard, B. (1992) *Genes Dev.* **6**, 1783–1798
- Suzuki, E., Guo, K., Kolman, M., Yu, Y., and Walsh, K. (1995) *Mol. Cell. Biol.* **15**, 3415–3423
- Tae-Hee, H., and Prywes, R. (1995) *Mol. Cell. Biol.* **15**, 2907–2915
- Castello, A., Cadefau, J., Cusso, R., Testar, X., Hesketh, J. E., Palacin, M., and Zorzano, A. (1993) *J. Biol. Chem.* **268**, 14998–15003
- Ren, J. M., Semenkovich, C. F., Gulve, E. A., Gao, J., and Holloszy, J. O. (1994) *J. Biol. Chem.* **269**, 14396–14401
- Kawanaka, K., Higuchi, M., Ohmori, H., Shimegi, S., Ezaki, O., and Katsuta, S. (1996) *Horm. Metab. Res.* **28**, 75–80
- Garvey, W. T. (1992) *Diabetes Care* **15**, 396–417
- Gajewski, K., Kin, Y., Lee, Y. M., Olson, E. N., and Schulz, R. A. (1997) *EMBO J.* **16**, 515–522
- Cripps, R. M., Black, B. L., Zhao, B., Lien, C.-L., Schulz, R. A., and Olson, E. N. (1998) *Genes Dev.* **12**, 422–434
- Yang, S., Galanis, A., and Sharrocks, A. (1999) *Mol. Cell. Biol.* **19**, 4028–4038
- Ornatsky, O. I., Cox, D. M., Tangirala, P., Andreucci, J. J., Quinn, Z. A., Wrana, J. L., Prywes, R., Yu, Y., and McDermott, J. C. (1999) *Nucleic Acids Res.* **27**, 2646–2654
- Zhao, M., Ligu, N., Kravchenko, V., Kato, Y., Gram, H., Di Padova, F., Olson, E., Ulevitch, R., and Han, J. (1999) *Mol. Cell. Biol.* **19**, 21–30
- Zetser, A., Gredinger, E., and Bengal, E. (1999) *J. Biol. Chem.* **274**, 5193–5200
- De Angelis, L., Borghi, S., Melchionna, R., Berghella, L., Baccarani-Contri, M., Parise, F., Ferrari, S., and Cossu, G. (1998) *Proc. Natl. Acad. Sci. U. S. A.* **95**, 12358–12363
- Ornatsky, O. I., and McDermott, J. C. (1996) *J. Biol. Chem.* **271**, 24927–24933



## EXHIBIT 3

## Cooperative Transcriptional Activation by the Neurogenic Basic Helix-Loop-Helix Protein MASH1 and Members of the Myocyte Enhancer Factor-2 (MEF2) Family\*

(Received for publication, July 23, 1996)

Brian L. Black<sup>‡§</sup>, Keith L. Ligon<sup>¶</sup>, Yuan Zhang<sup>‡</sup>, and Eric N. Olson<sup>‡¶</sup>

From the <sup>‡</sup>Department of Molecular Biology and Oncology, Hamon Center for Basic Cancer Research, University of Texas Southwestern Medical Center, Dallas, Texas 75235 and the <sup>¶</sup>Department of Biochemistry and Molecular Biology, University of Texas M. D. Anderson Cancer Center, Houston, Texas 77030

Establishment of skeletal muscle and neural cell types is controlled by families of myogenic and neurogenic basic helix-loop-helix (bHLH) proteins, respectively. Myogenic bHLH proteins have been shown to activate skeletal muscle transcription in collaboration with members of the myocyte enhancer factor-2 (MEF2) family of MCM1-agamous-deficiens-serum response factor (MADS)-box transcription factors, which are expressed in differentiated myocytes and neurons. Here, we show that the neurogenic bHLH protein MASH1 interacts with members of the MEF2 family and that this interaction, mediated by the DNA binding and dimerization domains of these factors, results in synergistic activation of transcription through either the MASH1 or the MEF2 DNA binding site. Consistent with their involvement in activation of neuronal gene expression, members of the MEF2 family are expressed in P19 embryonal carcinoma cells that have been induced to form neurons following treatment with retinoic acid. These results suggest that members of the MEF2 family perform similar roles in synergistic activation of transcription in myogenic and neurogenic lineages by serving as cofactors for cell type-specific bHLH proteins.

Recent studies suggest that there are parallels between the mechanisms that regulate differentiation in the myogenic and neurogenic lineages (1). Formation of skeletal muscle is controlled by a family of myogenic basic helix-loop-helix (bHLH)<sup>1</sup> proteins, MyoD, myogenin, Myf5, and MRF4, which are expressed specifically in skeletal muscle and can activate the complete program for skeletal muscle differentiation when expressed in several non-muscle cell types (2). Similarly, the

formation of central and peripheral neurons in *Drosophila* has been shown to be controlled by the achaete-scute family of bHLH factors, which are expressed in neuronal precursors and differentiated neurons (1). Two mammalian achaete-scute homologs (MASH) have been identified (3). One of these factors, MASH1, is expressed in subsets of cells in the peripheral and central nervous systems and is required for the formation of the peripheral nervous system during mouse embryogenesis (4–6). Cell type-specific bHLH proteins like the myogenic and neurogenic factors form heterodimers with a family of ubiquitous bHLH factors known as E proteins, which includes the products of the *E2A* gene, *E12* and *E47*, *HEB*, and the *Drosophila* *daughterless* gene product (7–9). These heterodimers bind the E box consensus sequence, CANNTG, which is found in the control regions of numerous muscle-specific genes, as well as other cell type-specific genes (7).

Myogenic bHLH proteins activate muscle-specific transcription in collaboration with members of the myocyte enhancer factor-2 (MEF2) family of transcription factors (10). There are four vertebrate *mef2* genes, *mef2a*, *mef2b*, *mef2c*, and *mef2d* (11–17), whose products bind as homo- and heterodimers to an A/T-rich DNA consensus sequence associated with numerous muscle-specific genes (18). MEF2 proteins are members of the MADS (MCM1-Agamous-Deficiens-serum response factor) family of transcription factors. The MADS domain and the adjacent MEF2 domain encompass the first 86 amino acids, and together these domains mediate DNA binding and dimerization (10). Recent studies have shown that members of the MEF2 family interact directly with heterodimers formed between myogenic bHLH proteins and E proteins and that the DNA binding and dimerization domains of these two different classes of transcription factors mediate this interaction (19, 20). In addition to being expressed in differentiated muscle cells, members of the MEF2 family are expressed in the developing brains of vertebrates in specific patterns that correlate with neuronal differentiation (13, 21, 22). Similarly, the single *mef2* gene in *Drosophila*, *D-mef2*, is expressed in developing muscle and in the central and peripheral nervous systems (23).

Like differentiating skeletal muscle cells, differentiating neurons exit the cell cycle irreversibly and up-regulate an array of tissue-specific genes. Given the high levels of MEF2 expression in differentiated neurons and the similar roles of bHLH proteins in specifying myogenic and neurogenic cell fates, we examined whether MEF2 factors might act as cofactors for the neurogenic bHLH protein MASH1 in a manner analogous to their interaction with myogenic bHLH factors. Our results show that MEF2 factors interact directly with MASH1/E12 heterodimers to synergistically activate transcription. These results suggest that MEF2 factors are cofactors

\* This work was supported by grants from the National Institutes of Health, the Muscular Dystrophy Association, the Robert A. Welch Foundation, and the Human Sciences Frontiers Program (to E. N. O.). The costs of publication of this article were defrayed in part by the payment of page charges. This article must therefore be hereby marked "advertisement" in accordance with 18 U.S.C. Section 1734 solely to indicate this fact.

<sup>§</sup> American Cancer Society postdoctoral fellow.

<sup>¶</sup> To whom correspondence should be addressed: Dept. of Molecular Biology & Oncology, Hamon Center for Basic Cancer Research, University of Texas Southwestern Medical Center at Dallas, 5323 Harry Hines Blvd., Dallas, TX 75235-9148. Tel.: 214-648-1191; Fax: 214-648-1196; E-mail: eolson@hamon.swmed.edu.

<sup>1</sup> The abbreviations used are: bHLH, basic helix-loop-helix; CAT, chloramphenicol acetyltransferase; DBD, DNA binding domain; DMEM, Dulbecco's modification of minimal essential medium; FCS, fetal calf serum; MADS, MCM1-agamous-deficiens-serum response factor; MASH, mammalian achaete-scute homolog; MCK, muscle creatine kinase; NCAM, neural cell adhesion molecule; RA, retinoic acid; PAGE, polyacrylamide gel electrophoresis; VP16, herpes virus virion protein 16; MEF2, myocyte enhancer factor-2.

that positively modulate the transcriptional activities of bHLH proteins in both myogenic and neurogenic lineages.

#### MATERIALS AND METHODS

**Cell Culture and Western Blots**—10T1/2 cells were maintained in DMEM supplemented with 10% fetal calf serum (FCS). P19 embryonal carcinoma cells were maintained in DMEM supplemented with 7.5% calf serum and 2.5% FCS. P19 cells ( $5 \times 10^5$  cells/plate) were aggregated in 60-mm bacterial Petri dishes for 4 days. For cells treated with retinoic acid (RA), RA was added at a concentration of  $1 \mu\text{M}$  for the first 48 h of aggregation. Following aggregation, the P19 cell aggregates were dispersed and replated in 60-mm tissue culture plates and were maintained for an additional 4 days. All cells were fed with fresh medium every 48 h.

Western blots were performed as described previously (24). Briefly, cells were lysed in cracking buffer, and equivalent quantities of total cellular protein were separated by SDS-PAGE and transferred to nitrocellulose membranes. Proteins were detected using an enhanced chemiluminescence kit (Amersham Corp.). The polyclonal rabbit anti-MEF2A antibody was purchased from Santa Cruz Biotechnology. The polyclonal anti-MEF2D (kindly provided by Ron Prywes, Columbia University) and anti-MEF2C antibodies have been described (24). Monoclonal anti-NCAM and  $\alpha$ -tubulin were purchased from Sigma.

**Plasmids, Transfections, and CAT Assays**—The MEF2 expression plasmids used in this study are described elsewhere (25) and encode the MEF2 factors in plasmid pCDNA1/amp (Invitrogen, Inc.). The full-length MASH1 cDNA was expressed under control of the Rous sarcoma virus long terminal repeat in plasmid pRSVSV40 and was kindly provided by David Anderson (26). The full-length MASH1 and MASH1 bHLH cDNAs were also expressed as Myc-tag fusions in plasmid pCS2MT(+) (27). No differences in activation or interaction were observed for full-length MASH1 expressed under control of either promoter. The stability and expression of MASH1 and MASH1 bHLH were confirmed *in vitro* and *in vivo* using the Myc-tag vectors by *in vitro* translation and Western blot, respectively (data not shown). The E12 expression plasmid encodes a partial cDNA containing the E12 bHLH region, but lacking a transactivation domain (7). The E-box-dependent reporter, 4RtkCAT, contains four tandem copies of the right E-box from the muscle creatine kinase (MCK) enhancer and has been described previously (28). MASH1/E12 heterodimers have been reported to activate transcription through the MCK E-box (29). The MEF2-dependent reporter plasmid, pE102MEF2 $\times$ 2CAT, which contains two copies of the MCK enhancer MEF2 site upstream of the embryonic myosin heavy chain promoter (12) and the GAL4-dependent reporter plasmid, pG5E1bCAT, have been described previously (20). Plasmids GAL (DBD)-E12 bHLH and GAL(DBD)-MASH1 bHLH encode the DNA binding domain (DBD) of yeast GAL4 (amino acids 1–147) fused to either the bHLH region of E12 or MASH1, respectively. Plasmids 1–117 and 1–117/VP16 encode amino acids 1–117 of MEF2C either alone or fused to the activation domain of the viral activator, VP16.

10T1/2 cells were transfected by calcium phosphate precipitation, and tri-hybrid assays were performed as described previously (20). In each transfection, 10-cm plates were transfected with 5  $\mu\text{g}$  of each plasmid. In transfections in which not all expression plasmids were transfected, 5  $\mu\text{g}$  of the appropriate parental expression plasmid without a cDNA insert were cotransfected such that all transfections received the same amount of DNA and the same amount of each expression plasmid. Lysates for CAT assays were prepared and normalized using standard techniques as described previously (25). Conversion to acetylated forms was analyzed by thin-layer chromatography and quantitated by PhosphorImager analysis (Molecular Dynamics, Inc.).

#### RESULTS

**MEF2 Factors Are Up-regulated during Neural Differentiation**—Previous studies of MEF2 gene expression in the developing mouse showed MEF2 transcripts present in the embryonic brain during the time of neural differentiation and development (13, 21, 22). The pattern of MEF2 expression in the developing central nervous system of the mouse overlaps with the expression of MASH1 during embryogenesis (4). Based on these studies, we were interested in whether MEF2 factors were expressed during differentiation of neuronal cells in culture. P19 embryonal carcinoma cells when aggregated in the presence of RA differentiate to form neurons with a few cells resembling other neuronal cell types such as astrocytes

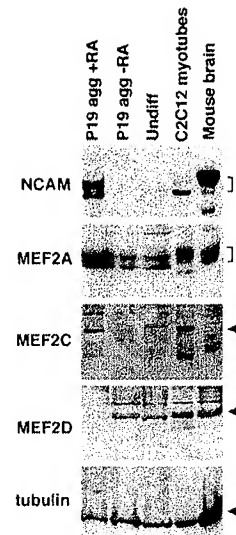


**FIG. 1. Western blot analyses of extracts from neuronal cells.** Extracts were prepared from differentiated and undifferentiated P19 cells as described under "Materials and Methods." Blots were probed with the antibodies indicated to the left of each panel. Arrows or brackets denote the positions of each of the indicated proteins. P19 cells were differentiated into neurons by aggregation and retinoic acid treatment (*agg +RA*), were differentiated into endodermal cells by aggregation in the absence of retinoic acid (*agg -RA*), or were undifferentiated (*undiff*). C2C12 myotube extracts and neonatal mouse brain extracts were included as controls for MEF2 protein and NCAM expression, respectively. The MEF2 proteins identified by Western blot comigrated with *in vitro* translated MEF2 proteins, which were specifically detected by the antibodies used (not shown). The size of each protein was confirmed by comparison with the migration of Bio-Rad kaleidoscope high molecular weight markers (not shown). Equivalent levels of total protein were loaded into each lane as verified by staining of SDS-PAGE gels with Coomassie Brilliant Blue (data not shown). The ubiquitously expressed protein  $\alpha$ -tubulin was also analyzed to confirm the Coomassie staining results.

and glial cells (30–32). Aggregation of P19 cells in the absence of RA results in differentiation to endodermal or mesodermal fates (30, 31, 33). We were particularly interested in this cell line, since upon aggregation of P19 cells in the presence of RA, MASH1 expression is dramatically up-regulated, and its expression persists until the after the cells are fully differentiated (26).

Fig. 1 shows the results of Western blot analyses performed on extracts isolated from P19 cells that had been differentiated by aggregation in the presence or absence of RA or were undifferentiated. The P19 cell extracts were compared with extracts isolated from C2C12 myotubes and from neonatal mouse brain for the expression of MEF2 proteins and the neural marker, NCAM. Analysis of NCAM expression showed a dramatic up-regulation in P19 cells differentiated in the presence of RA (Fig. 1), confirming the neural phenotype that nearly every cell in the population visually displayed following treatment with RA (data not shown).

Analysis of MEF2 protein expression in P19 cells (Fig. 1) showed that MEF2A was slightly up-regulated in RA-treated cells when compared with untreated cells. MEF2C was dramatically up-regulated upon neuronal differentiation of P19 cells. Blots probed with  $\alpha$ -MEF2C antiserum displayed almost no detectable MEF2C in undifferentiated or endodermally differentiated P19, whereas MEF2C was present in aggregated RA-treated P19 at levels nearly as high as in fully differentiated myotubes. In contrast, MEF2D was down-regulated upon neuronal differentiation. This result is consistent with the observation that MEF2D is involved in serum-mediated cell prolifera-

tion (34). The observation that MEF2C is up-regulated as P19 cells differentiate into neurons is consistent with the notion that MEF2C may be involved in neuronal maturation and suggests that MEF2C may collaborate with MASH1 to activate neuronal specific transcription. This idea is supported by the observation that MASH1 is also dramatically induced as P19 cells undergo neuronal differentiation but, like MEF2C, is not expressed in undifferentiated P19 cells or in P19 cells aggregated in the absence of RA (26). This idea is also supported by the overlapping patterns of MASH1 and MEF2C expression during embryogenesis (4, 21, 22).

**MEF2 Factors Interact with MASH1/E12 Heterodimers**—To determine whether MEF2 proteins interact directly with MASH1, we used a tri-hybrid assay in which a CAT reporter gene under control of the GAL4 DNA binding site was transfected into 10T1/2 fibroblasts with expression vectors encoding the bHLH region of E12 fused to the DNA binding domain of GAL4 along with MASH1, MEF2A, MEF2D, or MEF2C (Fig. 2B). A schematic representative of this assay is shown in Fig. 2A. The GAL4-E12 fusion protein, GAL(DBD)-E12 bHLH (GAL4-E12), failed to activate reporter gene expression alone (lane 2) or in the presence of only the MASH1 bHLH (lane 3). Likewise, GAL4-E12 bHLH plus MEF2C alone did not activate the CAT reporter (lane 7). However, when GAL4-E12 was expressed with the MASH1 bHLH and MEF2A, MEF2D, or MEF2C, activation of the reporter occurred (lanes 4–6). This activation ranged from 4- to 8-fold over the level of activation in the presence of GAL4-E12 alone. None of the MEF2 factors could activate transcription of the reporter alone or with GAL4-E12 alone. Only when the MASH1 bHLH, E12 bHLH, and MEF2 factors were all present together did activation occur.

To further analyze the interaction between MEF2 and MASH1/E12 heterodimers, we used a chimeric protein containing amino acids 1–117 of MEF2C, which includes the MADS and MEF2 domains, fused to the strong viral transactivator protein, VP16. We examined the ability of this chimeric protein (1–117/VP16) to interact with heterodimers formed between full-length MASH1 or the bHLH region of MASH1 and the E12 bHLH. As shown in Fig. 2C, 1–117/VP16 interacted with the E12/MASH1 bHLH heterodimer (lane 7), and strong transactivation of the CAT reporter occurred as a result of the potent activation domain of VP16 fused to MEF2. The strong activation provided by the VP16 transactivation domain allows examination of even relatively weak interactions. In spite of this, no interaction was observed between E12 homodimers and 1–117/VP16 (lane 5) or with GAL4-E12 plus 1–117/VP16 alone (lane 3), indicating that MEF2 can only interact with the heterodimer formed between MASH1 and E12 and not with E12 alone. These results also show that the bHLH region of MASH1 is all that is required for heterodimerization with E12 and subsequent interaction with MEF2. However, interaction between full-length MASH1 and MEF2 also occurred. When GAL4-E12 was expressed together with full-length MASH1, we observed a high level of reporter gene expression, since heterodimer formation brings the strong transcriptional activation domain of MASH1 in proximity to the minimal promoter (lane 8). However, strong synergism still occurred when GAL4-E12 was expressed with full-length MASH1 plus 1–117/VP16 (lane 9). These results demonstrate that MASH1/E12 heterodimers interact with the first 117 amino acids of MEF2, which contain the DNA binding and dimerization motifs present in the MADS and MEF2 domains.

Next, we wanted to more closely examine the regions within MEF2 required for interaction with MASH1/E12. To do this, we used a tri-hybrid system in which the bHLH region of MASH1 was fused to the DNA binding domain of GAL4 in plasmid GAL

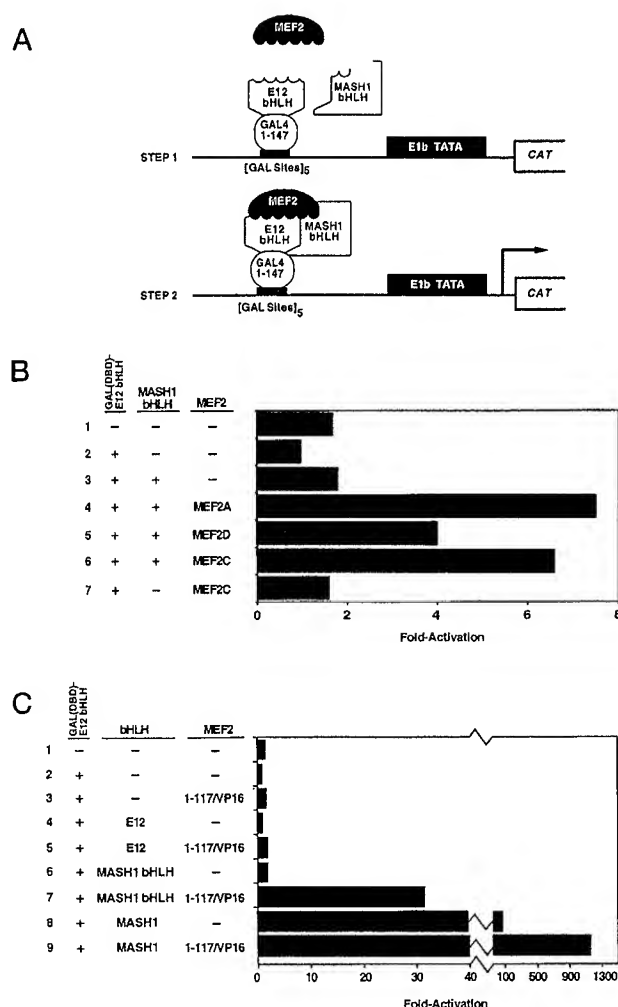
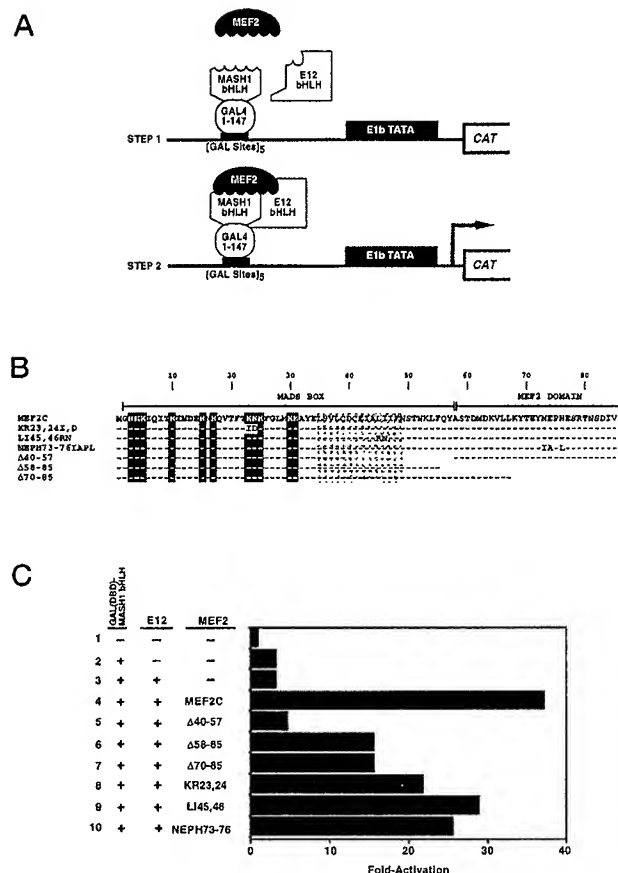


FIG. 2. Interaction between MEF2 factors and MASH1 detected by an *in vivo* tri-hybrid assay. A shows a schematic representation of the tri-hybrid assay used in these experiments. In B and C, 10T1/2 cells were transfected with the GAL4-dependent CAT reporter plasmid, pG5E1bCAT, and the indicated expression plasmids. Plasmids included are indicated by name or with a plus (+) and are described under "Materials and Methods." A minus indicates that the cDNA-encoding plasmid was not included. The results in B and C show the fold activation in CAT activity compared with reporter plus GAL(DBD)-E12 bHLH alone. Extracts used for the analysis in C were serially diluted such that each sample yielded activity in the linear range of the assay. Total extract was held constant in the serial dilutions by using lysate from untransfected 10T1/2 cells. Each panel shows a representative experiment. Similar results were achieved in each of three independent transfections and analyses.

(DBD)-MASH1 bHLH (GAL4-MASH1). A schematic representation is shown in Fig. 3A. In addition, plasmids encoding a truncated form of E12 containing its bHLH but lacking a strong activation domain and full-length MEF2C or various mutants of MEF2C were cotransfected. A schematic of the MEF2C mutants analyzed is shown in Fig. 3B. Analysis of the MEF2C deletion mutants showed that regions in both the MADS and MEF2 domains were important for interaction with MASH1/E12 heterodimers (Fig. 3C, lanes 5–7). In particular, deletion of residues 40–57 resulted in a complete loss of interaction with MASH1/E12 (lane 5). Since this region of MEF2 has been shown to be critical for homodimerization of MEF2C (35), we were interested in whether homodimerization was required for MEF2 to interact with MASH1/E12. Mutation of residues LI 45, 46, which are critical for MEF2 homodimerization (35), had



**FIG. 3. Mutational analysis of the determinants in MEF2 required for interaction with MASH1/E12.** *A* shows a schematic representation of the tri-hybrid assay used in these experiments. *B* shows a schematic representation of the MEF2C mutants analyzed in this experiment. The *blackened areas* denote amino acids essential for MEF2 DNA binding activity. The *stippled area* indicates the residues which mediate MEF2 homodimerization. Analysis of the DNA binding and dimerization of these mutants is described elsewhere (35). In *C*, 10T1/2 cells were cotransfected with the GAL4-dependent CAT reporter plasmid, pG5E1bCAT and GAL(DBD)-MASH1 bHLH and E12 expression plasmid (described under "Materials and Methods"). Also included were expression plasmids for MEF2C (wild-type or mutant) as indicated. The presence of GAL(DBD)-MASH1 bHLH and E12 is indicated with a *plus*. The absence of a cDNA-encoding plasmid is denoted by a *minus*. The fold activation in CAT activity compared with reporter alone in a representative experiment is shown. Nearly identical results were achieved in two independent transfections and analyses.

little or no affect on interaction with MASH1/E12 (*lane 9*). In fact, none of the mutations which changed only a few amino acid residues had a dramatic affect on the ability of MEF2 to interact with MASH1/E12. Therefore, we favor the idea that it is not a few residues within the MADS and MEF2 domains that are responsible for the interaction but rather that larger areas within those domains form a binding surface that mediates interaction with MASH1/E12.

**MEF2 and MASH1 Can Activate Transcription through Each Other's Binding Sites**—We also investigated whether MEF2 and MASH1 could interact to activate transcription through the DNA binding site of the other factor (*Fig. 4*). The heterodimer formed between the bHLH regions of MASH1 and E12 only weakly activated transcription of a CAT reporter linked to tandem copies of the right E-box from the MCK enhancer, because these regions of the proteins lack transcriptional activity (*Fig. 4A*). The weak activation which occurred was likely due to dimerization of the MASH1 bHLH with en-

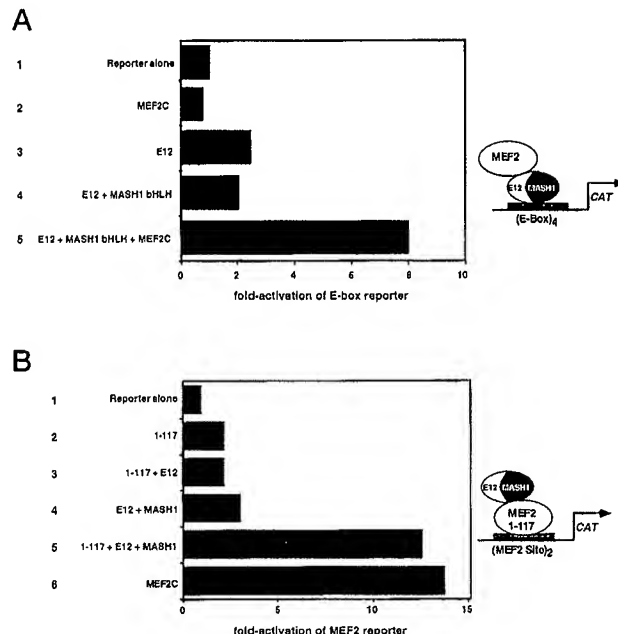


**FIG. 4. MEF2 and MASH1/E12 activate transcription through each other's binding sites.** 10T1/2 cells were transiently transfected with the E box-dependent reporter, 4RtkCAT (*A*), or a MEF2-dependent reporter, pE102MEF2×2CAT (*B*) along with expression vectors encoding E12, MASH1 bHLH, MASH1, or MEF2C, as indicated. Plasmids are described under "Materials and Methods." Values are expressed as the fold induction of CAT activity over the activity of the reporter alone. Each panel shows a representative experiment. Nearly identical results were achieved in two independent transfections and analyses. The diagrams to the right of each panel illustrate how we envision transcriptional activation to be occurring through protein-protein interactions.

ogenous E12, which has a strong transactivation domain. Similarly, full-length MEF2 was unable to activate this reporter gene because the reporter lacks a MEF2 binding site (*Fig. 4A, lane 2*). However, when the bHLH regions of MASH1 and E12 were expressed together with full-length MEF2C, the reporter gene was expressed at high levels (*Fig. 4A, lane 5*). We interpret these results to indicate that the bHLH heterodimer binds the E-box in the reporter and serves as a platform to recruit MEF2 with its transcriptional activation domain, resulting in CAT expression.

Likewise, the DNA binding region of MEF2C, encoded by amino acids 1–117, was unable to activate a CAT reporter gene linked to two copies of the MEF2 site (*Fig. 3B, lane 2*), because amino acids 1–117 of MEF2C do not encode an activation domain (35). This reporter also failed to respond to full-length MASH1 containing its strong activation domain in the presence of E12, because the reporter lacks a binding site for bHLH proteins (*lane 4*). However, when MEF2/1–117 was expressed with full-length MASH1 and E12 bHLH, the reporter gene was expressed at high levels (*lane 5*). In this case, the DNA binding domain of MEF2 appears to recruit the MASH1/E12 bHLH heterodimer to the DNA, and the MASH1 activation domain activates transcription of the reporter gene.

#### DISCUSSION

The results of this study show that members of the MEF2 family interact with heterodimers formed between the neurogenic bHLH protein, MASH1 and E12. The interaction between MEF2 and MASH1/E12 allows either type of factor to activate transcription through the binding site of the other. Considered together with previous studies (19, 20), these results suggest that interactions between MEF2 factors and cell type-specific

bHLH proteins are important for activation of tissue-specific transcription in both the myogenic and neurogenic cell lineages.

In contrast to the myogenic bHLH factors, which can induce muscle differentiation in transfected non-muscle cells, forced expression of MASH1 does not activate neuronal differentiation (26). We have transfected 10T1/2 cells with MASH1 and MEF2 expression vectors and also have not observed activation of neuronal genes. Likewise, we did not observe conversion to neuronal cell fates in P19 cells which were transfected with MASH1 plus MEF2, but were otherwise untreated with RA.<sup>2</sup> Thus, while MEF2 appears to serve as a cofactor for MASH1, these two proteins alone are insufficient to initiate neurogenesis under the conditions of transfection assays. Whether these two factors require additional coregulators remains to be determined.

While this manuscript was in preparation, Mao and Nadal-Ginard reported that MEF2A could cooperate with MASH1 to activate transcription (36). Our results are in general agreement with theirs, but they differ in two respects. In our experiments, MASH1 and MEF2 were able to activate transcription through either factor's binding site when only one of the factors was bound to DNA. In contrast, they reported that both factors needed to bind DNA to cooperatively activate transcription. They also used bacterially expressed proteins *in vitro* and found that MASH1 and MEF2 could interact directly without a need for E12. In our *in vivo* tri-hybrid assays, we found that MASH1 required E12 to efficiently interact with MEF2 proteins. In addition, while we have primarily focused on MEF2C, our results extend the analysis of the interactions to include MEF2A, MEF2C, and MEF2D.

The high levels of MEF2 expression in neuronal cell lines and in differentiated neurons *in vivo* suggest that MEF2 is a regulator of neuron-specific gene expression. We have analyzed the control regions of numerous neuronal genes that have been characterized, and we have identified MEF2 consensus sites within several neuronal genes from mammals and *Drosophila*.<sup>2</sup> In the case of the neuronally restricted *Drosophila* T5 *scute* gene, a perfect consensus MEF2 site overlaps the TATA box in the promoter (37). In addition, there are three functional E-boxes in close proximity to the MEF2 site (37–39). The arrangement of the MEF2 site and the E-boxes in the *scute* gene is strikingly similar to the arrangement of those sites in several muscle-specific promoters where MEF2 and bHLH factors have been shown to collaborate with each other and to activate transcription through each other's binding sites (25, 40–42). These observations and results of this study, taken together with previous studies of myogenesis (19, 20), suggest that members of the MEF2 family of transcription factors serve as general potentiators of cell type-specific transcription in both myogenic and neurogenic lineages by collaborating with tissue-specific bHLH factors.

**Acknowledgments**—We thank A. Tizenor for assistance with graph-

ics, T. Davis for editorial assistance, and R. Prywes and D. Anderson for reagents. We thank Jane Johnson for critical review of the manuscript and for helpful discussions.

#### REFERENCES

- Jan, Y. N., and Jan, L. Y. (1993) *Cell* **75**, 827–830
- Olson, E. N. (1990) *Genes Dev.* **4**, 1454–1461
- Johnson, J. E., Birren, S. J., and Anderson, D. J. (1990) *Nature* **346**, 858–861
- Lo, L. C., Johnson, J. E., Saito, T., and Anderson, D. J. (1991) *Genes Dev.* **5**, 1524–1537
- Guillemot, F., and Joyner, A. L. (1993) *Mech. Dev.* **42**, 171–185
- Guillemot, F., Lo, L. C., Johnson, J. E., Auerbach, A., Anderson, D. J., and Joyner, A. L. (1993) *Cell* **75**, 463–476
- Murre, C., McCaw, P. S., Vaessin, H., Caudy, M., Jan, L. Y., Jan, Y. N., Cabrera, C. V., Buskin, J. N., Hauschka, S. D., Lassar, A. B., Weintraub, H., and Baltimore, D. (1989) *Cell* **58**, 537–544
- Kadesch, T. (1993) *Cell Growth Differ.* **4**, 49–55
- Hu, J.-S., Olson, E. N., and Kingston, R. E. (1992) *Mol. Cell. Biol.* **12**, 1031–1042
- Olson, E. N., Perry, M., and Schulz, R. A. (1995) *Dev. Biol.* **172**, 2–14
- Pollock, R., and Treisman, R. (1991) *Genes Dev.* **5**, 2327–2341
- Yu, Y. T., Breitbart, R. E., Smoot, L. B., Lee, Y., Mahdavi, V., and Nadal-Ginard, B. (1992) *Genes Dev.* **6**, 1783–1798
- Leifer, D., Krainc, D., Yu, Y. T., McDermott, J. C., Breitbart, R., Heng, J., Neve, R. L., Kosofsky, B., Nadal-Ginard, B., and Lipton, S. A. (1993) *Proc. Natl. Acad. Sci. U. S. A.* **90**, 1546–1550
- McDermott, J. C., Cardoso, M. C., Yu, Y. T., Andres, V., Leifer, D., Krainc, D., Lipton, S. A., and Nadal-Ginard, B. (1993) *Mol. Cell. Biol.* **13**, 2564–2577
- Breitbart, R., Liang, C., Smoot, L. B., Laheru, D., Mahdavi, V., and Nadal-Ginard, B. (1993) *Development (Camb.)* **118**, 1095–1106
- Martin, J. F., Schwarz, J. J., and Olson, E. N. (1993) *Proc. Natl. Acad. Sci. U. S. A.* **90**, 5282–5286
- Martin, J. F., Miano, J., Hustad, C. M., Copeland, N. G., Jenkins, N. A., and Olson, E. N. (1994) *Mol. Cell. Biol.* **14**, 1647–1656
- Gossett, L. A., Kelvin, D. J., Sternberg, E. A., and Olson, E. N. (1989) *Mol. Cell. Biol.* **9**, 5022–5033
- Kaushal, S., Schneider, J. W., Nadal-Ginard, B., and Mahdavi, V. (1994) *Science* **266**, 1236–1240
- Molkentin, J. D., Black, B. L., Martin, J. F., and Olson, E. N. (1995) *Cell* **83**, 1125–1136
- Lyons, G. E., Micales, B. K., Schwarz, J. J., Martin, J. F., and Olson, E. N. (1995) *J. Neurosci.* **15**, 5727–5738
- Leifer, D., Golden, J., and Kowall, N. W. (1994) *Neuroscience* **63**, 1067–1079
- Schulz, R. A., Chromey, C., Lu, M.-F., Zhao, B., and Olson, E. N. (1996) *Oncogene* **12**, 1827–1831
- Firulli, A. B., Miano, J. M., Weizhen, B. I., Johnson, A. D., Casscells, W., Olson, E. N., and Schwarz, J. J. (1996) *Circ. Res.* **78**, 196–204
- Black, B. L., Martin, J. F., and Olson, E. N. (1995) *J. Biol. Chem.* **270**, 2889–2992
- Johnson, J. E., Zimmerman, K., Saito, T., and Anderson, D. J. (1992) *Development (Camb.)* **114**, 75–87
- Rupp, R. A., Snider, L., and Weintraub, H. (1994) *Genes Dev.* **8**, 1311–1323
- Weintraub, H., Davis, R., Lockshon, D., and Lassar, A. (1990) *Proc. Natl. Acad. Sci. U. S. A.* **87**, 5623–5627
- Johnson, J. E., Birren, S. J., and Anderson, D. J. (1992) *Proc. Natl. Acad. Sci. U. S. A.* **89**, 3596–3600
- Mummery, C. L., Feijen, A., Molenaar, W. H., Van den Brink, C. E., and DeLaat, S. W. (1986) *Exp. Cell Res.* **165**, 229–242
- McBurney, M. W., Reuhl, K. R., Ally, A. I., Nasipuri, S., Bell, J. C., and Craig, J. (1988) *J. Neurosci.* **8**, 1063–1073
- Bain, G., Ray, W. J., Yao, M., and Gottlieb, D. I. (1994) *Bioessays* **16**, 343–348
- Jones-Villeneuve, E. M. V., McBurney, M. W., Rogers, K. A., and Kalnins, V. I. (1982) *J. Cell Biol.* **94**, 253–262
- Han, T.-H., and Prywes, R. (1995) *Mol. Cell. Biol.* **15**, 2907–2915
- Molkentin, J. D., Black, B. L., Martin, J. F., and Olson, E. N. (1996) *Mol. Cell. Biol.* **16**, 2627–2636
- Mao, Z., and Nadal-Ginard, B. (1996) *J. Biol. Chem.* **271**, 14371–14375
- Villares, R., and Cabrera, C. V. (1987) *Cell* **50**, 415–424
- van Doren, M., Ellis, H. M., and Posakony, J. W. (1991) *Development (Camb.)* **113**, 245–255
- Martinez, C., Modolell, J., and Garrell, J. (1993) *Mol. Cell. Biol.* **13**, 3514–3521
- Edmondson, D. G., Cheng, T.-C., Cserjesi, P., Chakraborty, T., and Olson, E. N. (1992) *Mol. Cell. Biol.* **12**, 3665–3677
- Naidu, P. S., Ludolph, D. C., To, R. Q., Hinterberger, T. J., and Konieczny, S. F. (1995) *Mol. Cell. Biol.* **15**, 2707–2718
- Wong, M. W., Pisegna, M., Lu, M.-F., Leibham, D., and Perry, M. (1994) *Development (Camb.)* **166**, 683–695

<sup>2</sup> B. L. Black and E. N. Olson, unpublished observations.

## EXHIBIT 4

PATENT

**IN THE UNITED STATES PATENT AND TRADEMARK OFFICE**

*In re* Application of:

Eric N. OLSON

Serial No.: 10/043,658

Filed: January 9, 2002

For: METHODS FOR PREVENTING  
HYPERTROPHY AND HEART FAILURE  
BY INHIBITION OF MEF2  
TRANSCRIPTION FACTOR

Group Art Unit:

1632

Examiner:

Woitach, Joseph T.

Atty. Dkt. No.:

MYOG:024USC1/SLH

CERTIFICATE OF MAILING

37 C.F.R. § 1.8

I hereby certify that this correspondence is being deposited with the U.S. Postal Service with sufficient postage as First Class Mail in an envelope addressed to: Mail Stop Amendment, Commissioner for Patents, P.O. Box 1450, Alexandria, VA 22313-01450, on the date below:

May 9, 2005

Date

Steven L. Highlander

**DECLARATION OF TIM MCKINSEY UNDER 37 C.F.R. §1.132**

Mail Stop Amendment  
Commissioner for Patents  
P.O. Box 1450  
Alexandria, VA 22313-01450

Dear Sir:

I, Tim McKinsey, do declare the following:

1. I currently hold the position of Scientist II at Myogen, Inc., licensee of the above-captioned application. I also hold academic appointments in the Division of Cardiology at the University of Colorado Health Sciences Center and in the Department of Molecular Biology at the University of Colorado in Boulder. My education and training includes an undergraduate degree in Biological Sciences from University of Missouri and a Ph.D. in



Microbiology and Immunology from Vanderbilt University School of Medicine. I completed four years of post-doctoral training in the Department of Molecular Biology at the University of Texas Southwestern Medical School prior to moving to Colorado. I have published numerous original research papers and multiple reviews on the molecular mechanisms controlling heart muscle disease. In addition, I have given many invited lectures on the topic at universities and at national and international scientific meetings. For the past two years, I have been exclusively engaged in the discovery and validation of molecular drug targets for use in drug discovery in the field of heart failure. I am intimately familiar with the studies of MEF2 and Class II HDACs.

2. I am also familiar with the level of skill of scientists working in the field of cardiology and molecular biology as of the priority date of the referenced application. I consider one of ordinary skill in the art in this field of study to have a Ph.D. in biochemistry, chemistry, molecular biology, pathology or other related field, or an M.D., with 1-3 years of post-graduate study.
3. I have reviewed the specification and pending claims 1, 4, and 9 for the above-referenced case. The application describes and then subsequently claims the inhibition of MEF2 or MEF2 dependent gene transcription as a treatment for hypertrophy. I have also reviewed the examiner's assertions that the current patent specification does not give sufficient guidance for one of skill in the field of cardiac biology to practice the invention without having to undertake extensive experimentation.
4. The inventors' paradigm, as defined through the *in vitro* and *in vivo* models, is that in healthy heart tissue MEF2 is bound to and inactivated by Class II HDACs. A stress

signal or response leads to dissociation of this complex, followed by activation of a "fetal gene" cascade that invariably leads to hypertrophy. Inhibiting MEF2 dependent gene transcription, inhibiting MEF2 itself, or inhibiting the upregulation of a gene that is regulated by MEF2, is therefore considered anti-hypertrophic by the inventors.

5. I have reviewed the enclosed article by Zhang *et al.*, entitled "Class II Histone Deacetylases Act as Signal-Responsive Repressors of Cardiac Hypertrophy," *Cell*, 110:479-488 (2002), and have supplied my own review article McKinsey *et al.*, entitled "MEF2: a calcium-dependent regulator of cell division, differentiation and death," *TRENDS Biochem. Sci.*, 27:40-47 (2002), both of which support the inventor's claims relating to inhibition of MEF2 as a therapeutic target, and further explain the interaction between MEF2 and Class II HDACs in relation to cardiac hypertrophy. In Zhang *et al.*, the authors wanted to determine whether earlier reports of class II HDACs being potent repressors of MEF2 were indeed valid. The paper provides *in vivo* evidence that unphosphorylated Class II HDACs associate with and repress MEF2, and that pro-hypertrophic stimuli lead to phosphorylation-dependent release of class II HDACs from MEF2. Once HDACs are released, MEF2 can and does initiate transcription of fetal genes, leading to the development of hypertrophy. Signal resistant HDACs (see Fig. 2A) that are incapable of being phosphorylated are constitutive repressors of MEF2-dependent transcription and cardiac hypertrophy. The fact that these dominant repressive HDACs are anti-hypertrophic is not only validation of a role for HDACs in hypertrophy, it also shows direct proof that inhibiting MEF2 and MEF2 dependent gene upregulation is anti-hypertrophic. The reference also shows (See Fig. 4) that knocking out a Class II HDAC leads to loss of MEF2 regulation and development of profound and rapid cardiac

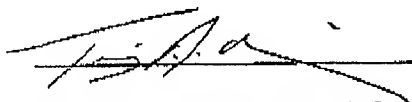
hypertrophy. These experiments are direct evidence and proof that inhibiting MEF2 would be a viable therapeutic regimen for the treatment of cardiac hypertrophy.

Additionally, McKinsey *et al.*, which is a review of the state of the art, further explains the interaction between MEF2 and class II HDACs and goes on to highlight the importance of MEF2 transcriptional activation as a key feature of a variety of cellular cascades. It is true that it has not been conclusively shown that direct inhibition of MEF2 ablates hypertrophy, those experiments have yet to be done, but this article addresses the importance of MEF2 and its interaction with not just class II HDACs, but calcineurin phosphatase and the CaM Kinases, all of which have been implicated as major players in hypertrophy. Read together, along with the specification, these articles demonstrate and validate a treatment for cardiac hypertrophy involving the inhibition of MEF2 or MEF2 dependent gene transcription.

6. I hereby declare that all statements made of my own knowledge are true and all statements made on information are believed to be true and further that the statements were made with the knowledge that willful false statements and the like so made are punishable by fine or imprisonment or both under § 1001 of Title 18 of the United States Code, and that such willful false statements may jeopardize the validity of this application or any patent issued thereon.

4-4-05

Date

  
Timothy A. McKinsey, Ph.D.

## EXHIBIT 5

**PATENT**

**IN THE UNITED STATES PATENT AND TRADEMARK OFFICE**

*In re* Application of:  
Eric N. OLSON

Serial No.: 10/043,658

Filed: January 9, 2002

For: METHODS FOR PREVENTING  
HYPERTROPHY AND HEART FAILURE  
BY INHIBITION OF MEF2  
TRANSCRIPTION FACTOR

Group Art Unit: 1632

Examiner: Woitach, J.

Atty. Dkt. No.: MYOG:024USC1/SLH

**DECLARATION OF TIMOTHY MCKINSEY UNDER 37 C.F.R. §1.131**

Mail Stop Amendment  
Commissioner for Patents  
P.O. Box 1450  
Alexandria, VA 22313-01450

I, Timothy McKinsey, to declare that:

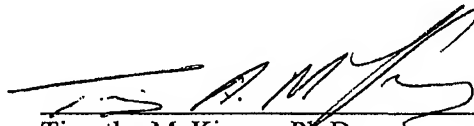
1. I currently hold the position of Scientist III at Myogen, Inc., licensee of the above-captioned application. I also hold academic appointments in the Division of Cardiology at the University of Colorado Health Sciences Center in Denver, CO, and in the Department of Molecular Biology in Boulder, CO. My education and training has been summarized previously in an earlier declaration filed in this prosecution.

2. I am familiar with the level of skill of scientists working in the field of cardiology and molecular biology as of the priority date of the referenced application. I consider one of ordinary skill in the art in this field of study to have a Ph.D. in biochemistry, chemistry, molecular biology, pathology or other related field, or an M.D., with 1-3 years of post-graduate study.

3. Attached to this declaration are two figures that describe an experiment performed in the laboratory of Dr. Eric Olson, the inventor of the present application and my former research advisor. Dr. Olson has recently provided these data in support of the application. The experiments involved the use of one month-old *MEF2D* knockout mice. Fig. A shows both the knockouts and wild-type littermates subjected to sham operation or thoracic aortic banding (TAB) for 20 days. TAB induced a 27% increase in heart weight-to-tibia length ratio, indicative of cardiac hypertrophy. The hypertrophic response to TAB was eliminated in animals lacking a functional *MEF2D* gene. Fig. B shows animals that were treated as described in Fig. A. Left ventricles were fixed and stained with hematoxylin (red) and Mason's trichrome (blue) to reveal cardiac muscle and fibrotic lesions, respectively. *MEF2D* null animals showed markedly reduced fibrosis in response to TAB. Thus, in my view, this figure shows the *MEF2D*, in addition to *MEF2A* and *MEF2C*, plays a role in pathological cardiac hypertrophy and remodeling.

4. I hereby declare that all statements made herein of my knowledge are true and that all statements made on information and belief are believed to be true; and further that these statements were made with the knowledge that willful false statements and the like so made are punishable by fine or imprisonment, or both, under Section 1001 of Title 18 of the United States Code and that such willful false statements may jeopardize the validity of the application or any patent issued thereon.

9-14-06  
\_\_\_\_\_  
Date

  
\_\_\_\_\_  
Timothy McKinsey, Ph.D.

## EXHIBIT 6

# Class II Histone Deacetylases Act as Signal-Responsive Repressors of Cardiac Hypertrophy

Chun Li Zhang,<sup>1</sup> Timothy A. McKinsey,<sup>1,4</sup>  
Shurong Chang,<sup>1</sup> Christopher L. Antos,<sup>1</sup>  
Joseph A. Hill,<sup>2</sup> and Eric N. Olson<sup>1,3</sup>

<sup>1</sup>Department of Molecular Biology  
University of Texas Southwestern Medical Center  
6000 Harry Hines Boulevard  
Dallas, Texas 75390

<sup>2</sup>Cardiovascular Division  
University of Iowa College of Medicine and Iowa  
City Veterans Affairs Medical Center  
Iowa City, Iowa 52242

## Summary

The heart responds to stress signals by hypertrophic growth, which is accompanied by activation of the MEF2 transcription factor and reprogramming of cardiac gene expression. We show here that class II histone deacetylases (HDACs), which repress MEF2 activity, are substrates for a stress-responsive kinase specific for conserved serines that regulate MEF2-HDAC interactions. Signal-resistant HDAC mutants lacking these phosphorylation sites are refractory to hypertrophic signaling and inhibit cardiomyocyte hypertrophy. Conversely, mutant mice lacking the class II HDAC, HDAC9, are sensitized to hypertrophic signals and exhibit stress-dependent cardiomegaly. Thus, class II HDACs act as signal-responsive suppressors of the transcriptional program governing cardiac hypertrophy and heart failure.

## Introduction

The adult myocardium responds to stress by hypertrophic growth, which is accompanied by an increase in size of cardiac myocytes, assembly of sarcomeres, and activation of a fetal cardiac gene program (Chien, 1999). Induction of fetal cardiac genes results in altered contractility and calcium handling and correlates with impaired cardiac function (Lowe et al., 2002). A variety of pathologic stimuli, including myocardial infarction, hypertension, contractile abnormalities, and pressure overload elicit the hypertrophic response. Autocrine and paracrine signaling pathways involving angiotensin II (ANGII), endothelin-1 (ET-1), and activators of the adrenergic system also contribute to myocyte hypertrophy.

Several calcium-dependent signaling molecules, including the calcium/calmodulin-dependent phosphatase calcineurin, calcium/calmodulin-dependent protein kinase (CaMK), and mitogen-activated protein kinases (MAPKs) have been implicated in the transduction of hypertrophic stimuli (Frey et al., 2000). However, relatively little is known of the terminal steps in these pathways that reprogram cardiac gene expression in the nucleus. It is also unclear how different intracellular sig-

naling pathways all result in the hypertrophic phenotype, and whether this reflects the convergence of these pathways on a common downstream target or crosstalk between signaling pathways at more upstream steps.

Histone acetyltransferases (HATs) and histone deacetylases (HDACs) govern gene expression patterns by being recruited to target genes through association with specific transcription factors (Jenuwein and Allis, 2001). HATs promote gene activation by acetylating nucleosomal histones, thereby relaxing chromatin structure. HAT activity is opposed by HDACs, which deacetylate histones, resulting in chromatin condensation and transcriptional repression (Johnson and Turner, 1999).

Vertebrate HDACs are categorized into three classes (Grozinger and Schreiber, 2002). Class I includes HDACs 1, 2, 3, and 8, which are expressed ubiquitously. Class II HDACs (4, 5, 7, and 9) are highly expressed in striated muscles and brain and contain N-terminal extensions that interact with positive and negative transcriptional cofactors. The N-terminal regions of class II HDACs also contain two conserved CaMK phosphorylation sites (McKinsey et al., 2000a, 2002). Phosphorylation of these sites leads to the binding of 14-3-3 proteins, which induces HDAC nuclear export and results in derepression of HDAC target genes (McKinsey et al., 2000b; Grozinger and Schreiber, 2000).

Among the targets of class II HDACs is myocyte enhancer factor-2 (MEF2), a MADS-box transcription factor highly expressed in myocytes (Black and Olson, 1998). Association of class II HDACs with MEF2 results in repression of MEF2 activity (McKinsey et al., 2002). This repressive influence can be relieved by CaMK-dependent phosphorylation of HDACs, which induces their dissociation from MEF2 (McKinsey et al., 2000a, 2000b; Lu et al., 2000a; Zhang et al., 2001b). MEF2-interacting transcriptional repressor (MITR) is a predominant splice variant of HDAC9 expressed in the heart (Sparrow et al., 1999; Zhou et al., 2001). MITR associates with MEF2 in a signal-responsive manner (Zhang et al., 2001b), but lacks a catalytic domain. Nevertheless, MITR efficiently suppresses MEF2 activity by recruiting other corepressors (Sparrow et al., 1999; Zhang et al., 2001a).

Here, we show that diverse hypertrophic signals *in vivo* lead to the activation of a cardiac HDAC kinase that phosphorylates the signal-responsive sites in class II HDACs and MITR. Mutant proteins lacking these phosphorylation sites act as signal-resistant repressors of cardiomyocyte hypertrophy and fetal cardiac gene expression *in vitro*. Conversely, HDAC9 knockout mice are super-sensitive to hypertrophic stimuli and spontaneously develop cardiac hypertrophy with advanced age. These findings demonstrate that class II HDACs act as signal-responsive repressors of cardiac hypertrophy.

## Results

### Activation of a Cardiac HDAC Kinase by Hypertrophic Stimuli

Class II HDACs and MITR possess a common structure with two conserved CaMK phosphorylation sites flank-

<sup>3</sup>Correspondence: eolson@hamon.swmed.edu

<sup>4</sup>Present address: Myogen, Inc., 7575 West 103rd Avenue, Westminster, Colorado, 80021.



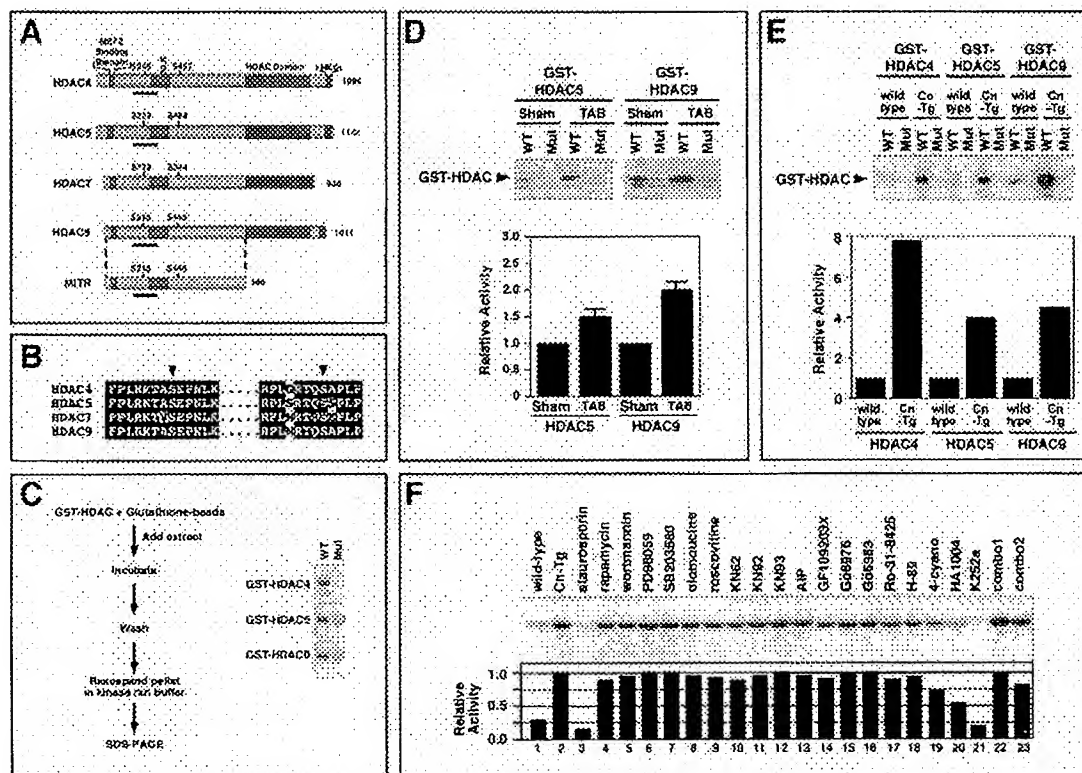


Figure 1. Elevated HDAC Kinase Activity in Hypertrophic Hearts

(A) Schematic diagram of class II HDACs. Class II HDACs have a bipartite structure, with a C-terminal catalytic (HDAC) domain and an N-terminal extension with a MEF2 binding domain. Conserved phosphorylation sites flank the nuclear localization sequence (NLS) and a nuclear export sequence (NES) is near the C terminus. MITR is a splice variant of HDAC9 that lacks an HDAC domain.

(B) Amino acid homologies surrounding the regulatory serines (arrowheads) in the class II HDACs.

(C) Schematic diagram of HDAC kinase assay. Kinase assays were performed with GST-HDAC substrates. The region of each HDAC that was used as substrate is underlined in (A). A kinase from heart lysates phosphorylates the wild-type (WT) substrates, but not mutant (Mut) substrates containing alanine in place of the regulatory serine residue.

(D and E) HDAC kinase assays were performed with heart extracts from thoracic aorta-banded (TAB) or sham-operated mice (D) or from wild-type (wt) or  $\alpha$ MHC-calcieneurin transgenic (Cn-Tg) mice. Values represent the average of at least three independent assays.

(F) HDAC kinase assays were performed with heart extracts derived from wild-type (lane 1) and Cn-Tg (lanes 2-23) mice in the absence (lanes 1 and 2) or presence (lanes 3-23) of diverse inhibitors (upper image). Kinase activity relative to that in extracts from Cn-Tg mice (lane 2) was determined (lower image). Inhibitors were added to reactions at concentrations 20 times the  $IC_{50}$ . Combo1 contained AIP and Go6983 and combo2 contained HA1004 and Go6983. Inhibitor experiments were performed at least three times with comparable results. A representative experiment is shown. For (D-F), enzyme activity was quantified as described in Experimental Procedures.

ing a nuclear localization sequence (NLS) near their N termini (Figures 1A and 1B). To determine whether a kinase specific for these phosphorylation sites might be activated in the heart in response to hypertrophic stimuli, we developed an *in vitro* kinase assay using portions of HDAC4, HDAC5, and HDAC9/MITR encompassing the conserved CaMK sites fused to GST as substrates (Figure 1C). Phosphorylation of GST-HDAC proteins was readily detected in this assay (Figure 1C, WT). GST-HDAC fusion proteins in which the CaMK sites (Ser-246 in HDAC4, Ser-259 in HDAC5, and Ser-218 in HDAC9/MITR) were mutated to alanines (Figure 1C, Mut) were not phosphorylated by cardiac extracts, demonstrating that the kinase activity is specific for the CaMK sites.

Constriction of the thoracic aorta in mice creates a pressure gradient in excess of 50 mm Hg and results in approximately a 50% increase in cardiac mass within 21 days (Hill et al., 2000). Analysis of cardiac extracts from sham-operated and thoracic aorta-banded (TAB) mice showed that pressure overload increased HDAC kinase activity 2.1- and 1.7-fold, using GST-HDAC9 and

GST-HDAC5 substrates, respectively ( $P < 0.05$ ; Figure 1D). Hypertrophic hearts from transgenic mice expressing activated calcineurin (Molkentin et al., 1998) also showed pronounced elevation of HDAC kinase activity (Figure 1E). Cardiac hypertrophy due to expression of activated forms of CaMK and the MAP kinase MEK5 in the heart also resulted in stimulation of HDAC kinase activity (data not shown).

To further characterize the HDAC kinase, we tested its sensitivity to a panel of inhibitors (Figure 1F and data not shown). The HDAC kinase was inhibited by staurosporin and K252a, which are general serine/threonine kinase inhibitors. The kinase was also partially inhibited by HA1004, which is a broad inhibitor known to inhibit CaMK, PKA, and PKG. However, the kinase was not inhibited by compounds that inhibit CaMK (KN62, KN93, or AIP), PKA (H-89 or 4-cyano-3-methylisouquinoline), PKC (GF109203X, Gö6976, Gö6983, or Ro-31-8425), MEK (PD98059), p38 (SB203580), cdk (olomoucine and roscovitine), or PI-3-kinase (rapamycin and wortmannin). The kinase was also not inhibited by inhibitors of

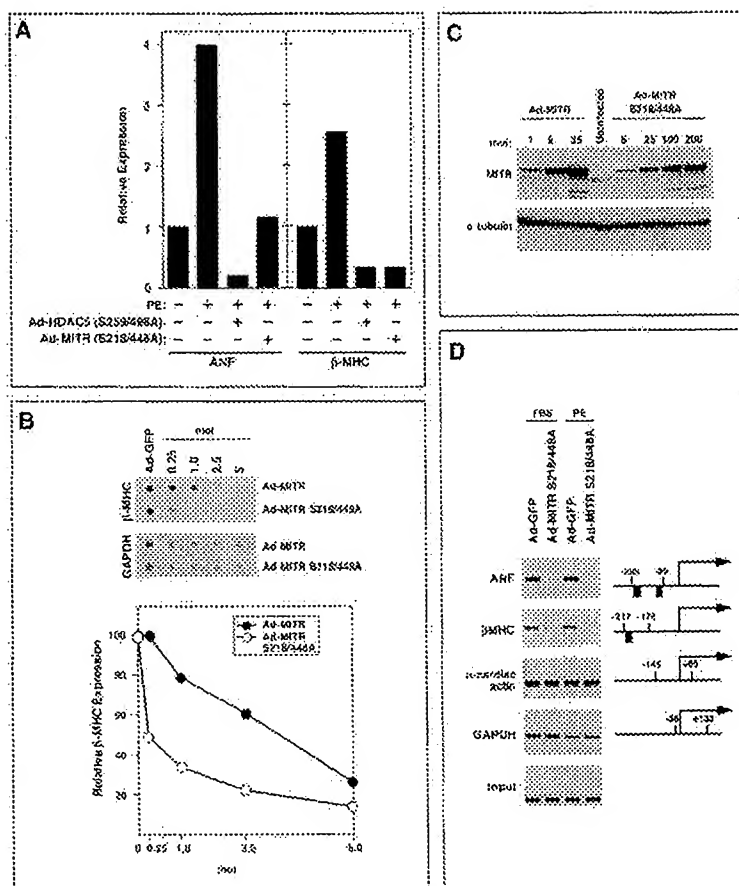


Figure 2. Inhibition of Fetal Gene Expression and Acetylation by Signal-Resistant MITR

(A) Neonatal rat cardiomyocytes were infected with adenoviruses encoding phosphorylation site mutants of HDAC5 (Ad-HDAC5 S259/498A) or MITR (Ad-MITR S218/448A) and were then stimulated with PE for 24 hr. Transcripts for ANF,  $\beta$ -MHC, and GAPDH were detected by dot blot. ANF and  $\beta$ -MHC expression are shown relative to that in untreated, uninfected controls and normalized to the level of GAPDH.

(B) Cardiomyocytes were infected with adenoviruses encoding Myc-tagged MITR or MITR S218/448A at the indicated multiplicity of infection (moi). Cells maintained in serum-free medium were stimulated with PE for 24 hr. The relative levels of  $\beta$ -MHC mRNA in Ad-MITR versus Ad-MITR S218/448A-infected cells were quantified by dot blot and normalized to the level of GAPDH.

(C) The expression of ectopic MITR in cardiomyocyte lysates was determined by Western blotting with an anti-Myc antibody (upper image). The blot was reprobed with an anti- $\alpha$ -tubulin antibody to reveal total protein input (bottom image).

(D) Soluble chromatin was prepared from cardiomyocytes infected with either Ad-GFP or Ad-MITR S218/448A and treated for 24 hr with FBS or PE. Chromatin was immunoprecipitated with an antibody specific for acetylated histone H3 and precipitated genomic DNA was analyzed by PCR using primers for ANF,  $\beta$ -MHC, GAPDH, and  $\alpha$ -cardiac actin promoters. Positions of primers (numbers) and the GATA sites (black boxes) relative to the transcription initiation sites of each gene are shown. The lower image shows a DNA input control in which PCR amplification was performed prior to immunoprecipitation.

PKG, Raf, or MLCK (data not shown). Combinations of the above inhibitors also failed to inhibit the kinase. Paradoxically, inhibitor combinations that contained HA1004 were less effective than HA1004 alone. We suspect this is due to counteracting effects of one inhibitor on the action of another.

These results demonstrate that diverse hypertrophic cues stimulate the activity of a kinase (or kinases) specific for the phosphorylation sites that inactivate class II HDACs and suggest that the kinase measured in this assay does not correspond to kinases previously implicated in hypertrophic signaling.

#### Signal-Resistant HDACs Inhibit Hypertrophy and Acetylation of Fetal Cardiac Genes

In light of the finding that cardiac hypertrophy was associated with enhanced HDAC kinase activity, which would be predicted to inactivate HDACs and MITR, we tested whether mutant proteins lacking the regulatory phosphorylation sites were able to prevent hypertrophic gene expression in primary rat cardiomyocytes. As shown in Figure 2A, the hypertrophic marker genes *atrial natriuretic factor* (ANF) and  $\beta$ -*myosin heavy chain* ( $\beta$ -MHC) are upregulated in cardiomyocytes stimulated with the adrenergic agonist phenylephrine (PE), a potent inducer of hypertrophy. Infection of cardiomyocytes with adenoviruses that expressed HDAC5 and MITR with serine-

to-alanine mutations at positions 259/498 and 218/448, respectively, abrogated the induction of these genes. The HDAC5 and MITR mutant proteins had no effect on expression of glyceraldehyde-3-phosphate dehydrogenase (GAPDH). Because MITR was effective in repressing fetal gene expression and is the predominant form of HDAC9 expressed in the heart, we used it in subsequent studies of the mechanisms involved in the blockade to hypertrophic signaling.

If the regulatory phosphorylation sites in MITR and class II HDACs are targets for hypertrophic stimuli, then wild-type HDAC proteins would be expected to be less effective inhibitors of hypertrophy than mutant proteins lacking these sites. To test this possibility, we compared the effects of wild-type MITR and the MITR S218/448A mutant on expression of  $\beta$ -MHC in cardiomyocytes treated with PE. As shown in Figure 2B, at comparable multiplicities of infection (moi's), Ad-MITR S218/448A was more than twice as effective in suppressing  $\beta$ -MHC expression than wild-type MITR. The activity of Ad-MITR S218/448A in this assay is an underestimate of its relative potency because the mutant protein accumulates to a level about 10-fold lower than the wild-type protein at the same moi (Figure 2C).

To determine whether signal-resistant MITR changed the acetylation state of histones associated with fetal cardiac genes, we performed chromatin immunoprecipitation.

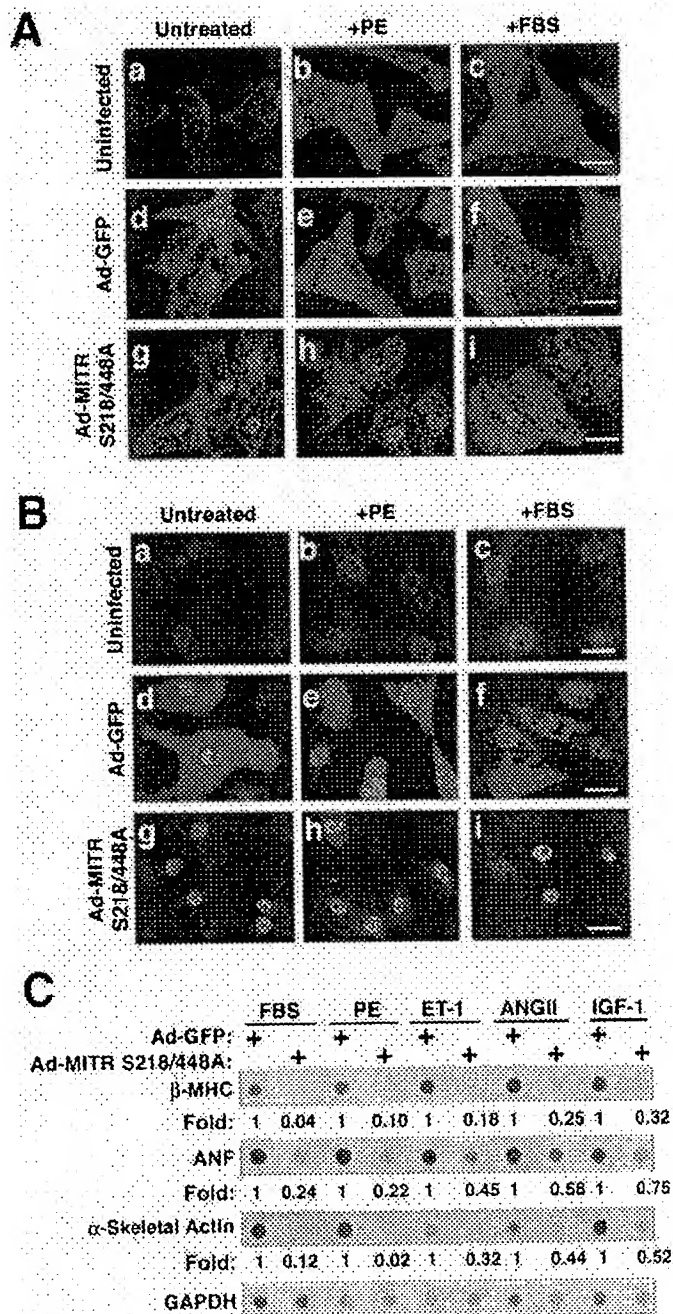


Figure 3. Prevention of Hypertrophy by MITR

(A and B) Cardiomyocytes were cultured either in the absence of virus or were infected with adenoviruses encoding GFP or Myc-tagged MITR S218/448A. After stimulation with PE or FBS for 24 hr, cells were fixed and stained with antibody against sarcomeric  $\alpha$ -actinin (A, red signal) or ANF (B, perinuclear red signal). Adenovirus-infected cells were identified by GFP fluorescence or costaining with anti-Myc antibody to reveal ectopic MITR (green signal). Scale bar equals 20  $\mu$ m. (C) Cardiomyocytes were cultured and infected with adenoviruses as described above. Cells maintained in serum-free medium were stimulated with FBS, PE, ET-1, ANGII, or IGF-1. After 24 hr, RNA was isolated and the indicated transcripts were measured by dot blot. Numbers indicate the expression level of each transcript in the presence of Ad-MITR S218/448A relative to Ad-GFP and normalized to GAPDH.

tation (ChIP) assays with an antibody specific for acetylated histone H3. Associated genomic DNA was then analyzed by PCR using primers specific for the promoter regions of the *ANF* and  $\beta$ -*MHC* genes. As a control, cardiomyocytes were infected with an adenovirus encoding green fluorescent protein (GFP). As shown in Figure 2D, the promoter regions of *ANF* or  $\beta$ -*MHC* are highly acetylated in cardiomyocytes infected with Ad-GFP and treated with either fetal bovine serum (FBS) or PE. In contrast, infection with Ad-MITR S218/448A significantly reduced acetylation of these promoters in the presence of hypertrophic stimuli. The *GAPDH* and  $\alpha$ -cardiac actin genes, which are not regulated during hypertrophy, did not show a change in histone acetyla-

tion in the presence of Ad-MITR S218/448A. Thus, there was a direct correlation between histone deacetylation and repression of fetal gene expression by signal-resistant MITR, suggesting that MITR repressed fetal genes by reducing the acetylation state of their promoters.

Neonatal cardiomyocytes assemble organized sarcomeres in the presence of hypertrophic agonists. Cardiomyocytes expressing the phosphorylation site mutant of MITR were unable to reorganize sarcomeres or upregulate expression of ANF protein in response to stimulation by PE or FBS (Figures 3A and 3B). Identical results were obtained with adenovirus encoding the HDAC5 S259/498A mutant (data not shown). Similarly, Ad-MITR S218/448A prevented induction of  $\beta$ -*MHC* and

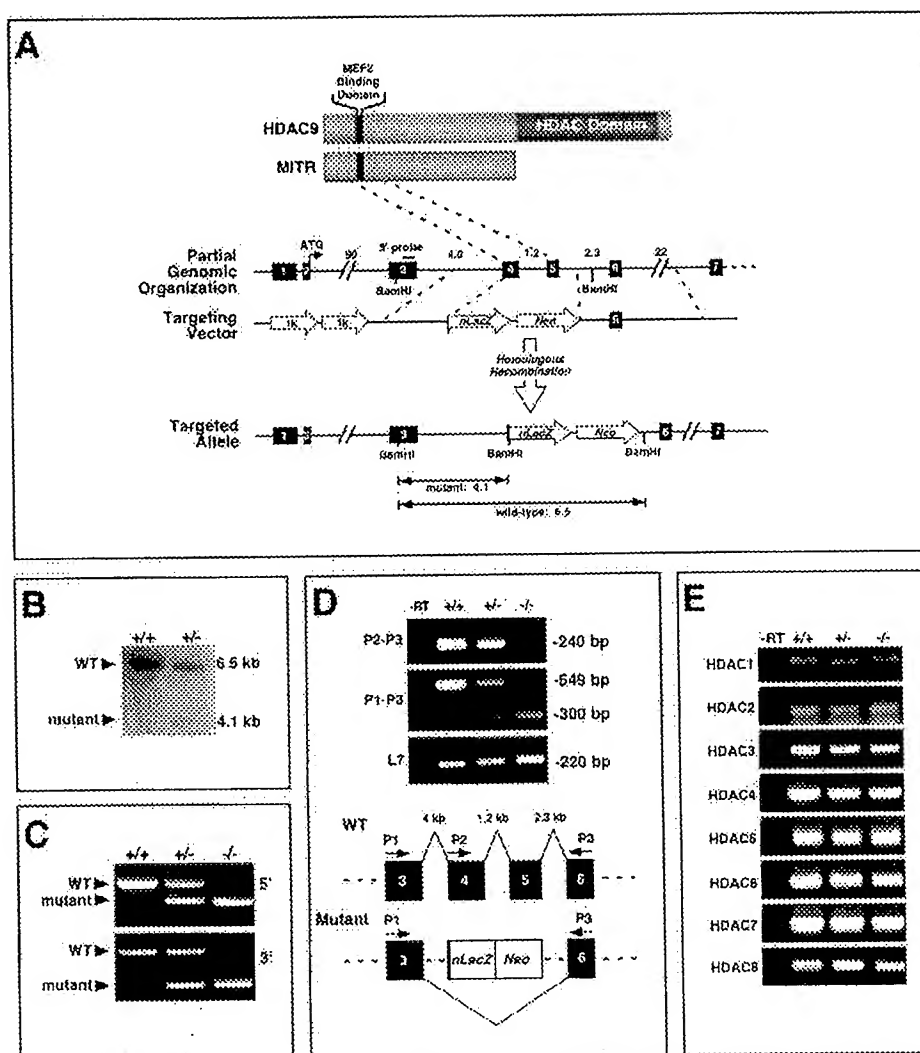


Figure 4. Targeting of Mouse *HDAC9*

(A and B) A diagram of the HDAC9 and MITR proteins is shown above the mouse *HDAC9* locus. Sizes of introns in kilobases (kb) and exons (filled boxes) are indicated. In the targeting vector, a nuclear *LacZ* (*nLacZ*) reporter was inserted in-frame with exon 4. Homologous recombination resulted in deletion of exons 4 and 5, which encode the MEF2 binding domain of HDAC9/MITR. Insertion of the *nLacZ* gene introduced a BamHI site that was used in conjunction with the indicated external 5' probe to distinguish the wild-type (6.5 kb) and mutant (4.1 kb) alleles by Southern blot (B).

(C) Genomic DNA from mice of the indicated genotypes was analyzed by PCR using primers specific for the 5' and 3' regions of the targeted mutation.

(D) The positions of the primers within *HDAC9* exons are shown (lower image). Targeting the *HDAC9* locus results in an aberrant mRNA splicing event between exons 3 and 6, as evidenced by the 300 base pair (bp) PCR product using primers P1 and P3, which is not present in wild-type controls. Sequencing of this RT-PCR product revealed a frameshift that introduced stop codons that prevent translation of sequences downstream of exon 3. L7 transcripts were amplified as a control for cDNA integrity.

(E) The consequences of *HDAC9* gene disruption on the expression of mRNA transcripts for HDACs 1–8 were assessed by semi-quantitative RT-PCR using heart RNA from mice of the indicated *HDAC9* genotypes.

*ANF* in response to FBS, ET-1, ANGII, and insulin-like growth factor-1 (IGF-1; Figure 3C). These findings suggested that phosphorylation of the regulatory serines in MITR and HDAC5 was necessary for hypertrophy in response to diverse agonists.

#### Generation of *HDAC9* Mutant Mice

To further investigate the potential involvement of class II HDACs as suppressors of cardiac hypertrophy in vivo, we inactivated the mouse *HDAC9*/MITR gene by homologous recombination in ES cells and generated *HDAC9* mutant mice (Figures 4A–4C). We chose to focus on

*HDAC9* because among the class II HDACs, it is expressed at the highest levels in the heart and because MITR, the primary product of the *HDAC9* locus, was highly effective in suppressing hypertrophy in vitro.

The targeted mutation deleted most of exon 4 and all of exon 5, which encode residues 99–176 that encompass the MEF2 binding domain of the protein (Figures 4A–4C). *HDAC9* mutant mice were obtained at predicted Mendelian ratios and showed no discernible pathological or histological abnormalities at early age (data not shown).

To confirm that the mutation created a null allele, we

performed RT-PCR analysis using primers representing exon sequences within and surrounding the targeted deletion region (Figure 4D). Using primer P2 (from deleted exon 4) and P3 (from exon 6), we detected a PCR product in RNA from hearts of wild-type and *HDAC9*<sup>+/-</sup> mice, but not of *HDAC9*<sup>-/-</sup> mice. In contrast, using primer P1 (from exon 3) and primer P3, RT-PCR products were detected in RNA samples from mice of all genotypes. In *HDAC9*<sup>+/-</sup> mice, products of 549 and 300 bp, corresponding to the wild-type and mutant transcripts, respectively, were detected, whereas in *HDAC9*<sup>-/-</sup> mice, only the mutant transcript was detected (Figure 4D). These results suggest that replacement of exon 4 and exon 5 of *HDAC9* with *LacZ-Neo* induced alternative splicing of the targeted allele, such that exon 3 was spliced to exon 6. This was confirmed by sequence analysis of RT-PCR products. Such splicing caused a frameshift and introduced two stop-codons immediately following exon 3 (data not shown). Thus, no functional HDAC9 or MITR protein is produced in homozygous mutants. Furthermore, due to such alternative splicing, the lacZ gene was not expressed in mutant mice (data not shown).

To determine whether other HDACs might be upregulated in mutant mice to compensate for the lack of HDAC9, we compared the expression of HDACs 1–8 in hearts from wild-type and mutant mice by RT-PCR. Transcripts encoding these other HDACs were expressed at normal levels in mutant hearts (Figure 4E).

#### *HDAC9* Mutant Mice Develop Age-Dependent Cardiac Hypertrophy and Are Hypersensitive to Pressure Overload

Although *HDAC9* mutant mice were initially normal, by eight months of age they developed cardiac hypertrophy and showed an average increase of 46% in heart weight/body weight ratios compared to age-matched wild-type controls ( $P < 0.001$ ; Figures 5A and 5B). In contrast, at one month of age, there was no significant difference in cardiac mass between wild-type and *HDAC9*<sup>-/-</sup> mice.

Despite the lack of an overt phenotype in young *HDAC9*<sup>-/-</sup> mice, we wondered whether they might be sensitized to hypertrophic stimuli, as would be predicted if HDAC9 was a suppressor of stress-induced signaling pathways. Since our earlier finding indicated that pressure overload stimulated a kinase that would inactivate class II HDACs, we compared the responses of wild-type and *HDAC9* mutant mice to thoracic aortic banding. Banding of the thoracic aorta of wild-type mice resulted in an average increase in left ventricular (LV) mass of 56% after 21 days (Figure 5C). In contrast, hearts from banded *HDAC9*<sup>-/-</sup> mice showed a 105% increase in LV mass over this period ( $P < 0.01$ ). These findings suggest that HDAC9 acts as a suppressor of the signaling mechanism that conveys a pressure stimulus to hypertrophic growth of the heart.

#### *HDAC9* Mutant Mice Are Sensitized to the Hypertrophic Effects of Activated Calcineurin

To further investigate the potential role of HDAC9 as a suppressor of hypertrophy, we asked whether *HDAC9*<sup>-/-</sup> mice were hypersensitive to calcineurin signaling. To address this issue, we crossed *HDAC9*<sup>-/-</sup> mice with mice

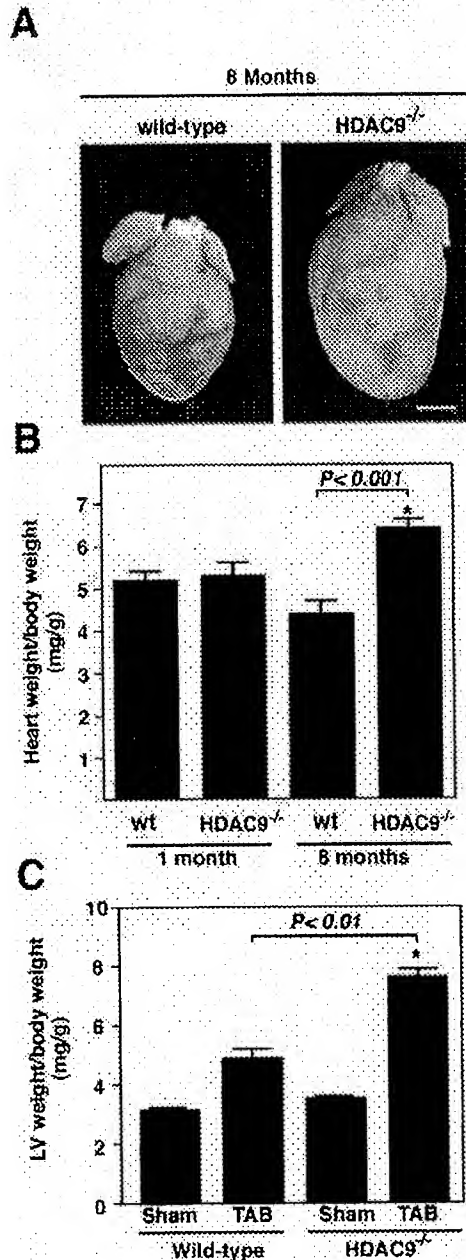
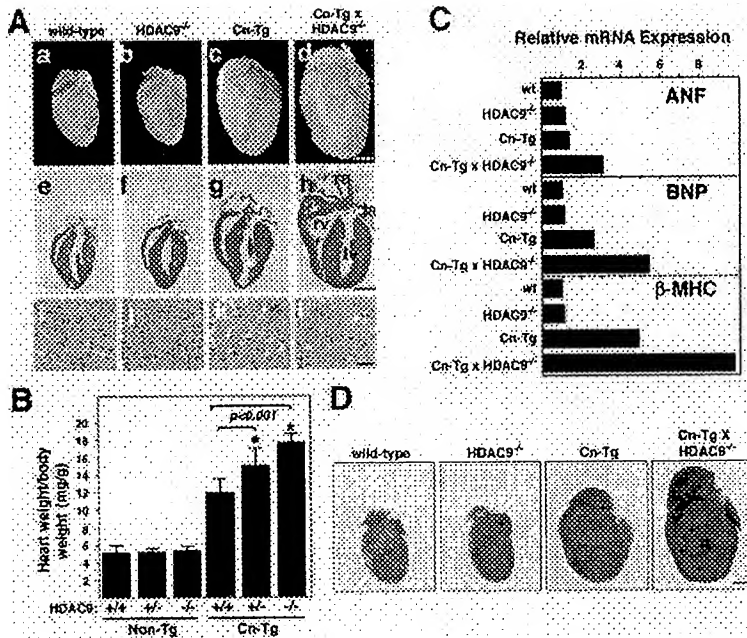


Figure 5. Cardiac Hypertrophy in *HDAC9* Mutant Mice

(A and B) *HDAC9* mutant mice and wild-type littermates were sacrificed at one and eight months of age and heart weight-to-body weight ratios were determined. Values represent the mean  $\pm$  standard deviation (SD).  $N = 5$ . Scale bar equals 2 mm. (C) Hypersensitivity to TAB. Six-to-eight-week-old mice were subjected to thoracic aortic banding (TAB) or to sham operation. Twenty-one days later, animals were sacrificed and the ratios of left ventricular (LV) mass-to-body weight were determined. At least five mice of each genotype were analyzed. Values represent the mean  $\pm$  SD.

bearing the  $\alpha$ -MHC-calcineurin transgene (Cn-Tg). Indeed, hearts from *HDAC9* mutants showed an exaggerated response to activated calcineurin (Figures 6A and 6B). Whereas activated calcineurin resulted in a 130% increase in cardiac mass by 4 weeks of age, the *HDAC9*



**Figure 6. HDAC9 Mutant Mice Are Hypersensitive to Calcineurin-Mediated Hypertrophy**

(A) HDAC9 mutant mice were bred with mice harboring the  $\alpha$ MHC-calcineurin transgene (Cn-Tg). Hearts from one-month-old mice of the indicated genotype were isolated (top images), sectioned, and stained with H and E (middle and bottom images). The bottom image shows high magnification images of H and E-stained cardiomyocytes from the ventricular septum. Scale bar equals 2 mm for top and middle, 20  $\mu$ m for bottom.

(B) Heart weight-to-body weight ratios of mice of the indicated genotypes were determined at four weeks of age. At least ten mice of each genotype were analyzed. Values represent the mean  $\pm$  standard deviation.

(C) Total RNA was isolated from hearts of mice of the indicated genotype and expression of transcripts for ANF, brain natriuretic peptide (BNP),  $\beta$ -MHC, and GAPDH was determined by Northern blot analysis. The relative abundance of transcripts was quantified and normalized to GAPDH.

(D) Wild-type or HDAC9 mutant mice were crossed to transgenic mice harboring a MEF2-dependent LacZ reporter gene. Offspring were bred with Cn-Tg mice. At least two littermates of each genotype were sacrificed at 8 weeks of age and cardiac MEF2 activity was detected by staining for  $\beta$ -galactosidase activity. Scale bar equals 2 mm.

mutants showed a 220% increase in response to calcineurin ( $P < 0.001$ ; Figure 6B). Massive hypertrophy was observed in the right and left ventricular walls and interventricular septum. Histological analysis demonstrated that the increase in cardiac mass was a reflection of the extreme hypertrophy of individual cardiomyocytes in HDAC9 mutant mice (Figure 6A, lower image). HDAC9<sup>-/-</sup> mice showed an enhanced cardiac growth response to calcineurin that was intermediate between that of wild-type and HDAC9<sup>-/-</sup> littermates (Figure 6B). The enhanced hypertrophy of HDAC9<sup>-/-</sup> hearts was mirrored by changes in fetal cardiac gene expression, as Northern blot analysis showed that transcripts for ANF, brain natriuretic peptide (BNP), and  $\beta$ -MHC were super-induced by calcineurin in the absence of HDAC9 (Figure 6C).

We considered the possibility that the exaggerated response of HDAC9<sup>-/-</sup> hearts to stress signaling might reflect subtle structural or functional cardiac abnormalities that are exacerbated by stress. However, echocardiography failed to reveal any abnormalities in cardiac function in HDAC9 mutant mice up to 8 months of age. We also considered whether noncardiac or systemic abnormalities could contribute to the sensitized phenotype of HDAC9 mutants, but we observed no abnormalities in lung, vascular system, or skeletal muscle of the mutants. Thus, we conclude that the phenotype represents a cell-autonomous abnormality of cardiac myocytes.

#### The Transcriptional Activity of MEF2 Is Hypersensitive to Calcineurin Signaling in HDAC9<sup>-/-</sup> Mice

Since MEF2 is activated by stress signals and repressed by class II HDACs, we used a line of transgenic mice,

which harbors a LacZ transgene controlled by three tandem copies of the MEF2 consensus binding site, to determine whether HDAC9 regulated the responsiveness of MEF2 to calcineurin signaling in the intact heart in vivo. This MEF2-LacZ transgene provides a read-out of MEF2 transcriptional activity and is only basally active in the postnatal heart (Naya et al., 1999). In the absence of calcineurin signaling, the MEF2-dependent reporter was expressed at low levels in both wild-type and HDAC9 mutant hearts. In contrast, MEF2 activity was elevated in the hearts of  $\alpha$ MHC-calcineurin transgenic mice, and in the HDAC9 mutant, MEF2-LacZ expression was activated to even higher levels in response to calcineurin signaling (Figure 6D). These findings demonstrate that MEF2 responds to signals for pathologic, but not physiologic hypertrophy and that the responsiveness of MEF2 to calcineurin signaling is negatively regulated by HDAC9 in vivo.

#### Discussion

Stress signals stimulate adult cardiomyocytes to undergo hypertrophy, which is associated with the activation of a fetal cardiac gene program that results in maladaptive changes in cardiac contractility and calcium handling. The results of this study show that stress signals stimulate an HDAC kinase that phosphorylates conserved regulatory serine residues in class II HDACs. Mutant forms of class II HDACs that cannot be phosphorylated render cardiac myocytes refractory to hypertrophic stimuli, and mice lacking HDAC9 are sensitized to stress signals that induce hypertrophy. A model consistent with these findings is shown in Figure 7.



### Activation of an HDAC Kinase by Hypertrophic Signals

CaMK activity is elevated in failing human hearts (Kirchhefer et al., 1999), and constitutively activated CaM kinases can induce cardiac hypertrophy in vivo and in vitro (Kato et al., 2000; Passier et al., 2000; Zhang et al., 2002). The ability of CaMK signaling to phosphorylate the conserved regulatory sites in MITR and class II HDACs in transfected cells (McKinsey et al., 2000a, 2000b; Zhang et al., 2001b) suggested that CaMK might be involved in the transduction of hypertrophic stimuli through HDACs in vivo. Indeed, our results demonstrate the existence of a protein kinase activity in cardiac extracts that phosphorylates the CaMK sites in MITR and class II HDACs and point to this enzyme as an effector in hypertrophic signaling pathways. However, the kinase detected in this assay does not appear to correspond to a typical CaMK, based on its insensitivity to all of the CaMK inhibitors we tested (KN62, KN93, and AIP), as well as its failure to bind a calmodulin affinity column and its activity in the presence of EGTA (data not shown). The kinase is also not recognized by an anti-CaMKIV antibody. Although the kinase was partially inhibited by HA1004, which is known to inhibit PKA, PKG, and CaMK, this inhibitor may also inhibit other untested or unknown kinases. Since other inhibitors for PKA, PKG, and CaMK do not inhibit the HDAC kinase, it does not appear that these kinases singly or in combination can account for the activity. Nevertheless, it is possible that the kinase is a CaMK-like kinase, since purified CaMK can phosphorylate the same sites in HDACs. The identity of this stress-responsive kinase remains to be determined.

The stimulation of HDAC kinase activity by stress signals in vivo, coupled with the ability of signal-resistant HDAC mutants to block hypertrophy of primary cardiomyocytes in the presence of diverse agonists in vitro, suggests that this kinase integrates multiple hypertrophic signaling pathways. Of course, activation of HDAC kinase activity by different hypertrophic stimuli need not be direct and could involve secondary pathways or autocrine signaling loops.

### Repression of Cardiac Hypertrophy by MITR and Class II HDACs

The phenotype of *HDAC9* mutant mice demonstrates that this HDAC acts in the adult heart to suppress the fetal gene program and hypertrophic growth. In the absence of stress, these mice showed normal cardiac size and function at young age, whereas at old age or when stressed by pressure overload or calcineurin activation, they showed a severely exaggerated hypertrophic response. Remarkably, deletion of only a single *HDAC9* allele was sufficient to sensitize animals to hypertrophic stimuli, resulting in a cardiac growth response intermediate between that of wild-type and *HDAC9*<sup>-/-</sup> mice. These findings demonstrate that the hypertrophic program is exquisitely sensitive to the repressive influence of HDAC9 and imply that, under conditions of stress, HDACs 4, 5, and 7, which are also expressed in the adult heart, cannot fully compensate for a reduction in HDAC9 expression.

The enhanced hypertrophic phenotype of *HDAC9* mutant mice, and the suppression of cardiomyocyte hypertrophy by overexpressed HDACs in vitro, also suggest

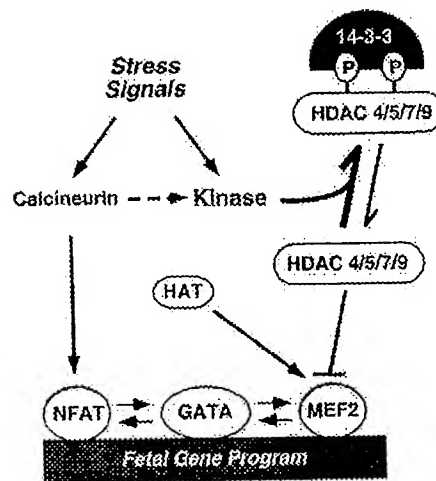


**Figure 7. Repression of Cardiac Hypertrophy by Class II HDACs**  
Class II HDACs (4, 5, 7, and 9) associate with MEF2 and inhibit hypertrophy and the fetal gene program. Stress signals stimulate an HDAC kinase that phosphorylates (P) HDACs at two conserved serine residues. HDAC kinase is also stimulated by calcineurin. When phosphorylated, HDACs bind 14-3-3, dissociate from MEF2, and are exported from the nucleus. Upon release of HDACs, MEF2 is free to associate with histone acetyltransferases (HATs) and to activate downstream target genes that drive a hypertrophic response. MEF2 also interacts with NFAT and GATA transcription factors, which have been implicated in hypertrophic gene expression.

that in order for stress signals to induce hypertrophy, the stimuli must exceed a threshold of repressive activity that represents the combined actions of class II HDACs. In *HDAC9* mutant mice, this threshold is lowered, with resulting exacerbation of the hypertrophic response. This sensitized phenotype also suggests that stress signals do not inactivate all the repressive activity of class II HDACs and that residual nonphosphorylated HDACs dampen the hypertrophic response. Otherwise, removing HDAC9 would not be expected to augment the hypertrophic response.

While *HDAC9* mutant mice show an enhanced response to stress signals, they do not show abnormal cardiac growth during postnatal development when the heart enlarges through physiologic hypertrophy. That simply eliminating HDAC activity is insufficient to cause hypertrophy suggests that the hypertrophic program also requires positive signals that are likely to be directed at other targets. (By analogy, releasing the brake of a car is insufficient to make it move without also stepping on the accelerator.) It is notable in this regard that MEF2 is activated by several stress response pathways through mechanisms independent of HDAC derepression (McKinsey et al., 2002).

The lack of enhanced hypertrophy during postnatal cardiac development in *HDAC9* mutant mice also suggests that the intracellular pathways that transduce pathologic and physiologic signals leading to hypertrophy are distinct and that HDAC9 responds specifically to stress signals that activate the fetal gene program. The selective activation of fetal cardiac genes by stress signals, but not during normal postnatal growth of the heart, supports the notion that pathologic and physio-

logic hypertrophy depends on different signaling pathways.

#### Transcriptional Targets for HDACs in the Hypertrophic Pathway

The super-activation of MEF2 activity in *HDAC9* mutant mice in response to calcineurin signaling indicates that MEF2 is a downstream target for repression by HDAC9/MITR in vivo. However, MEF2 need not be the sole transcriptional effector of the stress-response pathways governed by HDACs. It should also be pointed out that MEF2 interacts with GATA and NFAT transcription factors, which also associate with each other (Molkentin et al., 1998; Morin et al., 2000; Youn et al., 2000). These factors have each been shown to be capable of activating the fetal gene program in response to hypertrophic signaling (Liang et al., 2001; Molkentin et al., 1998). Thus, HDAC has the potential to repress hypertrophy-responsive genes by being recruited via MEF2 to gene regulatory regions that do not contain direct binding sites for MEF2 (see Figure 7).

The ability of HDACs to repress cardiac hypertrophy implies that HAT activity is required for hypertrophy and activation of the fetal gene program. Notably, the coactivators p300 and CBP, which possess HAT activity, have been shown to interact with the same region of MEF2 that interacts with class II HDACs and to be activated by the same signals that inactivate class II HDACs (Sartorelli et al., 1997; Impey et al., 2002). The signal-dependent dissociation of phospho-HDACs from MEF2 would therefore allow for the association of MEF2 with p300/CBP and consequent activation of stress-response and fetal cardiac genes.

#### Therapeutic Implications

Cardiac hypertrophy is associated with an increased risk of morbidity and mortality. Pathologic changes in the hypertrophic heart have been correlated with altered contractility that results from activation of the fetal cardiac gene program (Lowe et al., 2002). The realization that HDACs act as repressors of the hypertrophic program and stress-responsive substrates for an HDAC kinase suggests that therapeutic strategies to inhibit this kinase could be beneficial in the treatment of cardiac hypertrophy. Current strategies for treatment of hypertrophy and heart failure target early steps in hypertrophic signaling pathways, such as cell surface receptors, calcium channels and handling proteins, and components of the  $\beta$ -adrenergic receptor system. Given the plethora of signals that cause hypertrophy and heart failure, an alternative approach would be to target an effector common to many such pathways. Class II HDACs and their regulatory kinase(s) appear to represent such a point of convergence and as such represent potential therapeutic targets.

#### Experimental Procedures

##### HDAC Kinase Assays

Adult mouse hearts were homogenized in 1 ml of lysis buffer (PBS containing 1 mM EDTA, 0.1% Triton X-100, 1 mM PMSF, and protease inhibitor cocktail [Roche]). After brief sonication, lysates were clarified by ultra-centrifugation, and protein concentration was determined.

GST-HDAC substrates contained amino acids 208–310 of HDAC4,

218–328 of HDAC5, or 180–283 of HDAC9 fused to glutathione S-transferase (GST). GST-fusion proteins were also made with serine-to-alanine mutations at positions 246, 259, and 218 in HDACs 4, 5, and 9, respectively. GST-HDAC protein (1  $\mu$ g) was conjugated to glutathione-agarose beads. GST-HDAC-bound beads were washed with PBS and subsequently incubated with heart protein lysate (100  $\mu$ g) in lysis buffer for 2 hr at 4°C. Beads were washed twice with the same buffer and equilibrated with kinase reaction buffer (25 mM HEPES [pH 7.6], 10 mM  $MgCl_2$ , and 0.1 mM  $CaCl_2$ ). Beads were then resuspended in kinase reaction buffer (30  $\mu$ l) containing 12.5  $\mu$ M ATP and 5  $\mu$ Ci [ $\gamma$ - $^{32}$ P]-ATP and reactions were allowed to proceed for 30 min at room temperature. Reactions were then boiled, and phosphoproteins were resolved by SDS-PAGE, visualized by autoradiography, and quantified using a phosphorimager.

##### Transgenic Mice and $\beta$ -Galactosidase Staining

Mice bearing transgenes encoding a constitutively active form of calcineurin under control of the  $\alpha$ -MHC promoter, and mice carrying the *desMEF2-LacZ* transgene (MEF2 indicator mice) have been described (Molkentin et al., 1998; Naya et al., 1999). *LacZ* gene expression was determined as described (Naya et al., 1999).

##### Cardiomyocyte Cell Culture and Adenovirus Infections

Primary rat cardiomyocytes were prepared as described (Molkentin et al., 1998). Eighteen hours after plating, cells were infected with adenovirus for 2 hr and subsequently cultured in serum-free medium for 24 hr before stimulation for another 24 hr with PE (100  $\mu$ M; Sigma), ET-1 (100 nM; American Peptide Company, Inc), IGF-1 (100 ng/ml; American Peptide Company, Inc), ANGII (100 nM; American Peptide Company, Inc), or FBS (2.5%; Sigma).

Myc- and FLAG-tagged derivatives of MITR and HDAC5 and their signal-resistant counterparts (S218/448A and S259/498A, respectively) have been described (McKinsey et al., 2000a; Zhang et al., 2001b). For adenovirus production, cDNAs were cloned into the pAC-CMV vector and the resultant constructs were cotransfected into 293 cells with pJM17 using Fugene 6 (Roche). Primary lysates were used to reinfect 293 cells and viral plaques were obtained using the agar overlay method. Clonal populations of adenoviruses were amplified by reinfecting 293 cells and titered.

##### Immunocytochemistry

Primary cardiomyocytes plated on laminin-coated glass coverslips were fixed and stained as described (Zhang et al., 2001b). Fluorescent images were collected on a LSM 410 Zeiss confocal microscope and were processed with Adobe Photoshop. The following primary and secondary antibodies were used at 1:200 dilution: anti- $\alpha$ -actinin (EA-53; Sigma), anti-Myc (9E10 and A-14; Santa Cruz), anti-rat-ANF (IHC9103; Peninsula Laboratories, Inc.), Texas Red-conjugated anti-mouse or anti-rabbit IgG (Vector Labs), and fluorescein-conjugated anti-mouse or anti-rabbit IgG (Vector Labs).

##### RNA Isolation and Analysis

Total RNA was purified from cultured cells or intact hearts with Trizol reagent (Invitrogen) according to manufacturer's instructions. Northern and RNA dot blot analyses were performed with 20  $\mu$ g and 2  $\mu$ g, respectively, of total RNA. For RT-PCR, total RNA was used as a template for reverse transcriptase and random hexamer primers (Invitrogen). Sequences of oligonucleotide probes and primers are available upon request.

##### Chromatin Immunoprecipitation (ChIP) Assay

ChIP assays were performed as described (Lu et al., 2000b), using soluble chromatin prepared from cardiomyocytes. Equal amounts of chromatin from each sample (normalized by ethidium bromide staining of DNA) were immunoprecipitated with an anti-acetylated histone H3 antibody (Upstate Biotechnology). Ten percent of the precipitated DNA was subjected to 28 cycles of PCR in the presence of [ $^{32}$ P]-dCTP with primers specific for the *ANF*,  $\beta$ -*MHC*,  $\alpha$ -*cardiac actin*, or *GAPDH* promoters. As a control for DNA content, PCR reactions were also performed on chromatin samples prior to immunoprecipitation. Twenty percent of each reaction mixture was resolved through a 5% native polyacrylamide gel, visualized, and quantified using a phosphorimager (Molecular Dynamics). Primer sequences are available upon request.



# Generation of *HDAC9* Targeting Construct and Mutant Mice

The *HDAC9* targeting construct was generated using the pN-Z-TK<sub>2</sub> vector, which contains a nuclear *LacZ* (*nLacZ*) cassette and a *neo-mycin-resistance* gene (kindly provided by R. Palmiter). Following electroporation into the R1 ES cell line and positive-negative selection, 780 individual ES cell clones were isolated and analyzed by Southern blotting for homologous recombination. Four clones with a disrupted *HDAC9* gene were injected into 3.5-day mouse C57BL/6 blastocysts, and the resulting chimeric male mice were bred to C57BL/6 females to achieve germline transmission of the mutant allele.

## Thoracic Aorta Banding

Six-to-eight-week-old male wild-type and *HDAC9*<sup>-/-</sup> littermates underwent either a sham operation or were subjected to pressure overload induced by thoracic aorta banding as described (Hill et al., 2000).

## Acknowledgments

We are grateful to Yin-Chai Cheah for blastocyst injections, Hartmut Weiler for assistance with gene targeting, Robert Gerard for assistance with viruses, and Stuart Schreiber for providing HDAC plasmids. We thank James Richardson, Jeff Starks, and John Shelton for histological sections, and Alisha Tizenor for graphics. This work was supported by grants from the National Institutes of Health, the D.W. Reynolds Clinical Cardiovascular Research Center, the Texas Advanced Technology Program, and the Robert A. Welch Foundation to E.N.O. T.A.M. is a Pfizer Fellow of the Life Sciences Research Foundation.

Received: April 17, 2002

Revised: July 8, 2002

## References

Black, B.L., and Olson, E.N. (1998). Transcriptional control of muscle development by myocyte enhancer factor-2 (MEF2) proteins. *Annu. Rev. Cell Dev. Biol.* 14, 167–196.

Chien, K.R. (1999). Stress pathways and heart failure. *Cell* 98, 555–558.

Frey, N., McKinsey, T.A., and Olson, E.N. (2000). Decoding calcium signals involved in cardiac growth and function. *Nat. Med.* 6, 1221–1227.

Grozinger, C.M., and Schreiber, S.L. (2000). Regulation of histone deacetylase 4 and 5 and transcriptional activity by 14–3–3-dependent cellular localization. *Proc. Natl. Acad. Sci. USA* 97, 7835–7840.

Grozinger, C.M., and Schreiber, S.L. (2002). Deacetylase enzymes. Biological functions and the use of small-molecule inhibitors. *Chem. Biol.* 9, 3–16.

Hill, J.A., Karimi, M., Kutschke, W., Davisson, R.L., Zimmerman, K., Wang, Z., Kerber, R.E., and Weiss, R.M. (2000). Cardiac hypertrophy is not a required compensatory response to short-term pressure overload. *Circulation* 101, 2863–2869.

Impey, S., Fong, A.L., Wang, Y., Cardinaux, J.R., Fass, D.M., Obrietan, K., Wayman, G.A., Storm, D.R., Soderling, T.R., and Goodman, R.H. (2002). Phosphorylation of CBP mediates transcriptional activation by neural activity and CaM kinase IV. *Neuron* 34, 235–244.

Jenuwein, T., and Allis, C.D. (2001). Translating the histone code. *Science* 293, 1074–1080.

Johnson, C.A., and Turner, B.M. (1999). Histone deacetylases: complex transducers of nuclear signals. *Semin. Cell Dev. Biol.* 10, 179–188.

Kato, T., Sano, M., Miyoshi, S., Sato, T., Hakuno, D., Ishida, H., Kinoshita-Nakazawa, H., Fukuda, K., and Ogawa, S. (2000). Calmodulin kinases II and IV and calcineurin are involved in leukemia inhibitory factor-induced cardiac hypertrophy in rats. *Circ. Res.* 87, 937–945.

Kirchhefer, U., Schmitz, W., Scholz, H., and Neumann, J. (1999). Activity of cAMP-dependent protein kinase and Ca<sup>2+</sup>/calmodulin-dependent protein kinase in failing and nonfailing human hearts. *Cardiovasc. Res.* 42, 254–261.

Liang, Q., De Windt, L.J., Witt, S.A., Kimball, T.R., Markham, B.E., and Molkenin, J.D. (2001). The transcription factors GATA4 and GATA6 regulate cardiomyocyte hypertrophy in vitro and in vivo. *J. Biol. Chem.* 276, 30245–30253.

Lowes, B.D., Gilbert, E.M., Abraham, W.T., Minobe, W.A., Larrabee, P., Ferguson, D., Wolfel, E.E., Lindenfeld, J., Tsvetkova, T., Robertson, A.D., et al. (2002). Myocardial gene expression in dilated cardiomyopathy treated with beta-blocking agents. *N. Engl. J. Med.* 346, 1357–1365.

Lu, J., McKinsey, T.A., Nicol, R.L., and Olson, E.N. (2000a). Signal-dependent activation of the MEF2 transcription factor by dissociation from histone deacetylases. *Proc. Natl. Acad. Sci. USA* 97, 4070–4075.

Lu, J., McKinsey, T.A., Zhang, C.L., and Olson, E.N. (2000b). Regulation of skeletal myogenesis by association of the MEF2 transcription factor with class II histone deacetylases. *Mol. Cell* 6, 233–244.

McKinsey, T.A., Zhang, C.L., Lu, J., and Olson, E.N. (2000a). Signal-dependent nuclear export of a histone deacetylase regulates muscle differentiation. *Nature* 408, 106–111.

McKinsey, T.A., Zhang, C.L., and Olson, E.N. (2000b). Activation of the myocyte enhancer factor-2 transcription factor by calcium/calmodulin-dependent protein kinase-stimulated binding of 14–3–3 to histone deacetylase 5. *Proc. Natl. Acad. Sci. USA* 97, 14400–14405.

McKinsey, T.A., Zhang, C.L., and Olson, E.N. (2002). MEF2: a calcium-dependent regulator of cell division, differentiation and death. *Trends Biochem. Sci.* 27, 40–47.

Molkenin, J.D., Lu, J.R., Antos, C.L., Markham, B., Richardson, J., Robbins, J., Grant, S.R., and Olson, E.N. (1998). A calcineurin-dependent transcriptional pathway for cardiac hypertrophy. *Cell* 93, 215–228.

Morin, S., Charron, F., Robitaille, L., and Nemer, M. (2000). GATA-dependent recruitment of MEF2 proteins to target promoters. *EMBO J.* 19, 2046–2055.

Naya, F.J., Wu, C., Richardson, J.A., Overbeek, P., and Olson, E.N. (1999). Transcriptional activity of MEF2 during mouse embryogenesis monitored with a MEF2-dependent transgene. *Development* 126, 2045–2052.

Passier, R., Zeng, H., Frey, N., Naya, F.J., Nicol, R.L., McKinsey, T.A., Overbeek, P., Richardson, J.A., Grant, S.R., and Olson, E.N. (2000). CaM kinase signaling induces cardiac hypertrophy and activates the MEF2 transcription factor in vivo. *J. Clin. Invest.* 105, 1395–1406.

Sartorelli, V., Huang, J., Hamamori, Y., and Kedes, L. (1997). Molecular mechanisms of myogenic coactivation by p300: direct interaction with the activation domain of MyoD and with the MADS box of MEF2C. *Mol. Cell. Biol.* 17, 1010–1026.

Sparrow, D.B., Miska, E.A., Langley, E., Reynaud-Deonauth, S., Kotucha, S., Towers, N., Spohr, G., Kouzarides, T., and Mohun, T.J. (1999). MEF-2 function is modified by a novel co-repressor, MITR. *EMBO J.* 18, 5085–5098.

Youn, H.D., Chatila, T.A., and Liu, J.O. (2000). Integration of calcineurin and MEF2 signals by the coactivator p300 during T-cell apoptosis. *EMBO J.* 19, 4323–4331.

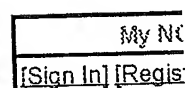
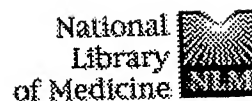
Zhang, C.L., McKinsey, T.A., Lu, J.R., and Olson, E.N. (2001a). Association of COOH-terminal-binding protein (CtBP) and MEF2-interacting transcription repressor (MITR) contributes to transcriptional repression of the MEF2 transcription factor. *J. Biol. Chem.* 276, 35–39.

Zhang, C.L., McKinsey, T.A., and Olson, E.N. (2001b). The transcriptional corepressor MITR is a signal-responsive inhibitor of myogenesis. *Proc. Natl. Acad. Sci. USA* 98, 7354–7359.

Zhang, T., Johnson, E.N., Gu, Y., Morissette, M.R., Sah, V.P., Gigena, M.S., Beike, D.D., Dillmann, W.H., Rogers, T.B., Schulman, H., et al. (2002). The cardiac-specific nuclear  $\delta$ (B) isoform of Ca<sup>2+</sup>/calmodulin-dependent protein kinase II induces hypertrophy and dilated cardiomyopathy associated with increased protein phosphatase 2A activity. *J. Biol. Chem.* 277, 1261–1267.

Zhou, X., Marks, P.A., Rifkind, R.A., and Richon, V.M. (2001). Cloning and characterization of a histone deacetylase, HDAC9. *Proc. Natl. Acad. Sci. USA* 98, 10572–10577.

## EXHIBIT 7



All Databases PubMed Nucleotide Protein Genome Structure OMIM PMC Journals Books  
 Search PubMed for

Limits Preview/Index History Clipboard Details

Display Abstract Show: 20 Sort Send to Text

About Entrez

Text Version

Entrez PubMed

Overview

Help | FAQ

Tutorial

New/Noteworthy

E-Utilities

PubMed Services

Journals Database

MeSH Database

Single Citation Matcher

Batch Citation Matcher

Clinical Queries

LinkOut

My NCBI (Cubby)

Related Resources

Order Documents

NLM Catalog

NLM Gateway

TOXNET

Consumer Health

Clinical Alerts

ClinicalTrials.gov

PubMed Central

☐ 1: Curr Opin Cell Biol. 2002 Dec;14(6):763-72.

Related Articles

**FULL-TEXT ARTICLE**

## Signaling chromatin to make muscle.

McKinsey TA, Zhang CL, Olson EN.

Myogen, Inc., 7575 West 103rd Avenue, Westminster, CO 80021, USA.

Several findings published within the past year have further established key roles for chromatin-modifying enzymes in the control of muscle gene expression, and have thus refined our thinking of how chromatin structure influences muscle differentiation, hypertrophy and fiber type determination. We discuss the interplay between chromatin-modifying enzymes and myogenic transcription factors, signaling mechanisms that impinge on these transcriptional complexes, and how these multicomponent regulatory cascades may be exploited in the development of novel therapeutics to more effectively treat myopathies in humans.

Publication Types:

- Review
- Review, Tutorial

PMID: 12473352 [PubMed - indexed for MEDLINE]

Display Abstract Show: 20 Sort Send to Text

Write to the Help Desk

NCBI | NLM | NIH

Department of Health & Human Services

Privacy Statement | Freedom of Information Act | Disclaimer

Mar 2 2005 14:57:42